UNIVERSITÄT BONN
Rheinische Friedrich-Wilhelms-
Universität Bonn

Neuroinvasion and cerebral ischemia as possible sources for α-synuclein prions in Parkinson's disease

Dissertation zur Erlangung
des Doktorgrades (Dr. rer. nat.)
der Mathematisch-Naturwissenschaftlichen Fakultät
der Rheinischen Friedrich-Wilhelms-Universität Bonn

Vorgelegt von:

Stephanie Lohmann
aus
Moers, Deutschland

Bonn 2021

Angefertigt mit Genehmigung der Mathematisch-Naturwissenschaftlichen Fakultät der Rheinischen Friedrich-Wilhelms-Universität Bonn

1. Gutachter: Prof. Dr. Erdem Gültekin Tamgüney
2. Gutachter: Prof. Dr. Jörg Höhfeld

Tag der Promotion: 26.05.2021
Erscheinungsjahr: 2021

Statement of originality

I certify that the content of this thesis is the product of my own work. All the assistance received in preparing this thesis and sources have been acknowledged and I have clearly referenced all sources used in this work.
This thesis has not yet been submitted to another examination institution – neither in Germany nor outside Germany – neither in the same nor in a similar way.

Partial results of the presented work (Peripheral challenge study) have been published:

Lohmann S, Bernis ME, Tachu BJ, Ziemski A, Grigoletto J, Tamgüney G:
'**Oral and intravenous transmission of α-synuclein fibrils to mice**'
Acta Neuropathologica; 2019, 138 (4):515-533. doi: 10.1007/s00401-019-02037-5 *

_____ _____

Place, Date Signature

Table of Content

Table of Content I
Abstract III
List of Figures IV
List of Tables IV
List of Abbreviations V
1 Introduction 1
1.1 Synucleinopathies and Parkinson's disease 1
1.2 Native α-synuclein 2
1.3 Accumulation of α-synuclein 3
1.4 Posttranslational modifications of α-synuclein 4
1.4.1 Phosphorylation 4
1.4.2 Nitration and oxidation 4
1.4.3 Truncation 5
1.4.4 Ubiquitination and Sumoylation 5
1.5 Toxicity of α-synuclein 5
1.5.1 Cellular stress 5
1.5.2 Loss of dopaminergic neurons 7
1.5.3 Protein degradation 8
1.5.4 Neuroinflammation 8
1.6 Transmission of α-synuclein 10
1.6.1 Cell-to-cell transmission 10
1.6.2 Spreading within the nervous systems 11
1.7 Prion-like behavior 11
1.8 Stroke as a neurodegenerative condition 12
1.8.1 Stroke 12
1.8.2 Stroke in Parkinson's disease 13
1.9 Mouse models of Parkinson's disease 14
1.9.1 Toxin-induced mouse models 14
1.9.2 Genetic mouse models of PD 14
1.10 Aim 16
2 Material and Methods 17
2.1 Material 17
2.2 Methods 20
2.2.1 Preparation of recombinant α-synuclein fibrils 20
2.2.2 Animals 21
2.2.3 Mouse tissue preparation 26
2.2.4 Histological analysis 26
2.2.5 Biochemical analysis 27
2.2.6 Data Analysis 29

2.2.7 Statistics 29
3 Results 30
3.1 Peripheral challenge study 30
3.1.1 Transmission of α-synuclein fibrils leads to severe neurological disease 30
3.1.2 Diseased mice accumulate pathological α-synuclein in the CNS 32
3.1.3 Distribution of pathological α-synuclein in the CNS of diseased mice 34
3.1.4 Neuropathology displays oligomeric and fibrillar α-synuclein 38
3.1.5 Pathological α-synuclein colocalizes with ubiquitin and p62 in the CNS 39
3.1.6 Pathological α-synuclein induces neuroinflammation in the brains of diseased mice 43
3.2 MCAO study 46
3.2.1 MCAO-treated mice display motor deficits 46
3.2.2 MCAO-treated mice display neuronal loss 47
3.2.3 MCAO-induced neuroinflammation 48
3.2.4 MCAO leads to a loss of dopaminergic neurons 52
3.2.5 MCAO causes α-synuclein to aggregate 53
4 Discussion 55
4.1 Peripheral challenge study 55
4.1.1 Intracerebral injection of α-synuclein fibrils causes neurological disease 55
4.1.2 Transmission of α-synuclein via peripheral routes causes pathology and neurological disease 58
4.1.3 Intravenous transmission causes neuropathology and neurological disease 60
4.1.4 Prion-like character of α-synuclein 61
4.2 MCAO study 62
4.2.1 Mild MCAO causes motor deficits and neurodegeneration 62
4.2.2 MCAO causes neuroinflammation 64
4.2.3 MCAO causes loss of dopaminergic neurons and neuropathology 64
5 Conclusion and future perspectives 68
6 Bibliography 69
7 Acknowledgement 87

Abstract

In synucleinopathies such as Parkinson's disease misfolding of α-synuclein, normally a cellular and soluble protein, leads to the accumulation of insoluble protein aggregates and to central nervous system disease (CNS). Misfolded α-synuclein acts as a seed, by recruiting native α-synuclein and inducing its misfolding into insoluble α-synuclein aggregates. Aggregated α-synuclein shows prion-like characteristics and spreads via cell-to-cell transmission throughout the central nervous system but also within the periphery, ultimately causing neurological disease.

Because the spatiotemporal spreading of pathological α-synuclein from the periphery to the CNS is not fully elucidated this work investigated and compared the spreading of pathological α-synuclein after intravenous or oral inoculation with that after intracerebral or intraperitoneal inoculation of TgM83$^{+/-}$ mice overexpressing the A53T mutant of human α-synuclein with α-synuclein fibrils. In accordance with previous studies, an infection rate of 100% was observed for intracerebrally and intraperitoneally injected mice. Moreover, this study is the first to show that a single intravenous injection of α-synuclein fibrils causes synucleinopathy in 100% of the challenged mice, and even a single oral gavage with α-synuclein fibrils results in 50% of the challenged mice in neurological disease. Diseased mice displayed aggregates of sarkosyl-insoluble and phosphorylated α-synuclein, which colocalized with ubiquitin and p62 and were accompanied by gliosis, indicative of neuroinflammation, throughout the CNS. In contrast, none of the control mice that were challenged with bovine serum albumin via the same routes developed any neurological disease or neuropathology. These findings show that aggregated α-synuclein behaves like a prion causing neuropathology and CNS disease, not only after intracerebral or intraperitoneal challenge but also by neuroinvasion after a single intravenous, or oral challenge.

Since cerebral ischemia increases the risk of developing Parkinson's disease (PD) without being clear what the underlying mechanism is, the second aim of this work was to study the impact of ischemic stroke on α-synuclein aggregation, which is known to cause PD. To investigate post-ischemic changes to the CNS, focal cerebral ischemia was induced by middle cerebral artery occlusion (MCAO) in transgenic mice overexpressing the A53T mutant of human of α-synuclein. Ischemic mice displayed significant motor deficits and loss of dopaminergic neurons in the substantia nigra at 360 days after MCAO. This was caused by a significantly increased amount of aggregated α-synuclein, which was accompanied by neuroinflammation as indicated by astrogliosis and microgliosis. In summary, cerebral ischemia induced a synucleinopathy with loss of dopaminergic neurons in the substantia nigra resulting in motor deficits in a mouse model of PD, which may explain why cerebral ischemia increases the risk of PD.

List of Figures

Figure 1.1: Native α-synuclein....3
Figure 1.2: α-Synuclein polymerization....4
Figure 1.3: Effects on α-synuclein aggregation and toxicity of pathological α-synuclein....7
Figure 1.4: Transmission mechanism from donor neuron to recipient neuron of α-synuclein, in a caudal-to-rostral manner....10
Figure 1.5: Pathological processes upon ischemic stroke....13
Figure 2.1: Experimental overview of the inoculation study....22
Figure 2.2: Experimental overview of the MCAO study....24
Figure 2.3: Middle cerebral artery occlusion (MCAO)....25
Figure 3.1: Intracerebral, intraperitoneal, intravenous, or oral challenge with α-synuclein fibrils lead to neurological disease in TgM83$^{+/-}$ mice....31
Figure 3.2: Aggregation of α-synuclein in the CNS of TgM83$^{+/-}$ mice challenged with α-synuclein fibrils....33
Figure 3.3: Detection of sarkosyl-insoluble aggregates of phosphorylated α-synuclein in the brains of TgM83$^{+/-}$ mice challenged with α-synuclein fibrils....34
Figure 3.4: Immunohistochemical analysis shows neuropathology in the CNS of TgM83$^{+/-}$ mice after challenge with α-synuclein fibrils for all four routes....36
Figure 3.5: Heat map showing the distribution of phosphorylated α-synuclein in TgM83$^{+/-}$ mice after challenge with α-synuclein fibrils for all four routes....37
Figure 3.6: Immunohistochemical analysis shows fibrillar and oligomeric α-synuclein in TgM83$^{+/-}$ mice after challenge with α-synuclein fibrils for all four inoculation routes....39
Figure 3.7: Aggregates of phosphorylated α-synuclein colocalize with ubiquitin in the CNS of inoculated TgM83$^{+/-}$ mice inoculated with α-synuclein fibrils....40
Figure 3.8: Aggregates of phosphorylated α-synuclein colocalize with p62 in the CNS of inoculated TgM83$^{+/-}$ mice inoculated with α-synuclein fibrils....42
Figure 3.9: Astrogliosis and microgliosis was significantly increased in TgM83$^{+/-}$ mice inoculated with human α-synuclein fibrils....45
Figure 3.10: MCAO-treated TgM83$^{+/-}$ mice gain weight....46
Figure 3.11: Middle cerebral artery occlusion in TgM83$^{+/-}$ leads to behavioral deficits....47
Figure 3.12: Immunohistochemical staining shows ipsilateral neuronal loss in TgM83$^{+/-}$ mice after MCAO....48
Figure 3.13: Immunhistochemical analysis shows induced ipsilateral microgliosis in TgM83$^{+/-}$ mice after MCAO....50
Figure 3.14: Immunhistochemical analysis shows induced ipsilateral astrogliosis in TgM83$^{+/-}$ mice after MCAO....51
Figure 3.15: Immunhistochemical analysis shows ipsilateral loss of dopaminergic neurons in TgM83$^{+/-}$ mice at 360 days after MCAO....53
Figure 3.16: The amount of aggregated α-synuclein was increased in the brains of TgM83$^{+/-}$ mice after MCAO....54

List of Tables

Table 1: Buffers and solutions used....17
Table 2: Summary of kits used....18
Table 3: Summary of primers used with their sequences....18
Table 4: Primary antibodies and their dilution....18
Table 5: Secondary antibodies used and their dilution....19
Table 6: Suppliers of software....19
Table 7: Incubation times in TgM83$^{+/-}$ mice after challenge with human α-synuclein fibrils or BSA via different routes....32

List of Abbreviations

Abbreviation	Meaning
BBB	blood brain barrier
BSA	bovine serum albumin
BSE	bovine spongiform encephalopathy
Ca^{2+}	calcium
CA	cornu ammonis
contra	contralateral
CJD	Creutzfeldt-Jakob disease
CNS	central nervous system
$CuSO_4$	copper sulfate
DAB	3-3'-diaminobenzidine
DAPI	4',6-diamidino-2-phenylindole
DG	dentate gyrus
dmx	dorsal motor nucleus X
dpi	days post inoculation
dps	days post surgery
E. coli	Escherichia coli
EDTA	ethylendiaminetetraacetic acid
ENS	enteric nervous system
ER	endoplasmic reticulum
EtOH	ethanol
FA	formic acid
GCI	glial cytoplasmic inclusions
GFAP	glial fibrillary acidic protein
HRP	horseradish peroxidase
i.c.	intracerebral
i.p.	intraperitoneal
i.v.	intravenous
Iba1	Ionized calcium-binding adapter molecule 1
ID	identification number
IF	immunofluorescence
ipsi	ipsilateral
IPTG	isopropyl-β-D-1-thiogalactopyranoside
kb	kilobase
kDa	kilo Dalton
LB	Lewy body
LN	Lewy neurite
LPS	lipopolysaccharide
MCAO	middle cerebral artery occlusion
MW	molecular weight

n	number of biological replicates
N	number of technical replicates
NaCl	sodium chloride
NeuN	neuronal nuclei
$(NH_4)_2SO_4$	ammonium sulfate
p	phospho
PAGE	polyacrylamide gel electrophoresis
PBS	phosphate-buffered saline
PCR	polymerase chain reaction
PD	Parkinson's disease
PFA	para-formaldehyde
PFF	preformed fibrils
pH	potential hydrogen
rpm	rotation per minute
ROS	reactive oxygen species
RT	room temperature
s.c.	subcutaneous
SD	standard derivation
SDS	sodium dodecyl sulfate
SEM	standard error of the mean
Ser129	serine 129
SN	substantia nigra
Snca	gene encoding mouse α-synuclein
syn	synuclein
TBS	Tris-buffered saline
Tg	transgenic
TH	tyrosine hydroxylase
UPS	ubiquitin-proteasome system
v/v	volume per volume
w/v	weight per volume
WB	western blot
WT	wild type
x g	times gravitational acceleration

1 Introduction

1.1 Synucleinopathies and Parkinson's disease

Synucleinopathies are a group of neurodegenerative disorders characterized by the intracellular deposition of misfolded and aggregated α-synuclein, such as in the cytoplasm and neurites of neurons in Parkinson's disease (PD) and dementia with Lewy bodies, or in the cytoplasm of oligodendrocytes in multiple system atrophy (Tamgüney and Korczyn, 2018). PD is the second most common neurodegenerative disease after Alzheimer's disease (Kalia and Lang, 2015). In addition to aging as the most critical risk factor for PD, several external factors are associated with an increased risk of developing PD. Those include environmental toxins, drug and pesticide exposure, dairy consumption, and history of traumatic brain injury or melanoma (Hubble et al., 1993; Park et al., 2005; Ascherio and Schwarzschild, 2016; Tysnes and Storstein, 2017). Most patients develop PD as a sporadic disease without known genetic predisposition. However, some familial cases have been described. These rare familial cases are mainly due to multiplications or missense mutations of *SNCA*, the gene encoding α-synuclein, but additional genetic mutations were found for several PARK genes, also known as familial PD genes (Polymeropoulos et al., 1997; Pankratz and Foroud, 2004; Hyun et al., 2013; Chan et al., 2017).

The pathological hallmarks of PD are intracellular Lewy bodies (LBs), or Lewy neurites (LNs), consisting of misfolded α-synuclein, and selective degeneration of dopaminergic neurons in the substantia nigra (SN) (Spillantini et al., 1997; A E Lang and Lozano, 1998; Anthony E. Lang and Lozano, 1998). The major component of LBs is accumulated pathological α-synuclein, although it was shown that ubiquitin and neurofilaments are also characteristics of LBs (Tofaris et al., 2003; Kanazawa et al., 2008). Braak and colleagues first observed that the accumulation of α-synuclein in the brain follows a stereotypic pattern. In postmortem PD brain, LBs were first found in the olfactory bulb and the dorsal motor nucleus of the vagal nerve (dmX) prior to motor impairment. It was observed that with disease progression, connected brain areas become affected as well. Braak and colleagues determined six stages for α-synuclein spreading within the brain (Heiko Braak *et al.*, 2003). Aggregated α-synuclein pathology in stage I and II is present in the olfactory bulb and the dmX including connected areas of the lower brainstem. In these two stages patients may suffer from loss of smell, and emotional and sleep disorders. During stage III, LBs propagate into midbrain regions, such as the amygdala and SN. Furthermore, patients may experience thermoregulation disorder. In stage IV, LB pathology reaches the thalamus and the interconnected meso- and allocortex and, thus, initiates the symptomatic phase of PD. At this stage, dopaminergic neurons of the SN are already severely damaged, so that the clinical major symptoms become apparent: bradykinesia, resting tremor, rigidity, and instability. In stage V and VI, the neocortex and the frontal lobe is

invaded, resulting in Lewy pathology throughout all motor and sensory brain regions. At the ultimate stage, patients suffer from psychiatric symptoms, visual hallucinations and dementia, in addition to the clinical motor symptoms (Heiko Braak *et al.*, 2003; Goedert, Clavaguera and Tolnay, 2010; Goedert *et al.*, 2014; Braak and Del Tredici, 2016). Most of the previously mentioned symptoms in PD may be explained by a loss of dopamine signaling due to synaptic dysfunction and loss of dopaminergic neurons (Jankovic, 2008). These characteristic motor symptoms are classically treated with dopamine replacement therapy, where L-3,4-dihydroxy-L-phenylalanine (L-DOPA), the precursor of dopamine, compensates the lack of dopamine within the brain (Abbott, 2010; Bastide *et al.*, 2015).

1.2 Native α-synuclein

The protein was named α-synuclein after its location in the presynaptic terminals in the electric organ of the electric ray *Torpedo californica* (Maroteaux, Campanelli and Scheller, 1988). Shortly after identification of α-synuclein, two additional members of the synuclein family were discovered: β-synuclein and γ-synuclein (Nakajo *et al.*, 1993; Jakes, Spillantini and Goedert, 1994; Lavedan *et al.*, 1998). Native α-synuclein is only present in vertebrates (George, 2002) and is mainly expressed in the brain (Jakes, Spillantini and Goedert, 1994; Iwai *et al.*, 1995). Although the cellular function of α-synuclein remains unclear, its affinity for synaptic vesicles (Maroteaux, Campanelli and Scheller, 1988; Kahle *et al.*, 2000), synapsin III (Zaltieri *et al.*, 2015), and the SNARE-protein synaptobrevin-2 (Burré *et al.*, 2010; Burré, Sharma and Südhof, 2014; Lou *et al.*, 2017) indicates an involvement in membrane-associated vesicle trafficking via the SNARE complex.

α-Synuclein is a 140 amino acid long cellular protein, encoded by the *SCNA* gene that has been mapped to the human chromosome 4q21-q23 (Polymeropoulos *et al.*, 1996). The 140 amino acids of the protein are divided into three major domains. The highly conserved N-terminal domain, which is also the membrane-binding domain, forms an amphipathic α-helix (Davidson *et al.*, 1998; Eliezer *et al.*, 2001; Chandra *et al.*, 2003). This domain consists of the first 60 amino acids and interestingly, also holds the mutation sites for all known missense mutations. The eight mutations A18T, A29S, A30P, E46K, H50Q, G51D, A53E and A53T, are linked to early onset of familial PD (Polymeropoulos *et al.*, 1997; Conway, Harper and Lansbury, 1998; Krüger *et al.*, 1998; Zarranz *et al.*, 2004; Appel-Cresswell *et al.*, 2013; Hoffman-Zacharska *et al.*, 2013; Kiely *et al.*, 2013; Pasanen *et al.*, 2014). The amino acids 61 to 95 form the hydrophobic 'non-amyloid-β component', shortened to 'NAC domain'. This domain holds the ability to form α-synuclein aggregates by changing the conformation from random coil to β-sheets (Ueda *et al.*, 1993). Additionally, it determines the binding affinity to cellular membranes (Fusco *et al.*, 2014). In contrast, the acidic C-terminal domain (amino acids 96-140) is mainly unstructured and therefore counteracts the

NAC aggregation by steric inhibition (Crowther *et al.*, 1998; Davidson *et al.*, 1998; Hoyer *et al.*, 2004). The C-terminal domain also holds various posttranslational modification sites (Uversky and Eliezer, 2009; Oueslati, Fournier and Lashuel, 2010) and a calcium binding site (Nielsen *et al.*, 2001) (Figure 1.1).

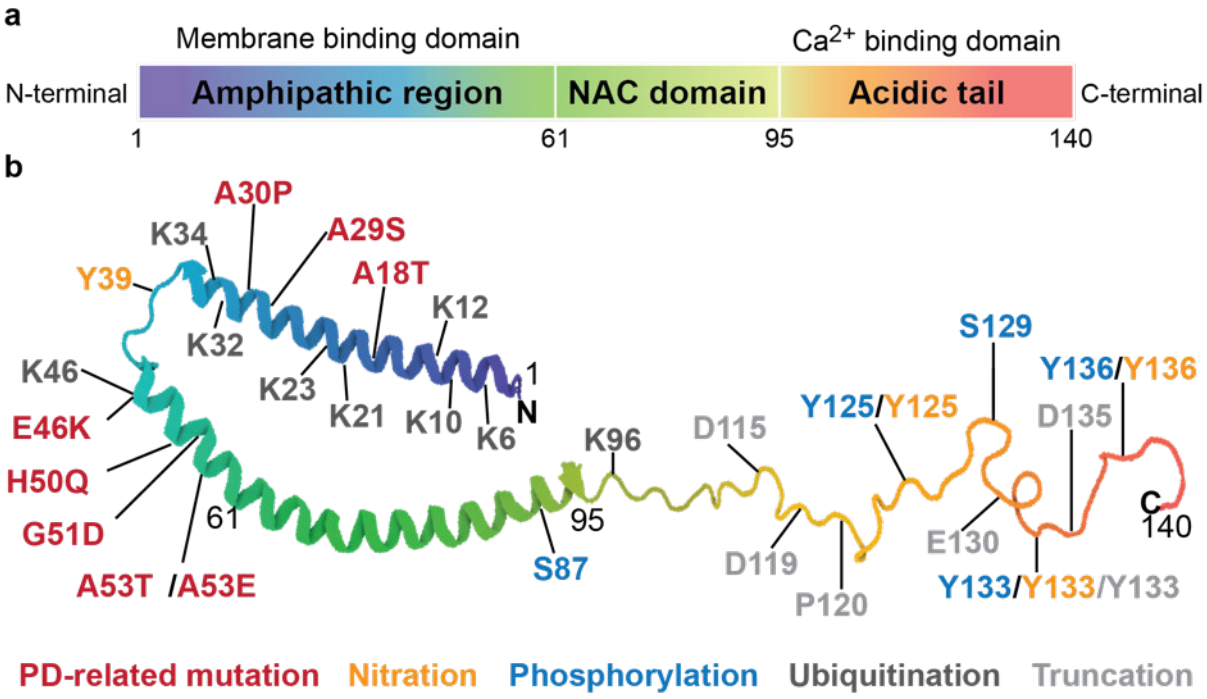

Figure 1.1: Native α-synuclein. α-synuclein consists of 140 amino acids, ranging from the membrane binding N-terminus over the non-amyloid-β component (NAC), to the Ca^{2+}-binding domain at the C-terminal domain (a). The secondary structure of α-synuclein (PDB: 1XQ8), as well as PD-related mutations and posttranslational modifications are presented according to their affected amino acids (b).

1.3 Accumulation of α-synuclein

Under physiological conditions, monomeric α-synuclein is either soluble or membrane bound (Davidson *et al.*, 1998; Eliezer *et al.*, 2001). Upon disease conditions and cellular stress, α-synuclein monomers can spontaneously misfold by undergoing conformational change, and form oligomers. These intermediate oligomers seem to exist in equilibrium with monomeric α-synuclein. Oligomeric α-synuclein acts as a template and recruits endogenous monomeric α-synuclein to self-assemble and form protofilaments, that ultimately accumulate into neurotoxic fibrils. α-Synuclein fibrils are rich in β-sheets and packed in parallel, thus resemble amyloids, the most stable protein configuration (Smith et al., 2006). Insoluble α-synuclein fibrils form inclusions either in the soma of neurons, defined as LBs, or in neuronal neurites, then called Lewy neurites (Figure 1.2) (Spillantini et al., 1997; Lashuel et al., 2002; Cremades et al., 2012; Horvath et al., 2012; Kalia et al., 2013; Tuttle et al., 2016).

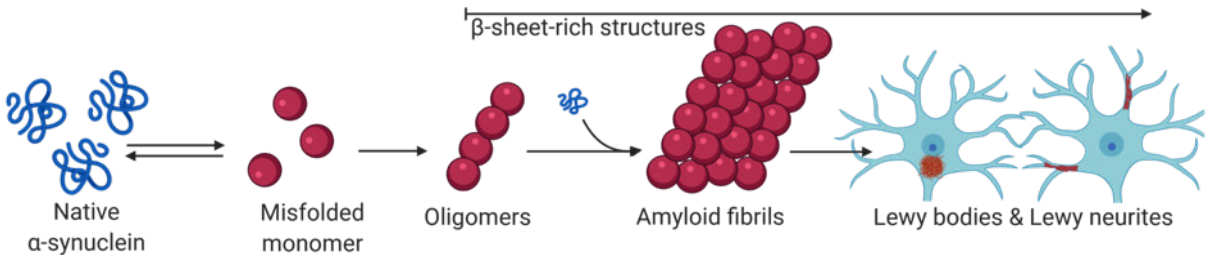

Figure 1.2: α-Synuclein polymerization. Spontaneously misfolding of α-synuclein leads to assembly of β-sheet-rich oligomeric α-synuclein, accumulating into amyloid fibrils, ultimately aggregating into Lewy bodies and Lewy neurites.

1.4 Posttranslational modifications of α-synuclein

There are various posttranslational modifications that affect the physiological function, aggregate formation, and thus neurotoxicity of α-synuclein. Most of these modification sites are located within the N- or C-terminal domain (Uversky and Eliezer, 2009; Oueslati, Fournier and Lashuel, 2010) (residues 1-60 and 96-140; Figure 1.1).

1.4.1 Phosphorylation

Posttranslational phosphorylation is controlled by various kinases, including casein kinase I and II, G protein-coupled receptor kinases, and polo-like kinase 2 (Feany and Bender, 2000; Fujiwara *et al.*, 2002; Inglis *et al.*, 2009; Bergeron *et al.*, 2014). Two common phosphorylation sites are at serine 87 and serine 129, which both can be found in aggregated α-synuclein (Okochi *et al.*, 2000; Fujiwara *et al.*, 2002). Although *Anderson et al.* found that the most dominant posttranslational modification of α-synuclein in LBs is phosphorylation at serine 129 (S129), which is nowadays known as one major hallmark of PD (Anderson *et al.*, 2006; Foulds *et al.*, 2013). In contrast, phosphorylation at tyrosine 125 has no impact on α-synuclein aggregation (Burai *et al.*, 2015), and the effect of phosphorylation at tyrosine 133 and 136 is still unclear (Feany and Bender, 2000; Ellis *et al.*, 2001; Ahn *et al.*, 2002).

1.4.2 Nitration and oxidation

Another posttranslational modification of α-synuclein is nitration, which occurs due to oxidative and nitrative stress and has also been detected in LBs of various synucleinopathies (Duda *et al.*, 2000; Giasson *et al.*, 2000). During this modification, the hydrogen atom at the phenol ring of the tyrosine is replaced by a nitro group to form 3-nitrotyrosine (Chavarría and Souza, 2013). This modification occurs specific at the tyrosine residues Y39, Y125, Y133, and Y136 of α-synuclein (Sevcsik *et al.*, 2011; Burai *et al.*, 2015). All four nitrated monomeric α-synuclein species lead to increased α-synuclein accumulation and therefore, may favor fibril formation (Figure 1.3) (Hodara *et al.*, 2004; Danielson *et al.*, 2009). Additionally, it was shown that increased levels of oxidative stress also lead to increased neuronal spreading of α-synuclein throughout the brain (Musgrove *et al.*, 2019).

1.4.3 Truncation

Posttranslational modification of full-length α-synuclein produces various truncated forms of the protein with molecular masses ranging between 10-15 kDa. These variations are also characteristically found in LBs and LNs (Baba *et al.*, 1998; Crowther *et al.*, 1998; Anderson *et al.*, 2006). Additionally, C-terminally truncated α-synuclein has been shown to increase the accumulation of full-length α-synuclein and, therefore, exhibits a seeding property (Murray *et al.*, 2003; Tofaris *et al.*, 2003; Hoyer *et al.*, 2004).

1.4.4 Ubiquitination and Sumoylation

Gomez-Tortosa and colleagues have shown that α-synuclein is co-localized with ubiquitin in LBs (Kuzuhara *et al.*, 1988; Gómez-Tortosa *et al.*, 2000). Detection of mono-, di-, or tri-ubiquitinated α-synuclein in inclusion bodies suggests that ubiquitination marks pathological changes in α-synuclein, rather than only targeting α-synuclein for turnover by the ubiquitin-proteasome machinery (Hasegawa *et al.*, 2002; Tofaris *et al.*, 2003; Nonaka, Iwatsubo and Hasegawa, 2004; Lee *et al.*, 2008). Ubiquitination of α-synuclein is possible at nine different lysine residues (K6, K10, K12, K21, K23, K32, K34, K46, and K96), where K6, K10 and K12 can also be ubiquitinated post aggregate formation (Nonaka, Iwatsubo and Hasegawa, 2005; Rott *et al.*, 2008). Depending on the side and the length of the ubiquitin chain these modifications can promote fibril formation or α-synuclein degradation (Hejjaoui *et al.*, 2011; Meier *et al.*, 2012; Abeywardana *et al.*, 2013; Haj-Yahya *et al.*, 2013). However, new findings have shown that ubiquitination at K6, K23, or K96 inhibits α-synuclein oligomerization (Moon et al., 2020). Additionally, inhibition of the ubiquitin-proteasome machinery and the autophagy-lysosomal degradation pathway has been shown to induce accumulation of phosphorylated α-synuclein (p-α-synuclein) at S129, suggesting that p-α-synuclein is degraded in a ubiquitin-independent manner (Chau et al., 2009; Machiya et al., 2010). Moreover, α-synuclein is covalently attached to small ubiquitin-related modifier (SUMO) via lysine residues (Dorval and Fraser, 2006). *Rott et al.* have shown that SUMOylation also enhances α-synuclein accumulation by inhibiting the ubiquitin-dependent degradation pathway (Rott *et al.*, 2017).

1.5 Toxicity of α-synuclein

1.5.1 Cellular stress

Posttranslational modifications and consequent oligomerization of α-synuclein play a key role in mitochondrial dysfunction. It has been shown that α-synuclein oligomers cause mitochondrial-associated membrane dysfunction, leading to inhibition of mitochondrial complexes, permeabilization of mitochondrial-like membranes, and increased mitochondrial fragmentation (Guardia-Laguarta et al., 2014; Plotegher, Gratton and Bubacco, 2014; Stefanovic et al., 2014; Subramaniam et al., 2014). Various α-synuclein missense mutations have a specific impact on mitochondrial damage. The H50Q mutation for example, leads to oligomerization and mitochondrial

fragmentation in hippocampal neurons (Appel-Cresswell et al., 2013; Khalaf et al., 2014), and the A53T mutation, along with phosphorylated α-synuclein at S129, leads to increased intracellular reactive oxygen species (ROS) levels resulting in enhanced mitochondrial fragmentation (Perfeito et al., 2014). Monomeric and oligomeric α-synuclein can also inhibit the mitochondrial protein import machinery by binding to the outer membrane (TOM) 20 receptor, additionally resulting in increased ROS production and loss of mitochondrial membrane potential (Rostovtseva et al., 2015; Di Maio et al., 2016).

Due to its membrane-binding ability, α-synuclein is directly interacting with synaptic vesicles and the membrane of the endoplasmic reticulum (ER) and the golgi apparatus. Overexpression of α-synuclein causes golgi fragmentation, leading to altered synaptic vesicle release and intracellular protein trafficking by rupture of synaptic vesicles, resulting in decreased neurotransmitter release (Gosavi *et al.*, 2002). It has been shown that 90% of aggregated α-synuclein is not located in LBs but in the neuronal presynapse, where it causes synaptic dysfunction (Kramer and Schulz-Schaeffer, 2007; Schulz-Schaeffer, 2010). Binding of oligomeric α-synuclein to several N-terminal domains of synaptobrevin induces vesicle clustering, limits synaptobrevin in the synapse, and thereby prevents SNARE complex formation and exocytosis. Thus, aggregated α-synuclein may also inhibit dopamine release, resulting in the common symptoms of synucleinopathies (Nemani *et al.*, 2010; Choi *et al.*, 2013).

Oligomeric α-synuclein also affects the axonal transport machinery by reducing microtubule stability, neuritic kinesin, and their dependent cargo transport, preventing microtubule assembly (Chen *et al.*, 2007; Zhou *et al.*, 2010; Prots *et al.*, 2013). Overexpression of α-synuclein also affects cellular Ca^{2+} influx, potentially by a pore-forming mechanism in a structure-specific manner, ultimately resulting in Ca^{2+}-dependent cell death (Danzer *et al.*, 2007; Angelova *et al.*, 2016; Ysselstein *et al.*, 2017). Destabilized Ca^{2+} homeostasis, golgi fragmentation, and synaptic dysfunction induces ER stress, promotes the activation of the unfolded protein response and, therefore, ultimately leads to cell death (Figure 1.3) (Conn *et al.*, 2004; Silva *et al.*, 2005; Smith *et al.*, 2005; Hoozemans *et al.*, 2007; Colla *et al.*, 2012; Heman-Ackah *et al.*, 2017).

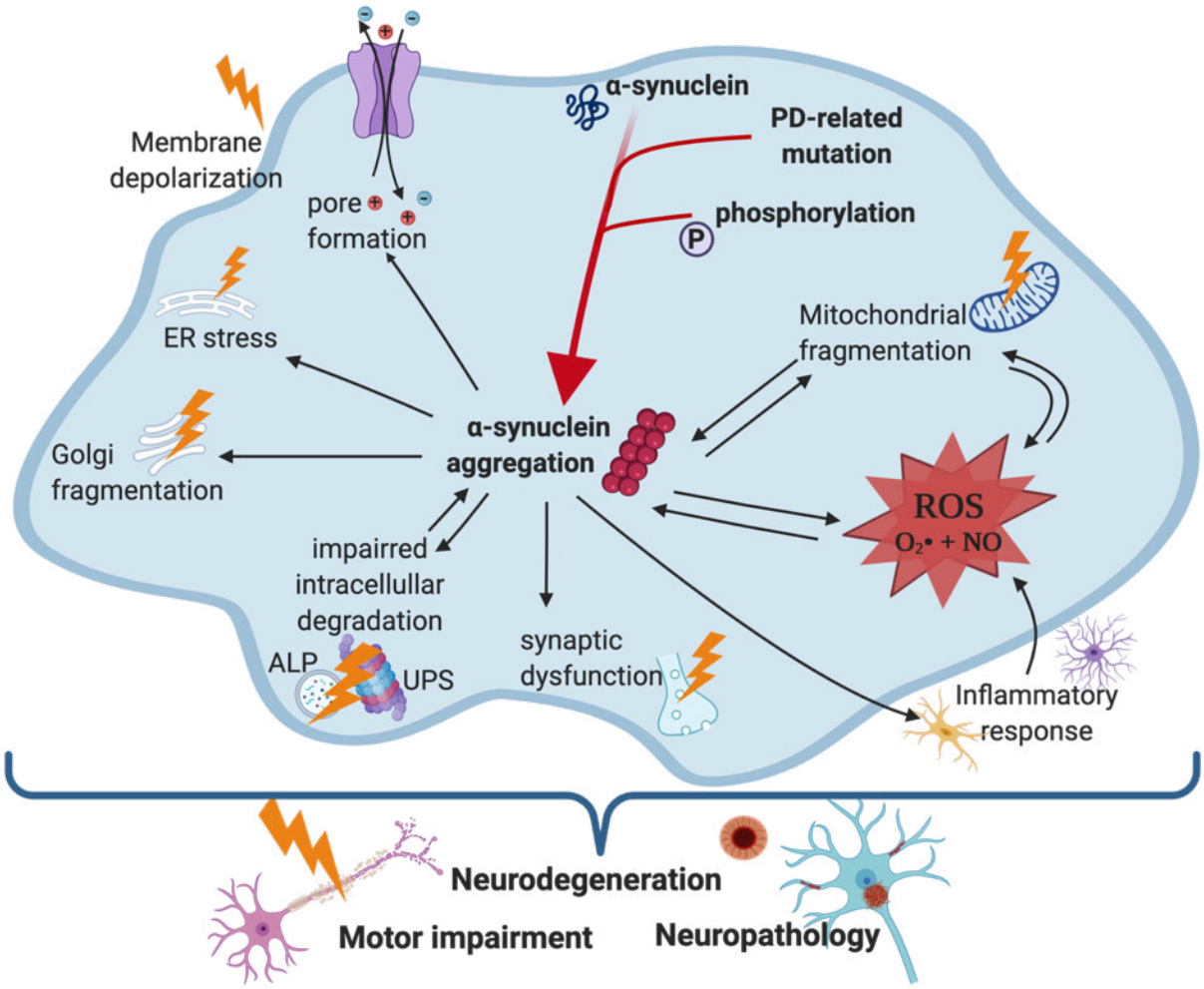

Figure 1.3: Effects on α-synuclein aggregation and toxicity of pathological α-synuclein. Aggregation of α-synuclein leads to endoplasmic reticulum (ER) stress, golgi fragmentation, synaptic dysfunction, membrane depolarization by a pore forming mechanism, and impaired intracellular degradation via the ubiquitin-proteasome system (UPS) and the autophagy-lysosome pathway (ALP), which in turn leads to enhanced accumulation of α-synuclein. Reactive oxygen species (ROS) are generated by α-synuclein aggregates, inclusions also cause mitochondrial fragmentation and induce neuroinflammation, both of which lead to additional ROS, resulting in increased α-synuclein aggregation. Ultimately, α-synuclein aggregation leads to neuropathology, causing neurodegeneration and motor impairment.

1.5.2 Loss of dopaminergic neurons

There are various cellular toxicity mechanisms following α-synuclein overexpression which cause damage to vulnerable neurons in different brain areas, such as the dorsal motor nucleus of the vagus, the putamen, and especially the substantia nigra pars compacta (Hirsch, 1994; Dickson, 2007; Sulzer and Surmeier, 2013). However, the most vulnerable neurons to be affected are dopaminergic neurons in the SN (Hirsch, Graybiel and Agid, 1988; Petrucelli *et al.*, 2002; Chung *et al.*, 2005). Toxicity of α-synuclein to dopaminergic neurons was shown in different models, ranging from *Drosophila, C. elegans*, rodents to different cell culture models, as well as in PD patients (Feany and Bender, 2000; Masliah *et al.*, 2000a; Zhou *et al.*, 2000; Lee *et al.*, 2002; Lakso *et al.*, 2003; Lin and Khoshbouei, 2019; Hoban *et al.*, 2020). Additionally, it has been shown that α-synuclein directly interacts with dopamine. Also, it negatively

regulates dopamine synthesis by binding to tyrosine hydroxylase (TH) and reducing its enzymatic activity. Thus, overexpression of α-synuclein reduces the conversion of L-tyrosine to L-DOPA catalyzed by TH (Abeliovich *et al.*, 2000; Perez *et al.*, 2002; Herrera *et al.*, 2008). Dopamine may also induce α-synuclein oligomerization via increased oxidative stress through dopamine oxidation (Fahn and Cohen, 1992; Lee *et al.*, 2011). Overexpression of α-synuclein and the degeneration of dopaminergic neurons in the SN ultimately results in dopamine loss in the basal ganglia. Thus, projecting to the striatum and motor cortex, brain areas responsible for motor behavior and movement, causing the characteristic motor symptoms of PD (Figure 1.3) (Hirsch, Graybiel and Agid, 1988; Michel, Hirsch and Hunot, 2016).

1.5.3 Protein degradation

There are currently two protein degradation pathways known that control the quality of cellular components and therefore, preserve cell homeostasis. One is the ubiquitin-proteasome system (UPS), which degrades short-lived proteins in the cytoplasm and the nucleus, and the other is the autophagy-lysosome pathway (ALP), which degrades long-lived proteins and abnormal cell organelles in the cytoplasm (Ciechanover, 2006). α-Synuclein can be tagged for degradation via the UPS by poly-ubiquitination, which also enables degradation via the ALP by noncovalently binding to the ubiquitin-binding protein p62/sequestome-1 (Webb *et al.*, 2003; Ebrahimi-Fakhari *et al.*, 2011). This protein works as a cargo receptor for autophagy, as it selectively interacts with LC3 on the phagophore membrane (Lamark *et al.*, 2009). Proteasomes efficiently degrade wild-type (WT) α-synuclein but fail to do so when α-synuclein is aggregated, as it cannot be entirely unfolded to fit into the narrow 20S core of the proteasome. Macroautophagy is more efficient in degrading α-synuclein aggregates (Ravikumar, Duden and Rubinsztein, 2002; Taylor, Hardy and Fischbeck, 2002). It has also been shown that WT α-synuclein is selectively recognized and translocated into lysosomes via the chaperone-mediated autophagy pathway. In contrast, the pathological α-synuclein A53T and A30P mutants bind to the LAMP2A receptor on lysosomes, where they inhibit their own uptake and degradation and that of other proteins (Cuervo *et al.*, 2004). Inhibition of autophagy ultimately leads to formation of inclusion bodies due to failure of the clearance mechanism and, therefore, promotes α-synuclein accumulation (Figure 1.3). These inclusion bodies are ubiquitinated for delivery to the UPS, but also bound to p62/sequestome-1 for p62-dependent autophagy (Rideout, Lang-Rollin and Stefanis, 2004; Rubinsztein, 2006). Thus, ubiquitin and p62 are used as markers for pathological α-synuclein aggregates resembling LBs (Kuusisto, Parkkinen and Alafuzoff, 2003; Kuusisto, Kauppinen and Alafuzoff, 2008).

1.5.4 Neuroinflammation

Neurodegenerative diseases are associated with neuroinflammation, characterized by microgliosis and astrogliosis (Hirsch and Hunot, 2009). Inflammation is induced upon overexpression or posttranslational modification of α-synuclein leading to neurotoxicity

of the altered protein. Intracellular Ca^{2+} influx, ROS, mitochondrial stress, ER stress, and activation of the unfolded protein response initiate the proinflammatory response via the NF-κB and JNK signaling pathways (Figure 1.3) (Klegeris *et al.*, 2008; Prabhakaran, Chapman and Gunasekar, 2011; Kim *et al.*, 2013).

Microglia are the tissue resident macrophages and the main immune cells in the CNS, maintaining homeostasis of the microenvironment by chemotaxis, phagocytosis, and secretion of various inflammatory mediators (Aschoff, 1924; Ransohoff and Cardona, 2010; Tremblay *et al.*, 2011). Upon brain injury, motile microglia get activated and produce specific cytokines that recruit additional immune cells, migrate to the injury, and extend their processes towards the lesion to isolate the injured tissue and maintain the microenvironment (McGeer *et al.*, 1987; Szalay *et al.*, 2016). During the inflammatory response inactivated, ramified microglia transform into amoeboid and active microglia (Davalos *et al.*, 2005; Nimmerjahn, Kirchhoff and Helmchen, 2005; Hines *et al.*, 2009; Stirling *et al.*, 2014). Microgliosis is induced in PD, as microglia activation has been detected in brain samples of PD patients and various animal models of PD, where microgliosis in the SN can even be detected before dopaminergic cells die (McGeer *et al.*, 1988; Ouchi *et al.*, 2005; Duffy *et al.*, 2018; Ferreira and Romero-Ramos, 2018). Extracellular α-synuclein promotes microglial activation via the NF-κB pathway, acts as an endogenous agonist for toll-like receptor 2, and may be a chemoattractant promoting microglial migration (Park *et al.*, 2008; Kim *et al.*, 2013; Wang *et al.*, 2015; Yun *et al.*, 2018).

Astrocytes are the most abundant glia cells in the brain and actively communicate with microglia, oligodendrocytes, other glia cells, and neurons. In addition, astrocytes maintain the homeostasis of the microenvironment in the brain, regulate synaptic transmission, control permeability of the blood-brain barrier and the homeostasis of water and ions, as well as the secretion of neurotrophins (Lee *et al.*, 2003; Sofroniew and Vinters, 2010; Allaman, Bélanger and Magistretti, 2011; Wilton, Dissing-Olesen and Stevens, 2019). After an immune response is induced by microglia, astrocytes become activated and build a barrier around the injury by surrounding the tissue and removing ions and neurotransmitters released from injured cells (Sofroniew and Vinters, 2010; Jeong *et al.*, 2014). Upon ROS detection, astrogliosis is directly induced to protect neurons from oxidative stress and to inhibit an excessive inflammatory response by regulating microgliosis (Tsacopoulos and Magistretti, 1996; Yang, Min and Joe, 2007; Kim *et al.*, 2010; Park *et al.*, 2012). Although α-synuclein is expressed in small amounts in astrocytes, they take up α-synuclein released from neurons in a toll-like receptor 4-independent way and induce neuroinflammation (Fellner *et al.*, 2013; Rannikko, Weber and Kahle, 2015). In postmortem PD tissue, α-synuclein accumulations have not only been found in neurons but also in astrocytes, suggesting that they play a role in the degradation of pathological α-synuclein to maintain a healthy microenvironment (Wakabayashi *et al.*, 2000; Lee *et al.*, 2010; Zhang *et al.*, 2016).

1.6 Transmission of α-synuclein

1.6.1 Cell-to-cell transmission

Cellular transmission of aggregated α-synuclein to neighboring neurons via different routes was shown in cell culture and mouse models. Oligomeric α-synuclein may be released by the donor neuron to the extracellular space from where it can enter a recipient neuron either by clathrin-mediated endocytosis (Figure 1.4, 1), direct diffusion through the plasma membrane (Figure 1.4, 2), or receptor-mediated endocytosis as seen after binding to lymphocyte-activation gene 3 (Figure 1.4, 3) (Desplats *et al.*, 2009; Abounit *et al.*, 2016; Mao *et al.*, 2016; Oh *et al.*, 2016). Additionally, membrane-bound exocytosis in an ATP13A2/PARK9, Rab11, and Ca^{2+}-dependent manner (Figure 1.4, 4), and lysosomal-vesicle trafficking through tunneling nanotubes (Figure 1.4, 5) have also been suggested as possible routes in the cell-to-cell propagation of α-synuclein (Figure 1.4) (Emmanouilidou *et al.*, 2010; Danzer *et al.*, 2012; Chutna *et al.*, 2014; Tsunemi, Hamada and Krainc, 2014). Upon uptake of oligomeric α-synuclein by a recipient neuron, endogenous monomeric α-synuclein is recruited to form larger α-synuclein aggregates and fibrils leading to Lewy pathology and neuronal death (Luk *et al.*, 2009; Volpicelli-Daley *et al.*, 2011).

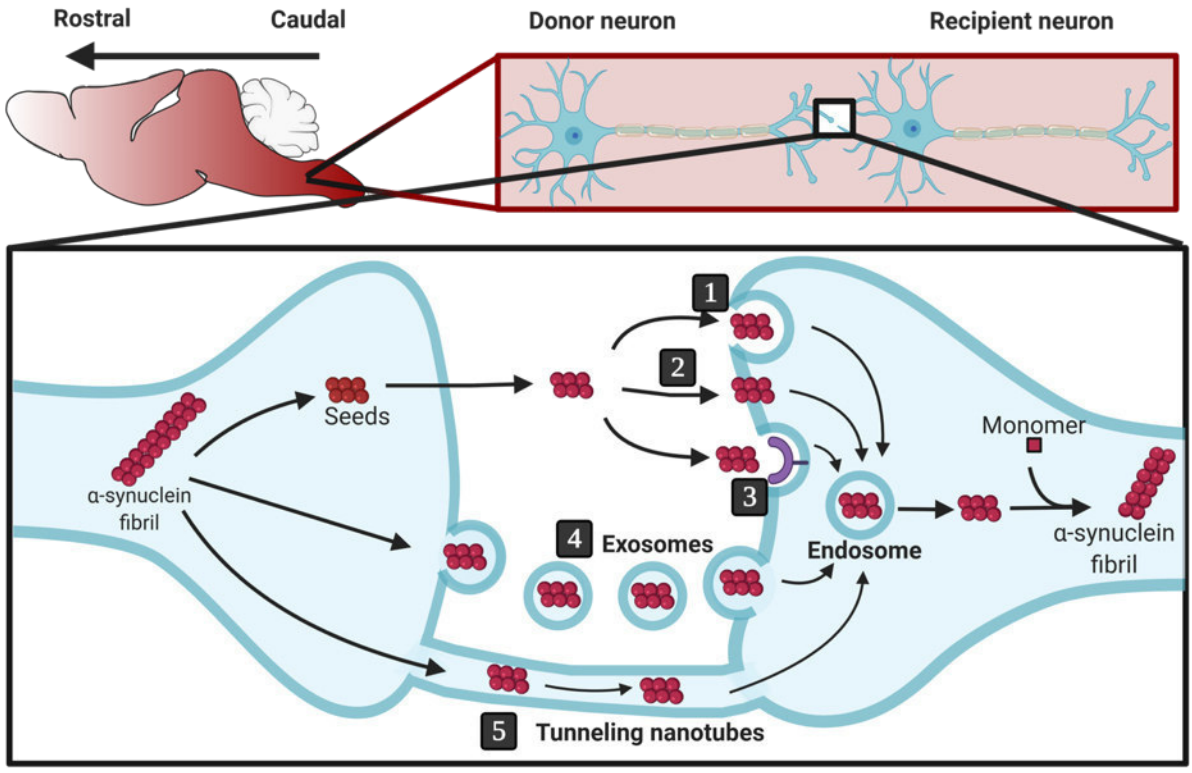

Figure 1.4: Transmission mechanism from donor neuron to recipient neuron of α-synuclein, in a caudal-to-rostral manner. Cellular transmission of oligomeric α-synuclein via endocytosis (1), diffusion (2), receptor-mediated endocytosis (3), membrane-bound exocytosis (4), or nanotubes connecting neurons (5). Based on Guo and Lee, 2014.

1.6.2 Spreading within the nervous systems

It has been shown that pathological α-synuclein spreads in a caudo-rostral manner within the brain but also spreads from the periphery to the brain (Masuda-Suzukake *et al.*, 2013; Ulusoy *et al.*, 2013; Holmqvist *et al.*, 2014; Bernis *et al.*, 2015). Preformed α-synuclein fibrils injected intraperitoneally, intramuscularly, or into the gastrointestinal tract can trans-synaptically spread into the brain via the vagus nerve and initiate LB pathology (Sacino, Brooks, Thomas, McKinney, Lee, *et al.*, 2014; Breid *et al.*, 2016; Uemura *et al.*, 2018; Kim *et al.*, 2019). Recent evidence demonstrates that pathological α-synuclein can even spread bidirectionally between connected areas throughout the peripheral nervous system (PNS), the enteric nervous system (ENS), and the CNS (Van Den Berge *et al.*, 2019a).

1.7 Prion-like behavior

Within the last decades, misfolded α-synuclein was discussed to show some prion-like behavior. Prions (PrP^{SC}) are β-sheet rich, infectious conformers of the native cellular prion protein (PrP^{C}), which only have little β-sheet structure, and promote self-polymerization by structural conversion of PrP^{C} into PrP^{SC} (Prusiner, 1991). The accumulation and propagation of PrP^{SC} ultimately causes transmissible spongiform encephalopathies, such as bovine spongiform encephalopathy (BSE) in cattle, chronic wasting disease (CWD) in deer and elk, and Creutzfeldt-Jakob disease (CJD) in humans (Prusiner, 1998; Tamgüney *et al.*, 2009). Prions have been classified into strains regarding the induced neuropathology and clinical outcome, as different strains and their conformations cause different diseases (Collinge and Clarke, 2007). Some prion strains can be transmitted across organisms and even via different routes and result in CNS disease, such as after intracerebral, intraperitoneal, intramuscular injection, and intravenous injection, blood transfusion, or oral uptake. Such a case was discovered for BSE prions from diseased cattle, which caused variant CJD in human after oral uptake (Hill *et al.*, 1997; Aguzzi and Polymenidou, 2004; Mabbott, 2017). So far, prion diseases are the only protein misfolding diseases known to be transmissible between and to humans.

However, there is growing evidence of parallels between prion diseases and other protein-misfolding diseases. Pathological α-synuclein strains have been shown to cause specific forms of disease in animal models, based on the mutation site, without altering characteristics, even after repeated passaging between different animal models (Woerman *et al.*, 2017, 2019). Moreover, caudal-to-rostral trans-synaptic propagation of α-synuclein, along with Braak's hypothesis (1.1) show that aggregated α-synuclein spreads throughout the whole CNS in a stereotypic, and therefore, prion-like manner, ultimately causing neurodegenerative disease (Kordower *et al.*, 2008; Masuda-Suzukake *et al.*, 2013; Peelaerts *et al.*, 2018). However, the exact molecular

mechanisms that trigger misfolding, fibrillization, LB formation, cell-to-cell transmission, and spreading of α-synuclein are poorly understood.

1.8 Stroke as a neurodegenerative condition

1.8.1 Stroke

Stroke is the second most common cause of death after heart disease causing 9% of all fatalities worldwide, and even silent strokes without any immediate clinical manifestation are observed in up to 28% of the population (Mozaffarian et al., 2016). Approximately 85% of all stroke cases are ischemic, and are associated with a risk that increases with age, as 18% of individuals over 45 years of age have already experienced symptoms of stroke (Howard et al., 2006). Other major risk factors are hypertension, sleep apnea, hyperlipidemia, diabetes mellitus, antithrombotic therapy, and tobacco and alcohol consumption (Guzik and Bushnell, 2017). Ischemic stroke with a cerebral blood flow threshold below 12 mL/min/100 g leads to oxygen deprivation in the tissue and loss of physiological cell functions, resulting in permanent tissue damage within seconds (Zaidat et al., 2012).

On a molecular basis, ischemia induces a cascade of events in the ischemic core leading to glutamate release, Ca^{2+}-influx, imbalance of membrane homeostasis, oxidative stress, ER stress, mitochondrial dysfunction, cytochrome c release, activation of caspases, and inflammatory responses. Ultimately, ischemic stroke results in neuronal death comprising apoptosis, autophagy, and necrosis. Reperfusion, the reoxygenation of the tissue after ischemia, leads to free radical formation, and, therefore, enhances the ischemic effects by causing an increase of reactive oxygen and nitrogen species. Upon reperfusion, the secondary neuronal injury also triggers inflammation and neuronal changes in brain regions connected to the ischemic core (Figure 1.5) (Lipton, 1999; Lo, Dalkara and Moskowitz, 2003; Sen *et al.*, 2009; Xing *et al.*, 2012; Lopez, Dempsey and Vemuganti, 2015; Zhao *et al.*, 2016a). Additionally, molecular mechanisms of ischemia-reperfusion are known to promote brain damage in chronic neurodegenerative disorders such as Alzheimer's disease (Qiu et al., 2010).

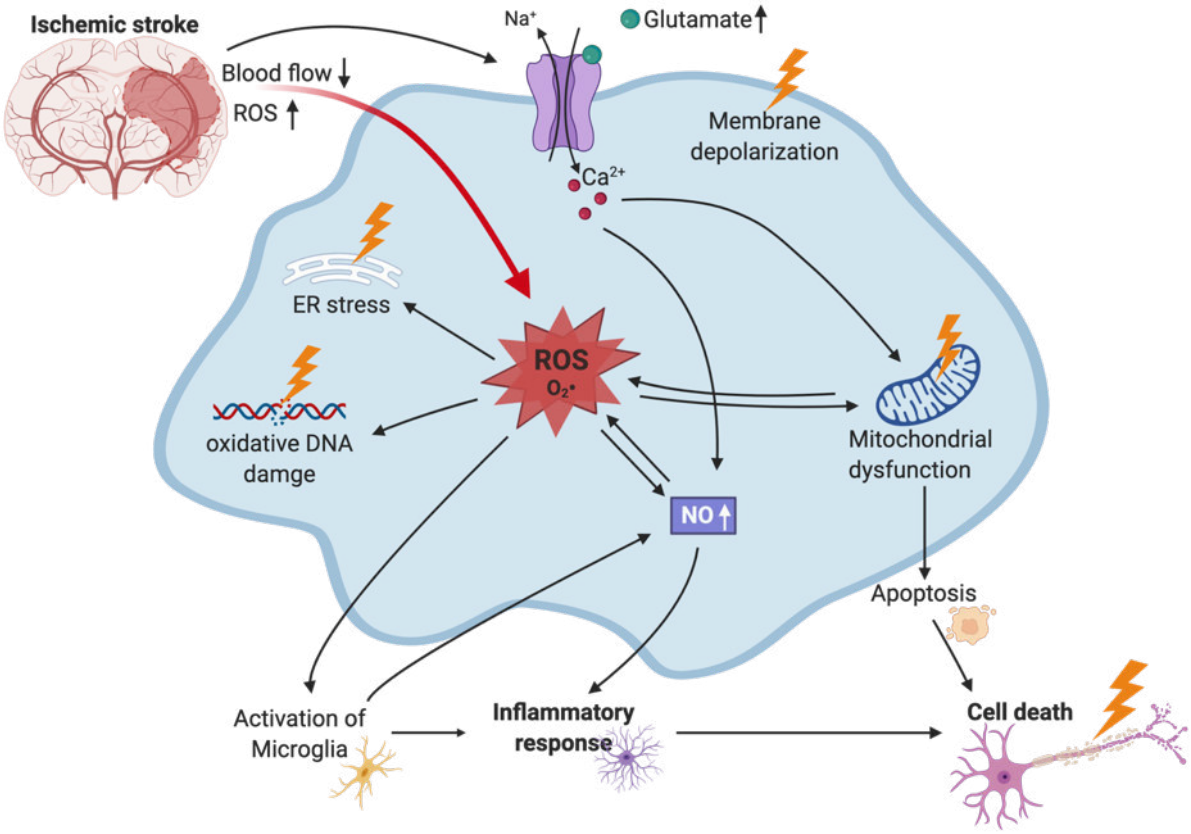

Figure 1.5: Pathological processes upon ischemic stroke. Cerebral ischemic cascades generate reactive oxygen species (ROS) causing endoplasmic reticulum (ER) stress, oxidative DNA damage, and increased nitric oxide (NO) levels, which trigger inflammatory responses and ultimately cell death. Additionally, Ca^{2+}-influx causes membrane depolarization and mitochondrial dysfunction and results in mitochondrial-dependent apoptosis and cell death.

1.8.2 Stroke in Parkinson's disease

Interestingly, the cellular responses in post-stroke tissue, including oxidative stress, ER stress, and mitochondrial dysfunction, seem to be similar to those that mediate the pathophysiological mechanisms causing α-synuclein aggregation and therefore, toxicity in PD (Figure 1.3 & Figure 1.5). Previous epidemiological studies reported an increased risk of PD after a stroke but also an increased risk of having a stroke after a PD diagnosis (Becker, Jick and Meier, 2010; Garcia-Gracia *et al.*, 2013; Huang *et al.*, 2019; Kummer *et al.*, 2019). In animal models of cerebral ischemia, it has been shown that neuronal death and inflammation not only occur in the striatum, where the ischemic core is localized, but also in the interconnected SN (Block, Dihné and Loos, 2005; Rodriguez-Grande *et al.*, 2013). Studies observed an increased level of α-synuclein in the ischemic core within the first hours up to 7 days of reperfusion (Hu *et al.*, 2006; Unal-Cevik *et al.*, 2011; Rodriguez-Grande *et al.*, 2013; T. H. Kim *et al.*, 2016). However, additional studies are needed to identify if ischemic stroke can cause α-synuclein aggregation and subsequently idiopathic PD.

1.9 Mouse models of Parkinson's disease

Mouse models of PD are either based on local or systemic transmission of neurotoxins or α-synuclein fibrils, or on transgenic mouse lines, or a combination of both. These models replicate most pathological features of PD, such as neurodegeneration and neuroinflammation, accompanied by severe PD-like motor symptoms.

1.9.1 Toxin-induced mouse models

In mice, PD-like disorders can be induced by transmission of neurotoxins or other chemical compounds, leading to a better understanding of the pathophysiology. For example, 1-methyl-4-phenyl-1,2,3,6-tetrahydropyridine (MPTP) systemic intoxication results in severe neurodegeneration in the SN, and development of the characteristic PD locomotor impairments without LB formation (Chiueh *et al.*, 1984; Langston *et al.*, 1999). Intracerebral injection of the neurotoxin 6-hydroxy-dopamine (6-OHDA) induces loss of nigrostriatal dopamine and dopaminergic neurons, motor behavioral abnormalities, and neuroinflammation, however, lacking α-synuclein accumulation (Ungerstedt, 1971; Perese *et al.*, 1989). The intoxication-model using the pesticide rotenone leads to parkinsonism, loss of nigrostriatal dopamine and dopaminergic neurons, and loss of myenteric neurons. Additionally, upon rotenone administration, inclusion bodies are observed, morphologically resembling LBs, as they are immune-positive for α-synuclein and ubiquitin (Betarbet *et al.*, 2000; Sherer *et al.*, 2003; Drolet *et al.*, 2009). Systemic administration with 1,1'-dimethyl-4,4'-bipyridinium (paraquat) also induces loss of dopaminergic neurons and dopamine in nigrostriatal regions, resulting in PD-like motor impairment. Chronic exposure to paraquat leads to an accumulation of α-synuclein-like aggregates in the SN and reduced expression of some nicotinic acetylcholine receptor subunits, resulting in an even more reduced dopamine release in the striatum (Brooks et al., 1999; Manning-Bog et al., 2002; O'Leary et al., 2008). All these intoxication models result in loss of dopaminergic neurons and motor impairment, typical for PD, however, most of them fail to mimic the important aggregation and spreading of α-synuclein in PD.

1.9.2 Genetic mouse models of PD

Synucleinopathies can be mimicked by transgenic mouse models overexpressing α-synuclein, or by induced overexpression, which can be achieved by using viral vectors driving the expression of WT or mutant α-synuclein. Injected adeno-associated virus vectors enhance nigral α-synuclein expression, leading to α-synuclein accumulation in the SN, loss of dopaminergic neurons, and thus to PD-like locomotor dysfunction (Koprich *et al.*, 2010; Dimant *et al.*, 2014; Peelaerts *et al.*, 2015a; Van der Perren *et al.*, 2015). Other well-known models showing PD-like phenotypes and the typical prion-like behavior are, for instance, transgenic (Tg) mouse lines overexpressing human WT, A53T, or A30P mutant α-synuclein under the murine prion promotor (PrP). PrP-driven expression of α-synuclein results in high expression levels in the brain and spinal cord but also in slightly elevated expression levels throughout

other tissues. Pathology in Tg mice causes synucleinopathies, and thus supports α-synuclein self-assembly and a toxic gain-of-function for aggregated α-synuclein (Giasson *et al.*, 2002; Lee *et al.*, 2002). Mice overexpressing α-synuclein suffer from ER stress, oxidative stress, and mitochondrial dysfunction, leading to activation of cell death pathways and ultimately resulting in LB pathology, neurodegeneration, and behavioral impairment. Thus, Tg mice represent the rapid onset of cellular mechanisms and symptoms that are present in familial PD, due to multiplications of the *SNCA* gene or specific missense mutation (Kirik *et al.*, 2002; Lo Bianco *et al.*, 2002; Singleton *et al.*, 2003; Farrer *et al.*, 2004; Ibáñez *et al.*, 2004). Synucleinopathy models based on inoculation with preformed α-synuclein fibrils help to investigate the prion-like spreading of α-synuclein, as these models are not limited to the brain and, thus, useful to investigate propagation from the periphery to the brain and vice versa (Holmqvist *et al.*, 2014; Breid *et al.*, 2016; Van Den Berge *et al.*, 2019a).

1.10 Aim

The first objective of this work was to investigate whether accumulated α-synuclein aggregates can neuroinvade the CNS from the periphery after intravenous or oral challenge and cause neurological disease. To this aim, a transgenic mouse model overexpressing the A53T mutant of human α-synuclein was challenged intravenously or orally with recombinant fibrils of human α-synuclein. Transmission via these two routes was compared with transmission after intracerebral and intraperitoneal challenge, to address the questions:

i. Are α-synuclein aggregates able to cross the brain-blood barrier and cause CNS disease after a single intravenous injection?
ii. Are α-synuclein aggregates able to cross the gastrointestinal wall and invade the CNS to cause neuropathology after a single oral transmission?

The second aim of this work was to identify the impact of ischemic stroke on α-synuclein aggregation and central neuroinvasion as a potential cause for synucleinopathies. The long-term consequences of an ischemic stroke on α-synuclein aggregation and the survival of dopaminergic neurons but also potential clearing mechanism via neuroinflammation should be investigated. To address these questions, a focal ischemia by middle cerebral artery occlusion (MCAO) was induced in transgenic mice, overexpressing the A53T mutant of human α-synuclein, which were subsequently examined over a period of 360 days for behavioral impairment, neuroinflammation, neurodegeneration, and α-synuclein aggregation.

2 Material and Methods

2.1 Material

Chemicals were purchased from Life Technologies (Carlsbad, USA), Roth (Karlsruhe, Germany), Sigma-Aldrich (St. Louis, USA), or Thermo Fischer Scientific (Waltham, USA), unless stated otherwise. All purchased chemicals were either classified as 'for research only' or "suitable for molecular biology" and fulfilled analytical quality grade. Consumables were purchased from BD Bioscience (Heidelberg, Germany), Eppendorf (Hamburg, Germany), Greiner Bio-One (Kremsmünster, Austria), Th. Geyer (Renningen, Germany), or VWR (Radnor, USA). Microscopic slides and coverslips were purchased from Thermo Fisher Scientific (Waltham, USA) and surgical instruments were purchased from Fine Science Tools (Foster City, USA).

Table 1: Buffers and solutions used

Buffer	Composition	
Blocking buffer	20% (v/v) 1% (v/v) 0.5% (v/v) 1×	Normal goat serum BSA Triton X-100 PBS
Citric buffer (CB)	9 mL 41 mL 450 mL	M Citric acid 0.1 M Sodium citrate dehydrate dH_2O
Copper (II) sulfate $CuSO_4$ solution	10 mM 50 mM	$CuSO_4$ Ammonium Acetate dH_2O pH 5
Paraformaldehyde (PFA) 0,4%	0,4% (w/v) 1×	Paraformaldehyde TBS pH 7.4
Primary antibody mix	1% (v/v) 1% (v/v) 0.25% (v/v) 1×	Normal goat serum BSA Triton X-100 PBS
Secondary antibody mix	1% (v/v) 1% (v/v) 1×	Normal goat serum BSA PBS
Tris-buffered saline (TBS) 10×	24 g 88 g Up to 1L	Trizma base NaCl dH_2O pH 7.6
TBS + Tween 20 (TBST) 0.05%	0.05% (v/v) 1×	Tween 20 TBS
TD4215	4% (w/v) 2% (v/v) 192 mM 25 mM 5% (w/v)	Sodium dodecyl sulfate (SDS) β-mercaptoethanol Glycine Tris Sucrose
Transfer buffer stock 10×	60.4 g 288 g Up to 2 L	Trizma base Glycin ddH_2O pH 8.6
Transfer buffer	50 mL 50 mL 450 mL	Transfer buffer stock (10X) MeOH dH_2O

Washing buffer, phosphate-buffered saline (PBS) + Triton X-100 (PBST)	0.25% (v/v) 1×	Triton X-100 PBS

Table 2: Summary of kits used

Kits	Company
alpha-Synuclein aggregation kit	Cisbio, Codolet, France
DNeasy Blood & Tissue Kit	Quiagen, Hilden, Germany
ImmPACT DAB, Peroxidase Substrate Kit	Vector Laboratories, Burlingame, USA
LuminocCt qPCR ReadyMix	Sigma, St. Louis, USA
Mouse on Mouse Immunodetection Kit	Vector Laboratories, Burlingame, USA
Mouse SNCα (Synuclein Alpha) ELISA kit	Elabscience, Houston, USA
Pierce BSA Protein Assay Kit	Thermo Fisher Scientific, Waltham, USA
SensoLyte α-Synuclein (human) ELISA Kit	AnaSpec, Fremont, USA
Vectastain Elite ABC HRP Kit	Vector Laboratories, Burlingame, USA

Table 3: Summary of primers used with their sequences

Primer	Description	Primer sequence [5' to 3']
oIMR1544	internal positive control fwd	CACGTGGGCTCCAGCATT
oIMR3580	internal positive control rev	TCACCAGTCATTTCTGCCTTTG
oIMR1770	Tg fwd	TGACGGGTGTGACAGCAGTAG
oIMR1771	Tg rev	CAGTGGCTGCTGCAATG
TmoIMR0025	Tg probe	[6FAM]CCCTGCTCCCTCCACTGTCTTCTGG[BHQ1]
TmoIMR0105	internal ctrl probe	[Cyanine5]CCAATGGTCGGGCACTGCTCAA[BHQ3]

Primary antibodies (Table 4) and secondary antibodies (Table 5) used in this thesis, their application and the corresponding concentrations are listed below.

Table 4: Primary antibodies and their dilution

Target (alternative name) [antibody clone]	Reference	Host	Dilution (IF/IHC)	Antigen Retrieval	Dilution (WB)
alpha-Synuclein [Syn211]	36-008, Merck Millipore	Mouse	1:20,000	Formic acid	
alpha-Synuclein (fibrillar) [Syn-F1]	847802, Biolegend	Mouse	1:500	CB	
alpha-Synuclein (oligomeric and fibrillar) [Syn-O2]	847602, Biolegend	Mouse	1:500	CB	
alpha-Synuclein (phospho S129) [EP1536Y]	AB51253, Abcam	Rabbit	1:200	CB	1:1,000

alpha-Synuclein (phospho S129) [pSyn#64]	015-25191, Wako	Mouse	1:1,200	CB	
alpha-Synuclein (phospho S129) [pSyn#64], biotin-conjugated	010-26481, Wako	Mouse	1:1,000	CB	
GAPDH	ab226408, Abcam				1:1,000
Glial fibrillary acidic protein (GFAP)	Z0334, Dako	Rabbit	1:500	CB	
Ionized calcium binding adaptor molecule 1 (Iba1)	019-19741, Wako	Rabbit	1:500	CB	
Neuronal Nuclei (NeuN) [A60]	MAB377, Merck Millipore	Mouse	1:1,000	CB	
p62 (sequestosome-1)	18420-1-AP, Proteintech	Rabbit	1:100	CB	
Tyrosine Hydroxylase (TH)	Ab152, Merck Millipore	Rabbit	1:1,000	CB	
Ubiquitin (Ubi-1)	MAB1510, Merck Millipore	Mouse	1:500	Formic acid	

Table 5: Secondary antibodies used and their dilution

Secondary antibody	Reference	Host	Dilution (IF)	Dilution (WB)
Alexa Fluor 488/594, anti-mouse IgG	A11001/A11005, Thermo Fisher Scientific	Goat	1:1,000	
Alexa Fluor 488/594, anti-rabbit IgG	A1108/A11012, Thermo Fisher Scientific	Goat	1:1,000	
Anti-rabbit IgG, HRP-conjugated	Cay10004301, Cayman Chemical	Goat		1:10,000

The following table lists software programs either used for data acquisition, evaluation, presentation of data, or preparation of pictures and graphs for this thesis Table 6.

Table 6: Suppliers of software

Product	Company name
Adobe Acrobat 9 Pro	Adobe Systems Inc., Mountain View, USA
Adobe Illustrator CS5	Adobe Systems Inc., Mountain View, USA
Adobe Photoshop CS5	Adobe Systems Inc., Mountain View, USA
BioRender	BioRender Biotech, Toronto, Canada
Fusion FX	Vilber Lourmat, Eberhardzell, Germany

Image J1	NIH, Wayne Rasband, Bethesda, USA
Mendeley	London, UK
Microsoft Office 2016	Microsoft Corporation, Redmond, USA
Omega Control	BMG Labtech, Ortenberg, Germany
Prism 8	GraphPad Software Inc., San Diego, USA
Zen 2010 (ZenBlue)	Carl Zeiss, Jena, Germany

2.2 Methods

2.2.1 Preparation of recombinant α-synuclein fibrils

The expression and purification of the recombinant human α-synuclein protein was conducted by Dr. Julius Tachu Babila (German Center of Neurodegenerative Diseases (DZNE), Bonn) and prepared as previously described (Breid *et al.*, 2016). Briefly, *Escherichia coli* strain BL21(DE3) cells harboring the pET-3a expression plasmid for human wild-type α-synuclein (pET-3a expression plasmid, Novagen) were grown in 1 L LB media consisting of ampicillin, chloramphenicol and 1% (v/v) glucose, at 37 ˚C to an optical density of 0.5 at 600 nm (OD_{600}). Protein expression was induced with 0.1 mM isopropyl-β-d-thiogalactopyranoside and the bacteria were grown at 37 °C for 5 h. Using osmotic shock, periplasmatic material was released into the buffer and cells were pelleted by centrifugation at 6,000 × g for 15 min at room temperature (RT). The pellet was taken up in 35% (w/v) sucrose solution containing 2 mM EDTA and 30 mM Tris-HCl (pH 7.2) and incubated for 15 min on a shaker at RT. Cells were harvested and resuspended in ice-cold water supplemented with 5 mM $MgSO_4$. Periplasmatic material was boiled for 20 min before being centrifuged at 21,000 × g for 30 min. For fractional ammonium sulfate precipitation, 19.4 g/100 mL $(NH_4)_2SO_4$ were added to the supernatant over a 10 min time period during gentle stirring on ice to achieve a 35% saturation. Following centrifugation at 21,000 × g for 30 min, additional 11.8 g/100 mL $(NH_4)_2SO_4$ was added during gentle stirring on ice for another 10 min, to increase the saturation up to 55%. The centrifugation step was repeated again and the pellet was resuspended in 10 mL water prior to three dialyses against 20 nM Tris-HCl (pH 8.0) for 3 h each. An ÄKTA pure chromatography system (GE Healthcare) was used to purify α-synuclein via Resource Q anion exchange chromatography with 20 mM Tris-HCl (pH 8.0) as binding and 500 mM NaCl in 10 mM Tris-HCl (pH 8.0) as elution buffer. A 30 mL linearly increasing gradient from binding towards elution buffer was used to release α-synuclein from the column. The fractions were pooled and dialyzed against 150 mM NaCl in 20 mM Tris-HCl (pH 7.2). The purified protein was agitated for 7 days at 37 ˚C and 900 rpm in an orbital thermomixer to obtain fibrils. α-Synuclein fibrils were diluted in PBS to a final concentration of 4.25 $\mu g/\mu L$ and sonicated on ice for 1 min with 40 pulses of 0.5 s with 1 s breaks and 50% amplitude using a Sonopuls mini20

sonicator. Generated human WT α-synuclein fibrils were verified to have low levels of endotoxins (>0.01 EU/mL) by use of the ToxinSensor™ Chromogenic LAL Endotoxin Assay Kit (Genscript) according to the manufacturer's instructions.

2.2.1.1 Atomic force microscopy

To evaluate the length distribution of the prepared α-synuclein fibrils, atomic force microscopy was performed by Alexandra Ziemski (Institut für Physikalische Biologie, Heinrich-Heine-Universität Düsseldorf). Therefore, 5 µL of sonicated fibrils were loaded onto a mica slide and incubated for 15 min at RT. The slide was washed three times with H_2O and dried with N_2. The fibrils were measured using the NanoWizard III (JPK BioAFM) with an OMCL-AC160TS cantilever (Olympus) in tapping mode in air. A total number of 547 fibrils were analyzed using the ruler tool in ImageJ to determine the length distribution of the prepared fibrils.

2.2.2 Animals

All experiments involving animals were approved by the animal care committee of the North Rhine-Westphalia State Environment Agency (LANUV). Mice were housed under standard conditions with a 12 h light-dark cycle with free access to food and water. Inoculation and MCAO experiments were performed on six- to eight-week-old C57BL/6J WT mice and hemizygous TgM83$^{+/-}$ (B6;C3-Tg[*Prnp*-SNCA*A53T]83Vle/J, The Jackson Laboratory) mice of both genders. TgM83$^{+/-}$ mice, overexpressing the A53T mutant of human α-synuclein under the prion promoter on a C57BL/6 background (Giasson *et al.*, 2002) were crossed to WT C57BL/6J mice and their progeny were genotyped for the presence of the transgene.

2.2.2.1 Genotyping

DNA-isolation

DNA was isolated either from small tail biopsies or from ear punches using the DNeasy Blood & Tissue Kit according to manufacturer's instruction. Briefly, biopsies were lysed in a Proteinase K containing buffer under shaking at 56 °C for 1 h. To separate cell debris, samples were centrifuged for 2 min at 6,000 × g and RNase A was added to the supernatant. After 2 min of incubation, a mix of 200 µL buffer AL and 200 µL EtOH was added to the sample, briefly mixed and loaded on silicia-membrane spin columns. DNA was purified by centrifugation at 6,000 × g for 1 min each with two washing steps with 500 µL buffer AW1 in between and a following centrifugation step at 20,000 × g for 3 min after adding 500 µL buffer AW2. DNA was eluted by 45 µL buffer AE and a final centrifugation at 6,000 × g for 1 min. Concentration of the isolated DNA was determined by photometric analysis using the FLUOstar omega microplate reader (BMG Labtech) and the extracted DNA was further used for genotyping using real-time polymerase chain reaction (PCR).

Real-time polymerase chain reaction

To determine the genotypes of murine progeny, 90 ng of isolated DNA was amplified by real-time PCR. An internal positive control as well as 6FAM- and Cyanine5-fluorescently labeled oligonucleotides binding downstream to one of the primers were used. All primer sequences used for the internal positive control, the amplification of the transgene as well as the labeled oligonucleotides are listed in Table 3. The master mix containing the primers, Taq Polymerase and the reference dye ROX was pipetted onto a PCR plate in triplicates before the sample was added. The sample plate was incubated for 2 min at 50 ˚C and the DNA was pre-denatured for 10 min at 95 ˚C, followed by 40 cycles of 15 s denaturing at 95 ˚C and annealing and extension at 60 ˚C for 1 min. The fluorescent reporter signal was normalized to the reference dye and the fluorescence signal was detected by the 7900 HT Fast Real Time PCR system.

2.2.2.2 Peripheral challenge study

Six- to eight-week-old TgM83$^{+/-}$ mice were intracerebrally inoculated either with 10 μg (2.3 μL) or 50 μg (12 μL) of sonicated human α-synuclein fibrils in PBS. For peripheral challenge, six- to eight-week-old TgM83$^{+/-}$ mice were inoculated intraperitoneally, intravenously or orally with 50 μg (12 μL) of sonicated human α-synuclein fibrils in PBS. Additionally, one group of animals was challenged orally with a high dose of 500 μg (120 μL) of human α-synuclein fibrils. Animals challenged intracerebrally, intraperitoneally, or intravenously with 50 μg (25 μL) bovine serum albumin (BSA) in 0.9% (w/v) saline solution, or orally challenged with 500 μg (250 μL) BSA in 0.9% (w/v) saline solution served as controls (Figure 2.1).

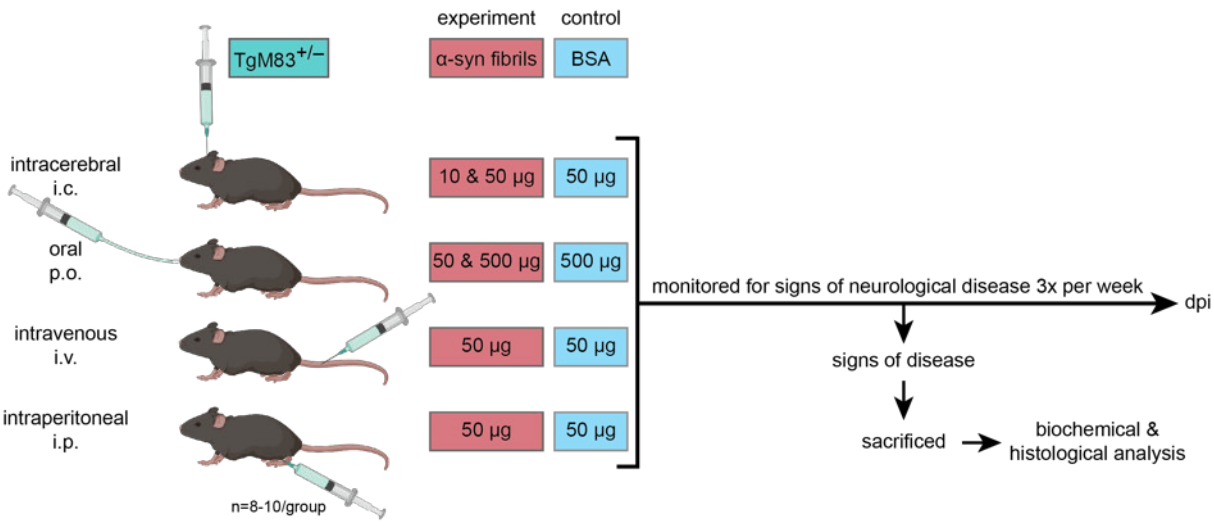

Figure 2.1: Experimental overview of the inoculation study. TgM83$^{+/-}$ mice overexpressing the A53T mutant of human α-synuclein were challenged intracerebrally, intravenously, intraperitoneally, or orally with fibrils made from recombinant human α-synuclein or with BSA as a control. Animals were sacrificed after developing neurological signs of disease. Neuropathology was analyzed by staining of brain and spinal cord tissue sections for pathological α-synuclein, by biochemistry for phosphorylated α-synuclein, and with a fluorescence resonance energy transfer (FRET) assay for aggregated α-synuclein.

All animals were weighed weekly and monitored three times per week for neurological signs of disease, such as weight loss, reduced grooming, ataxia, circling, kyphosis, paraparesis, and paralysis. Mice were sacrificed as soon as they showed clinical signs of neurological disease.

Intracerebral transmission

For intracerebral injection with α-synuclein fibrils or BSA, mice were weighed and carprofen was administered subcutaneously according to their bodyweight (5 mg/kg) 30 min prior to the surgery as an analgesic. Mice were anaesthetized by using a 1.5-2.0% isoflurane and oxygen gas mixture with a flow rate of 200 mL/min. To prevent dryness of the eyes during surgery, ointment (Bayer) was applied to cover the eyes, and hypothermia was prevented by placing the mice on a 37 ˚C warm heating pad in the stereotaxic frame (Kopf instruments). Mice were fixed by a palate bar and two additional ear bars. A small area on the head was disinfected with Braunol (B. Braun) and a 0.5 cm long midline incision on the scalp was made. The bregma was located and the injection coordinates were adjusted to +0.2 mm relative to the bregma and +2.0 mm relative to the midline on the stereotaxic frame and a 29-gauge disposable hypodermic syringe (VWR) was set to 2.6 mm below the dura to start the injection. An injection rate of 1.4 μL/min was used. The syringe was left in place for 5 additional minutes to avoid any loss of inoculum, before the needle was slowly retracted. The scalp was disinfected again and the incision was closed using a veterinary tissue adhesive (3M Vetbond). Mice were then transferred into a heated cage and constantly monitored until they completely recovered from surgery.

Intravenous transmission

Mice were weighed and anaesthetized by a 1.5-2.0% isoflurane/oxygen mixture with a flow rate of 200 mL/min for intravenous transmission. To dilate the tail vessels of the mice, the tail was warmed using an infrared lamp. The tail was then disinfected with 70% EtOH and the lateral tail veins were located. A 29-gauge needle (VWR) was inserted almost in parallel to the right lateral tail vein and 50 μg (12 μL) sonicated human α-synuclein fibrils or 50 μg (25 μL) BSA were slowly injected. After removing the needle, slight pressure was applied to the puncture site until the bleeding has stopped to prevent backflow of the inoculum. Mice were then transferred into a heated cage and monitored until they had completely recovered.

Intraperitoneal transmission

For intraperitoneal transmission, conscious mice were restrained by standard tail and scruff handling in the head-down position. Either 50 μg (12 μL) sonicated human α-synuclein fibrils or 50 μg (25 μL) BSA were injected into the right peritoneum using a 29-gauge disposable hypodermic syringe (VWR). Afterwards the mice were directly placed back in their cages.

Oral transmission

Conscious mice were restrained by normal tail and scruff handling for direct administration by oral gavage. They were held in an upright position and the neck was extended using a 20-gauge ball-tip disposable feeding needle (Sigma), which was gently passed through the mouth into the esophagus. Then 50 μg (12 μL) or 500 μg (120 μL) of sonicated human α-synuclein fibrils or 500 μg (250 μL) BSA were slowly administered. The feeding needle was removed slowly and mice were directly placed back in their cages, where they were monitored for a few minutes.

2.2.2.3 Middle cerebral artery occlusion study

Six- to eight-week-old TgM83$^{+/-}$ mice were subjected to either a middle cerebral artery occlusion (MCAO) or a sham control surgery (SHAM). To compare α-synuclein changes post MCAO over time, endpoints of the study were set to 14, 30, 90, 180 and 360 days post surgery (dps) (Figure 2.2).

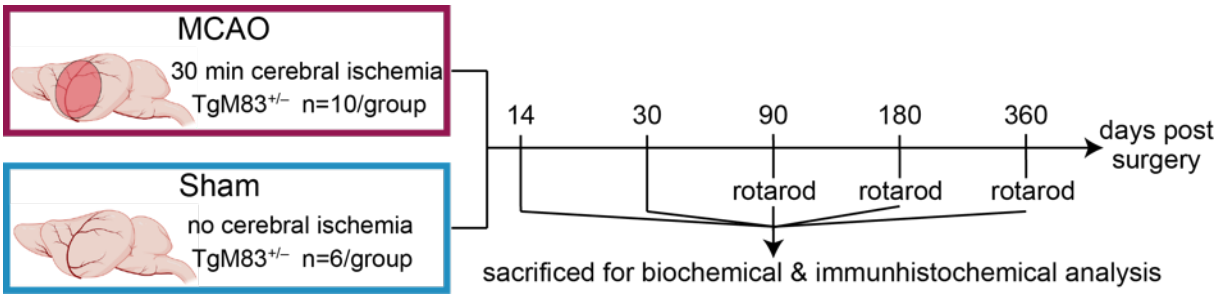

Figure 2.2: Experimental overview of the MCAO study. TgM83$^{+/-}$mice overexpressing the A53T mutant of human α-synuclein underwent surgery. Either a middle cerebral artery occlusion (MCAO) for 30 min or a sham surgery without occlusion of the artery was performed. Animals were sacrificed at 14, 30, 90, 180, or 360 days and neuropathology was analyzed by histology. A fluorescence energy transfer (FRET) assay was used to detect aggregated α-synuclein. Additionally, motor behavior of mice was tested at 90, 180, and 360 dps on a rotarod treadmill.

MCAO

Mice were weighed and carprofen was administered subcutaneously according to their bodyweight (5 mg/kg) 30 min prior to the surgery. Mice were anaesthetized in a 1.5-2.0% isoflurane and oxygen gas mixture with a flow rate of 200 mL/min. To prevent dryness of the eyes during surgery, ointment (Bayer) was applied to cover the eyes, and hypothermia was prevented by placing the mice on a 37 ˚C warm heating pad. The neck was shaved, the skin disinfected with Braunol (B. Braun) and a midline incision was made. The right common carotid artery (CAA) was carefully separated from surrounding tissue and the vagus nerve. A permanent ligation was made 4 mm proximal to the bifurcation, which splits the CCA into the external carotid artery (ECA) and the internal carotid artery (ICA) using 6/0 sutures (Feuerstein). The CCA was clipped proximal to the bifurcation and the ECA was also clipped with a vascular clamp (FST) to prevent backflow from the distal vasculature. A microincision into the CCA, distal to the permanent knot was made using spring scissors (FST), and a silicon-

coated filament (Doccol) was inserted into the CAA. Following insertion, the clip at the bifurcation was removed and the filament was gently guided into the ICA, until the tip occluded the middle cerebral artery (MCA), after 9 to 11 mm of filament insertion. The filament was fixed in this position for 30 min with an additional suture directly distal to the microincision (Figure 2.3).

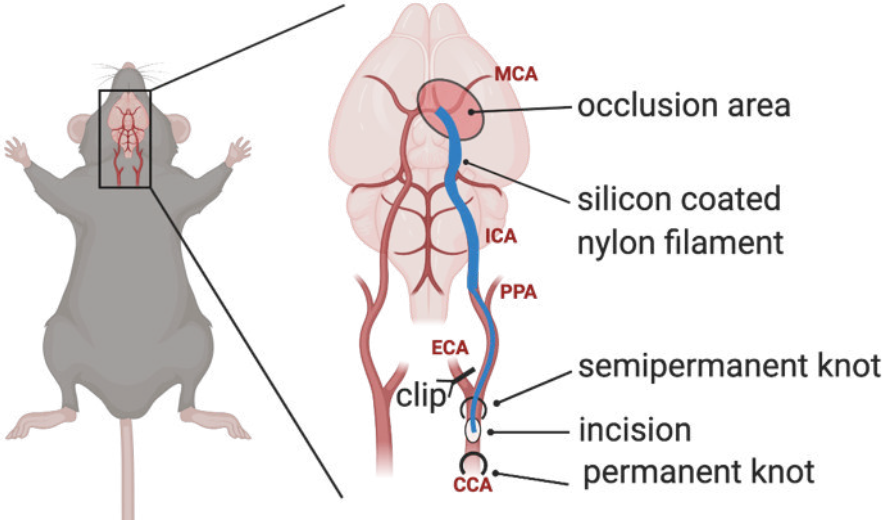

Figure 2.3: Middle cerebral artery occlusion (MCAO). The common carotid artery (CCA) was isolated and the blood flow was stopped by a permanent and a semi-permanent knot just before the bifurcation of the external carotid artery (ECA), which was also clipped. A silicone-coated nylon filament was inserted via a microincision into the CCA and guided through the internal common artery (ICA) until it reached the bifurcation to the middle cerebral artery (MCA). The filament was fixed in position to occlude the MCA for 30 min, before it was removed again.

During the incubation time a volume replenishment of 0.5 mL 0.9% (w/v) saline (B. Braun) was administered subcutaneously. After 30 min of MCAO, the filament was removed to allow natural reperfusion. To this aim, the suture was shortly opened to remove the filament and then directly closed with a permanent ligation. The vascular clamp at the ECA was removed and the neck incision was disinfected and closed with surgical sutures (Himed). Mice were then transferred into a heated cage and constantly monitored until they had completely recovered from surgery. Sham control mice underwent the same surgical procedure of ligation and microincision of the CCA but without insertion of a filament.

Rotarod

To evaluate general motor performance, coordination, and skill learning the rotarod test was used. The animals were subjected to the rotarod test 90, 180, and 360 days post surgery (dps). The mice were placed on the horizontal rotarod treadmill (Med associates Inc.) and the latency to fall was measured during a time period of 300 s, during which the speed accelerated from 4 to 40 rpm. Mice were subjected to four rotarod sessions, with a 10-min breaks in between of which the first run was considered as training session and was not scored.

2.2.3 Mouse tissue preparation

Animals showing signs of disease or reaching the endpoint of the study, were either sacrificed by spinal dislocation or with an overdose of ketamine/xylazine. For biochemical analysis, mice were sacrificed by spinal dislocation and organs were dissected, snap-frozen on dry ice, and stored at –80 ˚C.

For histological analysis, mice were sacrificed by intraperitoneal overdose with ketamine/xylazine and transcardially perfused with 8 mL ice-cold 0.9% saline (B. Braun), followed by 10% (v/v) ice-cold formalin neutral buffer solution (Sigma) using a perfusion pump (ISMATEC) until the mice were fixed. The organs were dissected and underwent post-fixation overnight in 10% (v/v) formalin neutral buffer solution. Prior to paraffin embedding, the organs were dehydrated in a series of graded ethanol baths (70%, 70%, 86%, 86%, 95%, 95%, 100%, 100% EtOH), transferred into two xylene baths (Sigma), and finally infiltrated with liquid paraffin (Leica) using an automated tissue processor (Leica) with each step lasting 2 h. Tissue sections were embedded using a paraffin embedding module (Leica) and finally cut into 6-μm thick coronal sections using a microtome (Leica). The sections were mounted on adhesive SuperFrost Plus slides (Thermo Fisher Scientific), dried overnight at 37 ˚C, and stored at 4 ˚C.

2.2.4 Histological analysis

2.2.4.1 Immunohistochemical analysis

For immunohistochemistry, tissue sections were first deparaffinized and then rehydrated through incubation in xylene and in a series of solutions with decreasing concentrations of ethanol to water, followed by heat-induced antigen-retrieval with citric buffer (pH 6.0). By incubation with 5% (v/v) hydrogen peroxide solution (Sigma) in methanol (Sigma) for 30 min, endogenous peroxidase activity in the tissue was inhibited. Tissue sections were blocked with 20% (v/v) normal goat serum and 1% (v/v) BSA in 0.5% (v/v) Triton X-100 in PBS for 1 h at room temperature. The appropriate primary antibody (Table 4) was diluted in 1% (v/v) normal goat serum, 1% (v/v) BSA, and 0.25% (v/v) Triton X-100 in PBS (PBST) and incubated overnight at RT. After washing once with PBST and twice with PBS, the tissue sections were incubated for 1 h with peroxidase-conjugated secondary antibody by use of the Mouse On Mouse kit (Vector Labs) diluted in 1% (v/v) normal goat serum and 1% (v/v) BSA in PBS at RT. That step was not necessary for the phospho- α-synuclein staining using the directly biotinylated #64 antibody (wako). After washing once with PBST and twice with PBS, peroxidase-positive structures were visualized by incubation with DAB (3-3'-diaminobenzidine, Vector Labs) for 20-40 s. The reaction was directly stopped with 3% (v/v) hydrogen peroxide solution. Tissue sections were counterstained with Mayer's hematoxylin (Merck), coverslipped with Eukitt (Sigma), and scanned using the Slide scanner AxioScan.Z1 (Carl Zeiss) and Zen Lite software.

2.2.4.2 Immunofluorescence analysis

For immunofluorescence, the 6-μm thick brain and spinal cord coronal sections were deparaffinized as described above. Tissue sections underwent heat-induced antigen-retrieval with citric buffer (pH 6.0) or, for staining for ubiquitin, with 70% (v/v) formic acid (Sigma). After washing twice with PBS, autofluorescence from the mouse tissue was quenched by incubation in $CuSO_4$ solution for 90 min at RT in the dark. Tissue sections were first washed with PBS, followed by blocking for 1 h in blocking buffer. The primary antibodies (Table 4) were diluted in primary antibody mix and incubated overnight at RT. Following one washing step with PBST and two with PBS, sections were incubated in secondary antibody-mix, as well as the appropriate Alexa Fluor 488- and Alexa Fluor 594-conjugated secondary antibodies (1:1,000, Thermo Fischer Scientific) and the nuclear marker DAPI (1:1,000, Thermo Fisher Scientific) for 1 h at RT. Tissue sections were once washed with PBST and twice with PBS, coverslipped using Fluoromount medium (Sigma), and analyzed with a LSM700 or LSM900 confocal laser scanning microscope (Carl Zeiss).

2.2.5 Biochemical analysis

2.2.5.1 Preparation of tissue homogenates

The Precellys 24 Dual homogenizer was used to prepare 25% (w/v) brain and 10% (w/v) spinal cord homogenates. Tissue samples were homogenized in ice-cold Ca^{2+}-and Mg^{2+}-free PBS (pH 7.4) in the presence of phosphatase and protease inhibitors by two 30 s cycles at 6500 rpm. Samples were then centrifuged at 1,000 $\times$ g for 5 min at 4 ˚C to separate tissue debris and the supernatant was adjusted to 750 mM NaCl before spinning at 1000 $\times$ g for 5 min at 4 ºC. Total protein concentration was determined using the Pierce BCA Protein Assay Kit (Thermo Fischer Scientific). PBS was used as blank, as well as diluent for standard preparation, and for a 1:10 or 1:50 pre-dilution of the tissue samples. All samples were analyzed in triplicates. Briefly, 15 μL of sample was first transferred to a 96-well plate to which 150 μL of detection solution (a mix of solution A and solution B at a 40:1 ratio) was added. The plate was first placed on a shaker for 30 s to ensure gentle mixing and then incubated at 37 ˚C for 30 min in the dark. The plate was cooled down to RT before fluorescence emission was measured at 562 nm on a FLUOstar omega microplate reader (BMG Labtech).

2.2.5.2 Sarkosyl-insoluble fractions

To separate sarkosyl-soluble from sarkosyl-insoluble α-synuclein aggregates, a volume of brain homogenate containing 500 μg of total protein was added to the same volume of 20% (w/v) *N*-lauroylsarcosyl to reach a final sarkosyl concentration of 10% (w/v) , which was incubated for 15 min on ice. Samples were centrifuged on 3 mL of a 10% sucrose cushion at 465.000 $\times$ g for 1 h at 4 ˚C in a TLA-110 rotor. The pellets

of the sarkosyl-insoluble proteins were resuspended in 50 µL freshly prepared TD4215 denaturing buffer and stored at –20 ˚C.

2.2.5.3 SDS-Page & Western blotting

To separate proteins from sarkosyl-insoluble fractions according to their molecular weight, they were subjected to SDS polyacrylamide gel electrophoresis of proteins (SDS PAGE). To this end fractions were thawed and heat denatured at 99 ˚C for 5 min at 700 rpm. The total volume of denatured sarkosyl fractions (50 µL) was loaded on a 4-12% Bis-Tris gel and separated in a morpholineethanesulfonic acid (MES) buffer system. For reference of the molecular weight, SeeBlue™ Plus2 Pre-stained Protein Standard (Life Technologies) was used. Proteins were size-separated by gel electrophoresis for about 180 min at 120 V. Proteins were then transferred onto methanol-activated poly-vinylidene difluoride (PDVF) membranes using the Semi-Dry Transfer Unit (Hoefer) for 75 min at 0.8 mA/cm^2. After cross-linking the membrane with 0.4% (v/v) paraformaldehyde in Tris-buffered saline (TBS) for 30 min at RT, membranes were blocked with 5% (w/v) skim milk in TBS with 0.05% Tween 20 (TBST) for 1 h to reduce unspecific antibody binding. Membranes were incubated with a primary antibody for phosphorylated α-synuclein (EP1536Y) overnight at 4 ˚C in 5% (w/v) skim milk in TBST. Following three washing steps with TBST for 15 min, membranes were incubated with specific anti-rabbit horseradish peroxidase-linked secondary antibody (1:10,000) for 1 h at RT. After washing three times for 10 min in TBST, equal amounts of SuperSignal West Dura extended-substrate were mixed and added to the membrane for 1 min at RT. Chemiluminescence signal was detected using the Fusion FX imaging system (Vilbert). To stain for total protein, membranes were washed 3 times for 15 min with TBST, prior to blocking with 5% (w/v) milk in TBST for 1 h at RT. Membranes were then probed with an antibody to glyceraldehyde 3-phosphate dehydrogenase (GAPDH) overnight at 4 ˚C in 5% (w/v) skim milk in TBST.

2.2.5.4 TR-FRET Immunoassay

Aggregation of human α-synuclein was quantified by homogeneous time resolved fluorescence technology (FRET). FRET assay for the inoculation experiments was performed by Dr. Maria Eugenia Bernis (DZNE, Bonn) and FRET assay for the MCAO experiments was performed by Dr. Jessica Grigoletto (DZNE, Bonn) following the manufacturer's instructions. Briefly, 1 µg of total protein from 25% (w/v) brain homogenate or 10% (w/v) spinal cord homogenate were prepared in triplicates by adding 1× lysis buffer. Pre-mixed antibodies, anti-h-α-Synuclein-d2 (acceptor) and anti-h-α-Synuclein-Tb-Cryptase (donor) were added to the sample. A negative control, Cryptase control and buffer control were prepared as suggested by the company. Twenty microliter of the final mix containing sample and antibody, as well as the controls were transferred on a 384-F-clear bottom plate (Greiner Bio-one), covered with a plate sealer, and incubated for 20 h at RT. Fluorescence emission was

measured at 665 nm for FRET-dependent acceptor fluorescence and at 620 nm for FRET-independent donor fluorescence on a CLARIOstar microplate reader (BMG Labtech). The ratio of both fluorescence emission values multiplied by 10,000 was directly proportional to the amount of human α-synuclein aggregates in each sample.

2.2.6 Data Analysis

2.2.6.1 Phospho-α-synuclein score

For quantification of pathology in different brain areas, coronal sections 0.26 mm, –1.70 mm, –3.28 mm, and –6.24 mm away from the bregma were analyzed for α-synuclein accumulation in neurites and somata using the pSyn#64 biotin-conjugated antibody specific for phosphorylated α-synuclein at Ser129. A scoring scheme from 0 to 5 was used (0: no pathology, 1: sparse pathology [few affected neurites, no affected soma], 2: mild pathology [more affected neurites, maximally 2 affected somata], 3: moderate pathology [some affected somata and neurites, but with large areas without pathology], 4: dense pathology [many affected neurites and somata], 5: severe pathology [large area covered with pathology]), based on Rey et al (Rey et al., 2016). For each inoculation route, the final score for each brain region was the average of the scores obtained for the left and right hemispheres of three animals. The scores were depicted as a color-coded heat map on a brain-section schematic based on the Allen Mouse Brain Atlas (Allen, 2007). Quantification was performed using ImageJ.

2.2.7 Statistics

For statistical analysis GraphPad Prism 8 was used. Data are presented as mean ± SD, unless stated otherwise. Treatment effects in different inoculation groups were compared using one-way ANOVA followed by the Holm-Šídák test. Both hemispheres of MCAO- and sham-treated animals were compared using one-way ANOVA followed by the Tukey's post-hoc test, unless stated otherwise. *P* values below 0.05 were considered statistically significant.

3 Results

Parkinson's disease is characterized by an accumulation of insoluble α-synuclein aggregates (Conway, Harper and Lansbury, 1998; Spillantini *et al.*, 1998) resulting in an increased immune response, increased ubiquitination, and a loss of dopaminergic neurons, and ultimately leads to CNS disease (Masliah *et al.*, 2000b; Leverenz *et al.*, 2007; Watanabe *et al.*, 2012). These morphological and functional changes between diseased and healthy control mice were investigated by behavioral analysis and scoring of inoculated mice, immunohistochemical and immunofluorescence analyses, as well as by biochemical analyses via western blotting and additional FRET assays of brain and spinal cord tissue samples.

3.1 Peripheral challenge study

The spreading of pathological α-synuclein was investigated after intracerebral, intraperitoneal, intravenous, or oral challenge with human α-synuclein fibrils in TgM83$^{+/-}$ mice. These transgenic mice overexpress human α-synuclein with a PD-associated mutation (A53T) (Giasson *et al.*, 2002). Hemizygous TgM83$^{+/-}$ mice have been demonstrated to remain healthy for over 650 days (Watts *et al.*, 2013). Mice were either challenged with human α-synuclein fibrils or with BSA, which served as a negative control, and were sacrificed after they developed clinical signs of neurological disease. Brain and spinal cord tissues were analyzed for pathological α-synuclein and other disease markers by immunohistochemical and biochemical analyses.

3.1.1 Transmission of α-synuclein fibrils leads to severe neurological disease

In order to study the propagation of pathological α-synuclein in TgM83$^{+/-}$ mice after challenge with human α-synuclein fibrils, first the length of the produced recombinant α-synuclein fibrils after sonication was determined. Atomic force microscopy (AFM) displayed the length of the fibrils according to a color scale (Figure 3.1a). An evaluation of the AFM image by statistical analysis revealed that the length of the majority of the sonicated α-synuclein fibrils was within a range of 25 to 70 nm (Figure 3.1b). Mice inoculated over the four routes with these fibrils were monitored for symptoms of neurological disease, such as ataxia, kyphosis, paralysis of the hindlimb, or generally motor impairments. All TgM83$^{+/-}$ mice intracerebrally injected with human α-synuclein fibrils did show signs of disease. Ten out of ten mice intracerebrally challenged with 10 μg α-synuclein fibrils developed disease within 156 ± 20 days (black dashed line; Figure 3.1c). Mice injected with higher doses (50 μg) of α-synuclein fibrils developed clinical signs of disease within 133 ± 4 days (black solid line). Intraperitoneal challenge with 50 μg α-synuclein fibrils led to signs of neurological damage in 10 out of 10 mice in 202 ± 35 days post injection (orange line). Neurological symptoms appeared in 10 out of 10 mice in 208 ± 20 days after intravenous challenge with 50 μg α-synuclein fibrils (pink line). Oral challenge of TgM83$^{+/-}$ mice with α-synuclein fibrils did not result

in full transmission. Two out of 8 animals orally challenged with 50 µg α-synuclein fibrils showed signs of disease at 220 and 350 days post oral gavage (blue dashed line), and 4 out of 8 mice orally challenged with 500 µg α-synuclein fibrils developed symptoms in 384 ± 131 days (blue solid line). Two mice out of each orally challenged group (50 µg [264 and 355 dpi] and 500 µg [150 and 192 dpi]) were found dead without showing detectable signs of disease. The cause of death for these four mice could not be determined due to advanced tissue decomposition. Control mice challenged intracerebrally, intraperitoneally, or intravenously with 50 µg BSA remained healthy during the entire observation time for up to 400 days post challenge (black dotted lines). Likewise, none of the oral control mice developed signs of neurological disease in over 570 days post challenge with 500 µg BSA (blue dotted lines; Figure 3.1c, Table 7).

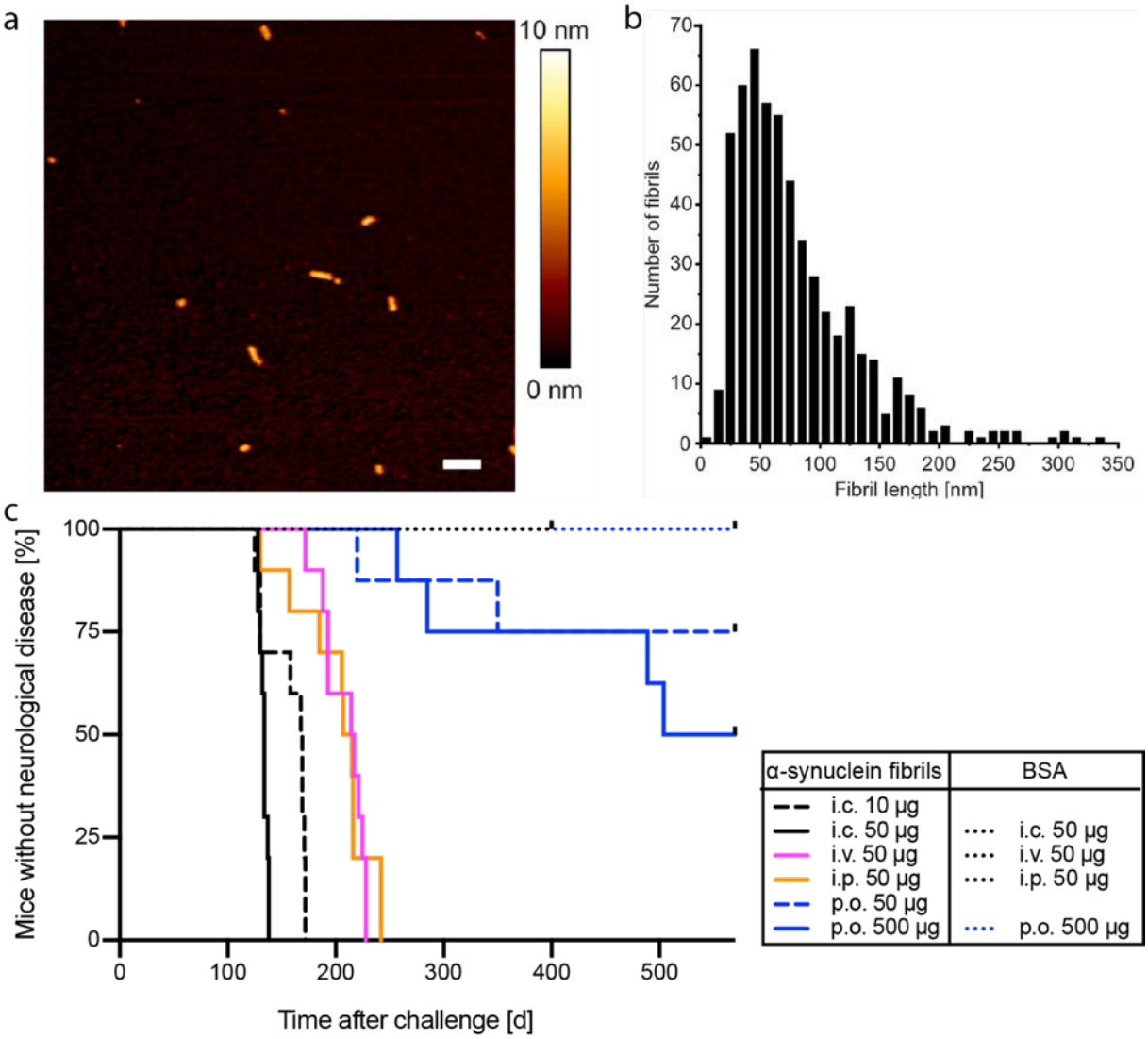

Figure 3.1: Intracerebral, intraperitoneal, intravenous, or oral challenge with α-synuclein fibrils lead to neurological disease in TgM83$^{+/-}$ mice. Atomic force microscopy image to determine the length of the sonicated α-synuclein fibrils used for inoculation. The color code indicates the height profile of the α-synuclein fibrils (a). The size distribution of sonicated α-synuclein fibrils was determined by statistical analysis of atomic force microscopy images (b). Kaplan-Meier survival curves showing the percentage of animals without disease over time. Signs of

neurological disease appeared in 2 out of 8 mice at 220 and 350 days post oral challenge with 50 µg of α-synuclein fibrils (p. o.; blue dashed line), and four out of 8 mice within 384 ± 131 days (mean ± SD) after oral challenge with 500 µg fibrils (p. o.; blue solid line). Ten out of 10 mice showed signs of neurological disease 208 ± 20 days post intravenous injection (i. v.; pink line) and 202 ± 35 days post intraperitoneal injection of 50 µg α-synuclein fibrils (i. p.; orange line). Intracerebral challenge with 10 µg or 50 µg α-syn fibrils resulted in neurological disease in 156 ± 20 days (i. c.; black dashed line) and 133 ± 4 days (black solid line), respectively, in 10 out of 10 mice in each group. There were no clinical signs of clinical disease detected in BSA-injected control mice (dotted lines, overlapping) (c). Scale bar = 200 nm. Published in Lohmann *et al.*, 2019.

Table 7: Incubation times in TgM83$^{+/-}$ mice after challenge with human α-synuclein fibrils or BSA via different routes.

Inoculation route	Inoculum type and amount [µg]	Mice with disease/ mice inoculated	Mean survival time ± SD [d]
Intracerebral	α-synuclein fibrils [10]	10/10	156 ± 20
	α-synuclein fibrils [50]	10/10	133 ± 4
	BSA [50]	0/8	≥ 400
Intraperitoneal	α-synuclein fibrils [50]	10/10	202 ± 35
	BSA [50]	0/8	≥ 400
Intravenous	α-synuclein fibrils [50]	10/10	208 ± 20
	BSA [50]	0/9	≥ 400
Oral	α-synuclein fibrils [50]	2/8	220 and 350
	α-synuclein fibrils [500]	4/8	384 ± 131
	BSA [500]	0/9	≥ 570

3.1.2 Diseased mice accumulate pathological α-synuclein in the CNS

Accumulation of pathological α-synuclein is a hallmark of PD (Spillantini *et al.*, 1997; Baba *et al.*, 1998). To investigate the relation between decreased survival of TgM83$^{+/-}$ mice challenged with human α-synuclein fibrils over different routes, and increased aggregation of α-synuclein, homogeneous time resolved fluorescence technology (FRET) assays were performed. This method allows quantification of levels of aggregated α-synuclein in brain and spinal cord homogenates. The amount of aggregated α-synuclein was highly increased in the CNS of TgM83$^{+/-}$ mice after intracerebral (black), intravenously (pink), intraperitoneally (orange), and after orally (blue) challenge with human α-synuclein fibrils, compared to the CNS of BSA-challenged control mice. All mice challenged with α-synuclein fibrils displayed higher amounts of aggregated α-synuclein in brain versus spinal cord tissue homogenates (Figure 3.2).

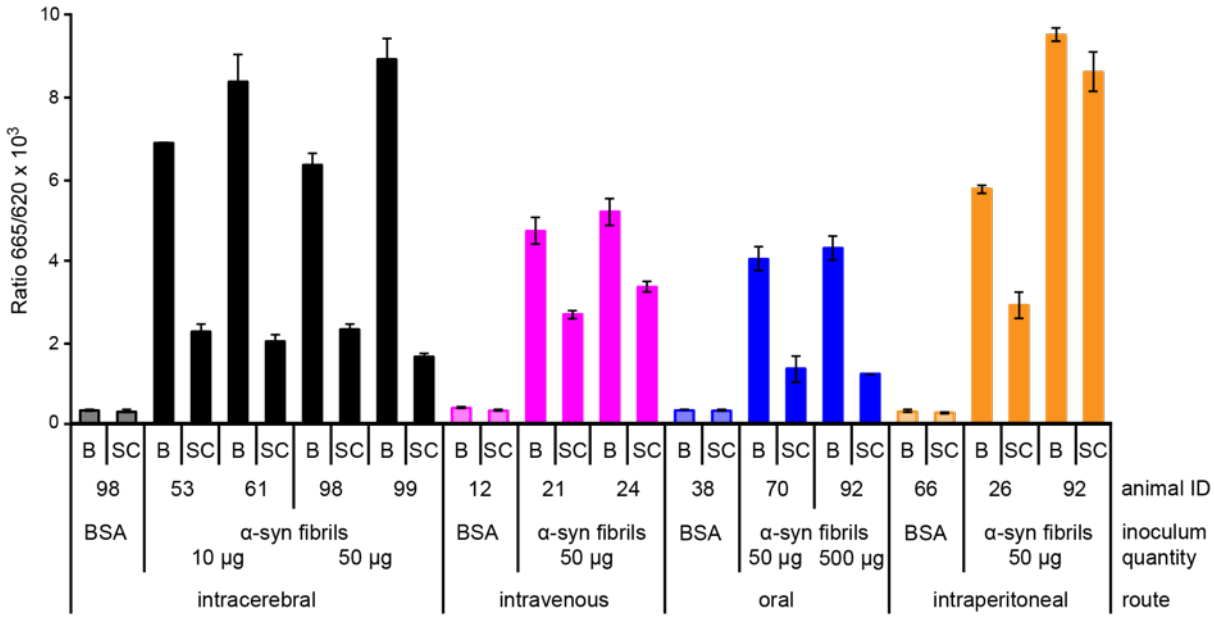

Figure 3.2: Aggregation of α-synuclein in the CNS of TgM83$^{+/-}$ mice challenged with α-synuclein fibrils. Levels of α-synuclein (α-syn) aggregation were quantified in brain and spinal cord homogenates of intracerebrally (black), intravenously (pink), intraperitoneally (orange), and orally (blue) challenged TgM83$^{+/-}$ mice using a FRET assay. Aggregated α-synuclein in the CNS was detected for every inoculation route when α-synuclein fibrils had been inoculated. In contrast, brain and spinal cord tissue homogenates of control mice injected with BSA did not contain any aggregated α-synuclein. Data shown as mean ± SD. Published in Lohmann *et al.*, 2019.

The tendency for α-synuclein to form detergent-insoluble aggregates in the CNS after challenge of TgM83$^{+/-}$ mice with α-synuclein fibrils was further shown by immunoblotting sarkosyl-insoluble fractions of brain homogenates against the EP1536Y antibody (Campbell *et al.*, 2001). This antibody recognizes phosphorylation at serine 129 (S129) of α-synuclein which is described as the most common modification leading to synucleinopathy lesions (Fujiwara *et al.*, 2002; Anderson *et al.*, 2006).

Western blot analysis showed sarkosyl-insoluble phosphorylated α-synuclein in brain tissue of all with α-synuclein fibrils challenged animals. Monomeric phosphorylated α-synuclein presented as a 14 kDa molecule and oligomeric species of phosphorylated α-synuclein presented as several additional high-molecular weight bands above the monomer. Interestingly, brains of intracerebrally injected mice seemed to contain less monomeric and oligomeric phosphorylated α-synuclein, compared to intraperitoneal, intravenous, or orally challenged mice. In contrast, brains of BSA-challenged control mice did not contain any detectable species of sarkosyl-insoluble phosphorylated α-synuclein (Figure 3.3).

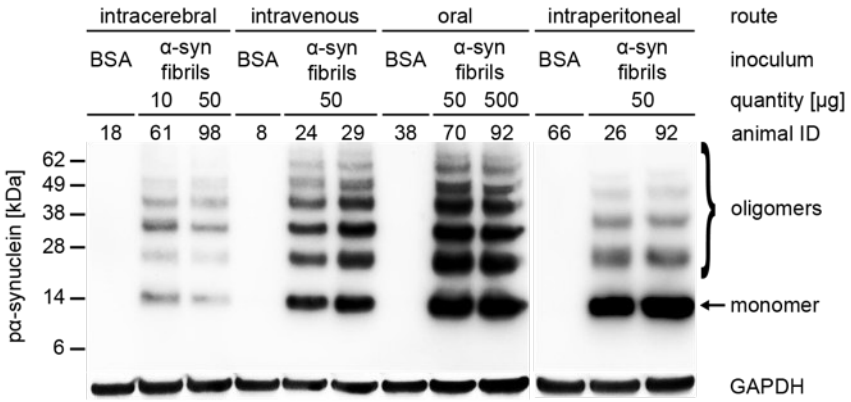

Figure 3.3: Detection of sarkosyl-insoluble aggregates of phosphorylated α-synuclein in the brains of TgM83$^{+/-}$ mice challenged with α-synuclein fibrils. Biochemical analysis via western blotting of sarkosyl-insoluble fractions from brain tissue shows phosphorylated α-synuclein as recognized by the EP1536Y antibody. Brain homogenates of TgM83$^{+/-}$ mice challenged with α-synuclein fibrils, regardless of the inoculation route, showed bands for sarkosyl-insoluble aggregates of phosphorylated α-synuclein, which presented as high-molecular weight bands above the 14 kDa band of monomeric, phosphorylated α-synuclein. In contrast, brain homogenates of BSA-injected control mice did not contain any sarkosyl-insoluble α-synuclein aggregates. Molecular masses are shown in kilodalton (kDa). Equal sample loading in each lane was controlled by detection of GAPDH. Published in Lohmann *et al.*, 2019.

Apart from the apparently lower amount of phosphorylated α-synuclein in intracerebrally inoculated animals, western blot and FRET assay provided similar results, showing increased levels of pathological α-synuclein in TgM83$^{+/-}$ mice after fibril inoculation, regardless of the route.

3.1.3 Distribution of pathological α-synuclein in the CNS of diseased mice

The influence of the different inoculation routes on α-synuclein aggregation and spreading in the CNS was investigated by analysis of different brain and spinal cord tissue sections with the pSyn#64 antibody recognizing phosphorylation at S129 of α-synuclein and an additional counterstaining with hematoxylin as a nuclear marker (Figure 3.4). Immunostaining visualized a strong accumulation of pathological α-synuclein throughout the whole brain and displayed a rostral to caudal pattern of pathology intensity in TgM83$^{+/-}$ mice for every inoculation route. Pathology was detected regardless of the route of inoculation in the frontal lobe, such as the motor cortex and striatum, in the parietal-temporal lobe, including the amygdala and the hypothalamus, and in the brain stem of challenged animals. Phosphorylated α-synuclein was present in neuronal cell bodies and neurites within these brain areas and the spinal cord of all mice challenged with α-synuclein fibrils. Interestingly, the hippocampus only showed α-synuclein pathology after intracerebral or oral challenge with α-synuclein fibrils but was not affected after intraperitoneal or intravenous

injection. None of the BSA-challenged control mice showed deposits of phosphorylated α-synuclein in any of these brain areas or the spinal cord.

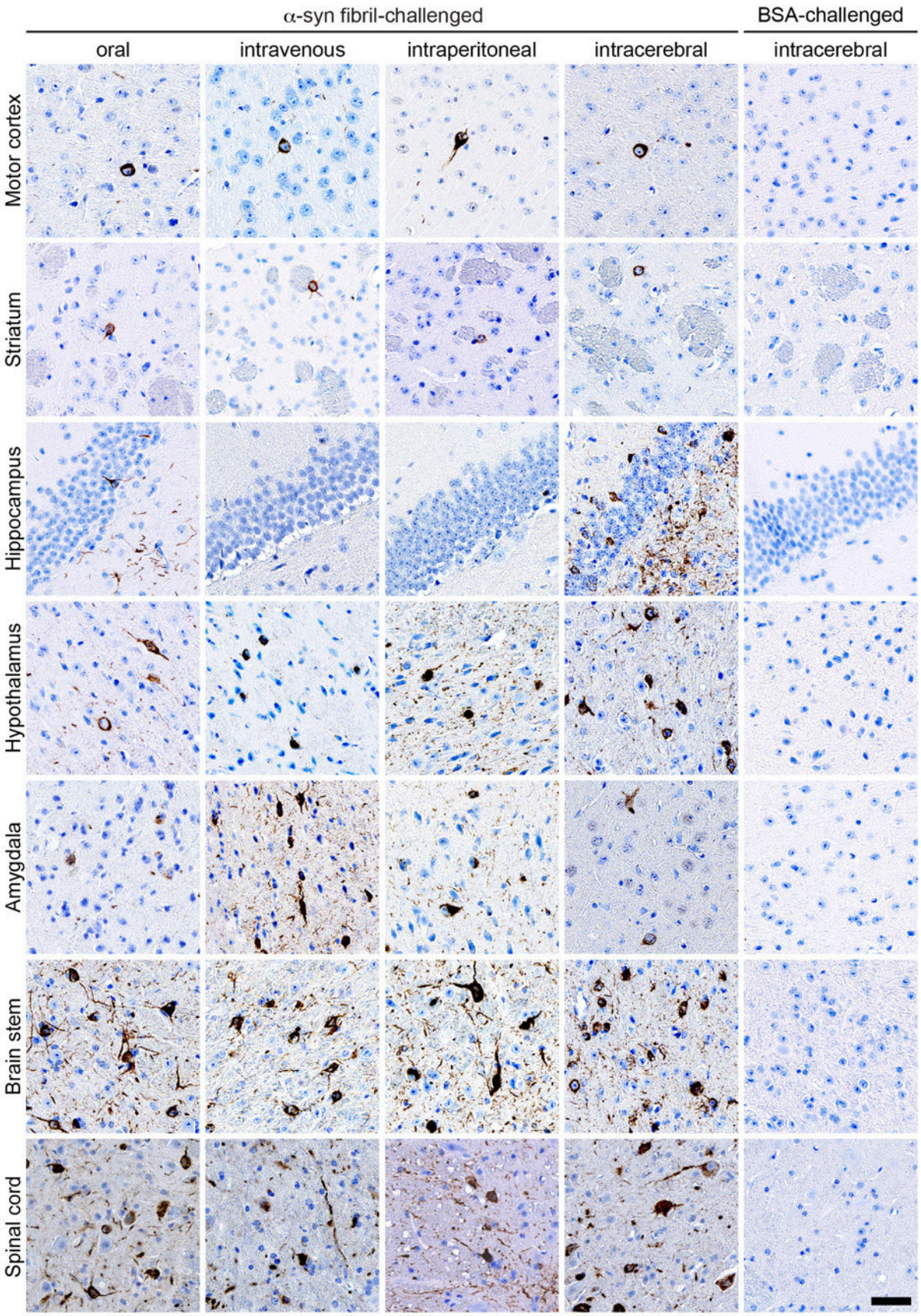

Figure 3.4: Immunohistochemical analysis shows neuropathology in the CNS of TgM83$^{+/-}$ mice after challenge with α-synuclein fibrils for all four routes. In TgM83$^{+/-}$ mice challenged intracerebrally, intraperitoneally, intravenously, or orally with α-synuclein (α-syn) fibrils, phosphorylated α-synuclein was present in neuronal cell bodies and neurites, as detected by staining with the pSyn#64 antibody recognizing phosphorylation at S129 of α-synuclein. Pathological α-synuclein was present throughout the brain, including the motor cortex, striatum, hippocampus, hypothalamus, amygdala, brain stem, as well as in the spinal cord. In contrast, none of the BSA-challenged mice showed any phosphorylated α-synuclein in the brain or the spinal cord. Scale bar = 50 µm. Published in Lohmann *et al.*, 2019.

Anatomical distribution of pathology in the form of phosphorylated α-synuclein deposits across the four inoculation groups was quantified. The findings were scaled from 0 to 5 reflective of no to severe pathology, and depicted as a heat map showing the extent of pathology in different brain regions (Figure 3.5). The most frontal sections at bregma 0.26 mm with mostly cortical regions showed none or just sparse pathology. Most pathology was detected in the primary and secondary motor cortex, where more affected neurites and somata were present in all four groups. Pathological α-synuclein was detected in the striatum and the lateral septal nucleus for all inoculation routes, with minor pathology presented after intraperitoneal challenge. At bregma –1.70 mm, affected neurites were spread throughout most of the cortical regions, showing less pathology after intravenous injection. A nearly identical amount of α-synuclein pathology was observed in the interbrain regions for all transmission routes. Here, the brains showed a sparse to mild pathology in the amygdala, a mild pathology throughout the thalamus, and a moderate pathology throughout the hypothalamus. Dense pathology was observed in the peduncular part of the lateral hypothalamus after oral and intravenous challenge. The hippocampal regions were not affected after intravenous or intraperitoneal challenge. However, sparse pathology was detected in all hippocampal regions after oral challenge. After intracerebral challenge mild pathology was detected in the CA1 region, moderate pathology in the CA3 region, and a severe pathology in the dentate gyrus. For sections from posterior areas, at bregma –3.28 mm no pathology was detected in any of the cortical regions for all but intracerebrally challenged mice, where sparse pathology was found in most cortical regions. Distribution of α-synuclein within the hippocampal regions showed sparse pathology for the oral route, and sparse to mild pathology in the CA1 and CA3 region, and moderate pathology in the dentate gyrus for the intracerebral route. An increased amount of pathology was observed in the midbrain region of all four groups, with sparse-to-mild pathology in the medial geniculate nuclei and a mild-to-moderate pathology in the parabrachial pigmented nucleus of the ventral tegmental area. The substantia nigra displayed a mild pathology after oral, intracerebral, and intraperitoneal challenge with α-synuclein fibrils and a moderate pathology was detected after intravenous injection. The superior colliculus indicated the following distribution pattern: mild-to-dense for intraperitoneal and intracerebral challenge, moderate-to-dense for intravenous challenge, and moderate-to-severe pathology for orally challenged mice. In the inner midbrain regions consistent moderate-to-dense pathology was observed in the lateral periaqueductal grey, the anterior pretectal

nucleus, the parvicellular part of the red nucleus, and the mesencephalic reticular formation consistent in all four groups. The only exception was a severe pathology in the mesencephalic reticular formation of orally challenged mice. At bregma –6.24 mm sparse-to-mild pathology was observed in the cerebellar nuclei, except for the cerebellum. Sparse pathology was also detected in the outer regions of the hindbrain, such as the inferior cerebellar peduncle and the spinal trigeminal tract. In contrast, moderate-to-dense pathology was present in the facial and the raphe magnus nuclei in all groups. Dense pathology was observed in the reticular nucleus after oral, intracerebral, and intraperitoneal challenge, and severe pathology after intravenous challenge.

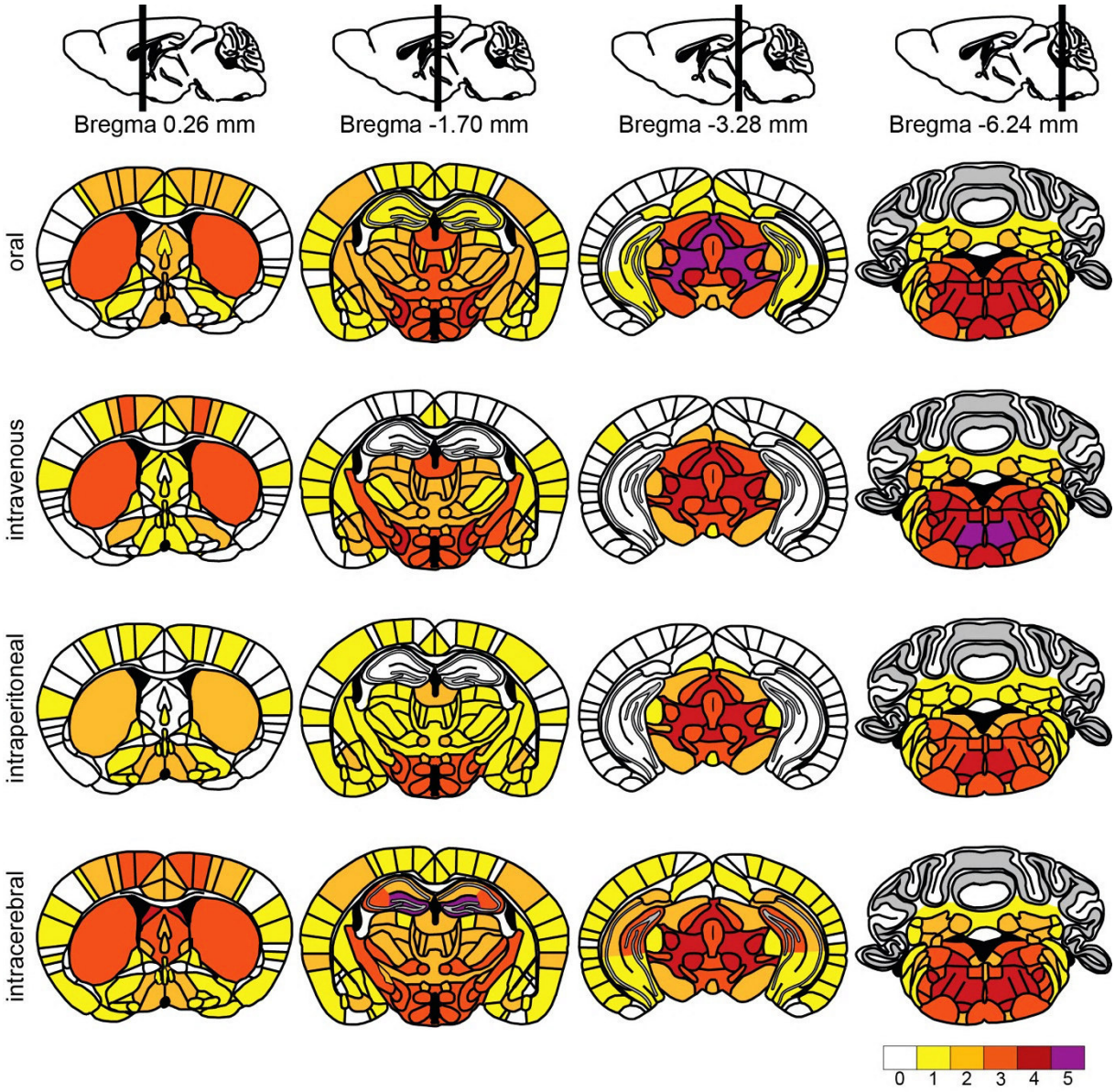

Figure 3.5: Heat map showing the distribution of phosphorylated α-synuclein in TgM83$^{+/-}$ mice after challenge with α-synuclein fibrils for all four routes. Distribution of phosphorylated α-synuclein in the brains of inoculated TgM83$^{+/-}$ mice with human α-synuclein fibrils was quantified and summarized on a scale from 0 to 5 reflective of no to severe pathology as a heat map for four coronal brain sections. n = 3/group. Published in Lohmann *et al.*, 2019.

Generally, oral, intracerebral, intraperitoneal, and intravenous challenge resulted in a consistent distribution of phosphorylated α-synuclein deposits but with overall less pathology after intraperitoneal challenge. One exception was the hippocampus, especially the dentate gyrus, showing pathology only after intracerebral and oral challenge but not after intravenous or intraperitoneal challenge with α-synuclein fibrils.

3.1.4 Neuropathology displays oligomeric and fibrillar α-synuclein

As synucleinopathies are characterized by the presence of oligomeric intermediates and ultimately fibrillar α-synuclein (Spillantini *et al.*, 1998; Giasson *et al.*, 1999), the conformation of the detected phosphorylated α-synuclein was further confirmed by immunohistochemistry. Hence, brain stem tissue sections, of TgM83$^{+/-}$ mice inoculated over different routes with human α-synuclein fibrils, which were shown to heavily accumulate phosphorylated α-synuclein, were prepared and probed with conformation specific antibodies. Here, the antibodies Syn-O2, recognizing early oligomers and late fibrils, and Syn-F1, specifically recognizing fibrillar α-synuclein (Vaikath et al., 2015) were used, and the tissue sections were counterstained with hematoxylin (Figure 3.6). Fibrillar and oligomeric α-synuclein was detected in all TgM83$^{+/-}$ mice challenged with α-synuclein fibrils, regardless of the route. Oligomeric and fibrillar α-synuclein mainly showed as intraneuronal inclusions but was also detected in neurites throughout the whole brain stem. In contrast, none of the BSA-challenged control mice showed fibrillar or oligomeric α-synuclein.

In summary, intracerebral, intraperitoneal, intravenous, and oral challenge of human α-synuclein fibrils lead to oligomeric and fibrillar conformations of phosphorylated α-synuclein in the brain of challenged TgM83$^{+/-}$ mice, resulting in insoluble inclusions that resemble Lewy bodies.

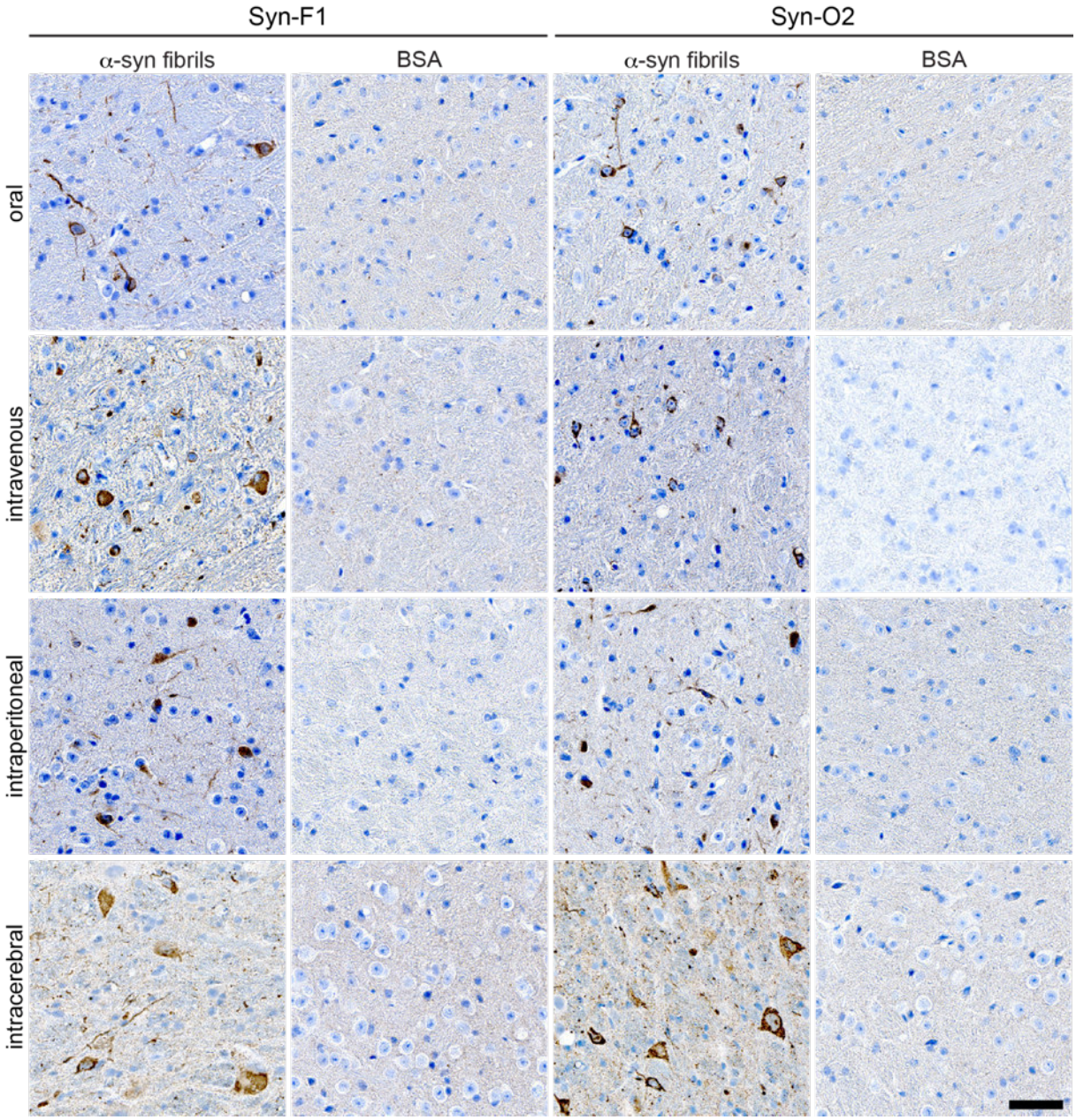

Figure 3.6: Immunohistochemical analysis shows fibrillar and oligomeric α-synuclein in TgM83$^{+/-}$ mice after challenge with α-synuclein fibrils for all four inoculation routes. Fibrillar and oligomeric α-synuclein was detected by the Syn-F1 and Syn-O2 antibodies, that recognize these specific conformers of pathological α-synuclein. Brain stem tissue sections of TgM83$^{+/-}$ mice challenged intracerebrally, intraperitoneally, intravenously, or orally with α-synuclein fibrils showed conformer specific α-synuclein in the soma and in neurites of affected neurons. None of the BSA-challenged mice showed any fibrillar or oligomeric α-synuclein. Scale bar = 50 µm. Published in Lohmann *et al.*, 2019.

3.1.5 Pathological α-synuclein colocalizes with ubiquitin and p62 in the CNS

Abnormal proteins are targets of the quality-control process and are directed towards the degradation machinery, including ubiquitin-mediated degradation by the proteasome. In line with this pathological α-synuclein in Lewy bodies has been shown

to be marked for degradation with ubiquitin without being efficiently removed (Lowe *et al.*, 1988; Kuusisto, Parkkinen and Alafuzoff, 2003; Masuda-Suzukake *et al.*, 2013). Hence, brain stem and spinal cord sections from TgM83$^{+/-}$ mice inoculated orally, intracerebrally, intraperitoneally, or intravenously with α-synuclein fibrils or BSA were double stained for phosphorylated α-synuclein (EP1536Y) and ubiquitin (MAB1510). Immunofluorescence staining confirmed co-localization of phosphorylated α-synuclein and ubiquitinated protein deposits in brain stem and spinal cord sections of diseased mice of all groups. In contrast, none of the healthy BSA controls showed deposits of phosphorylated α-synuclein or ubiquitin (Figure 3.7).

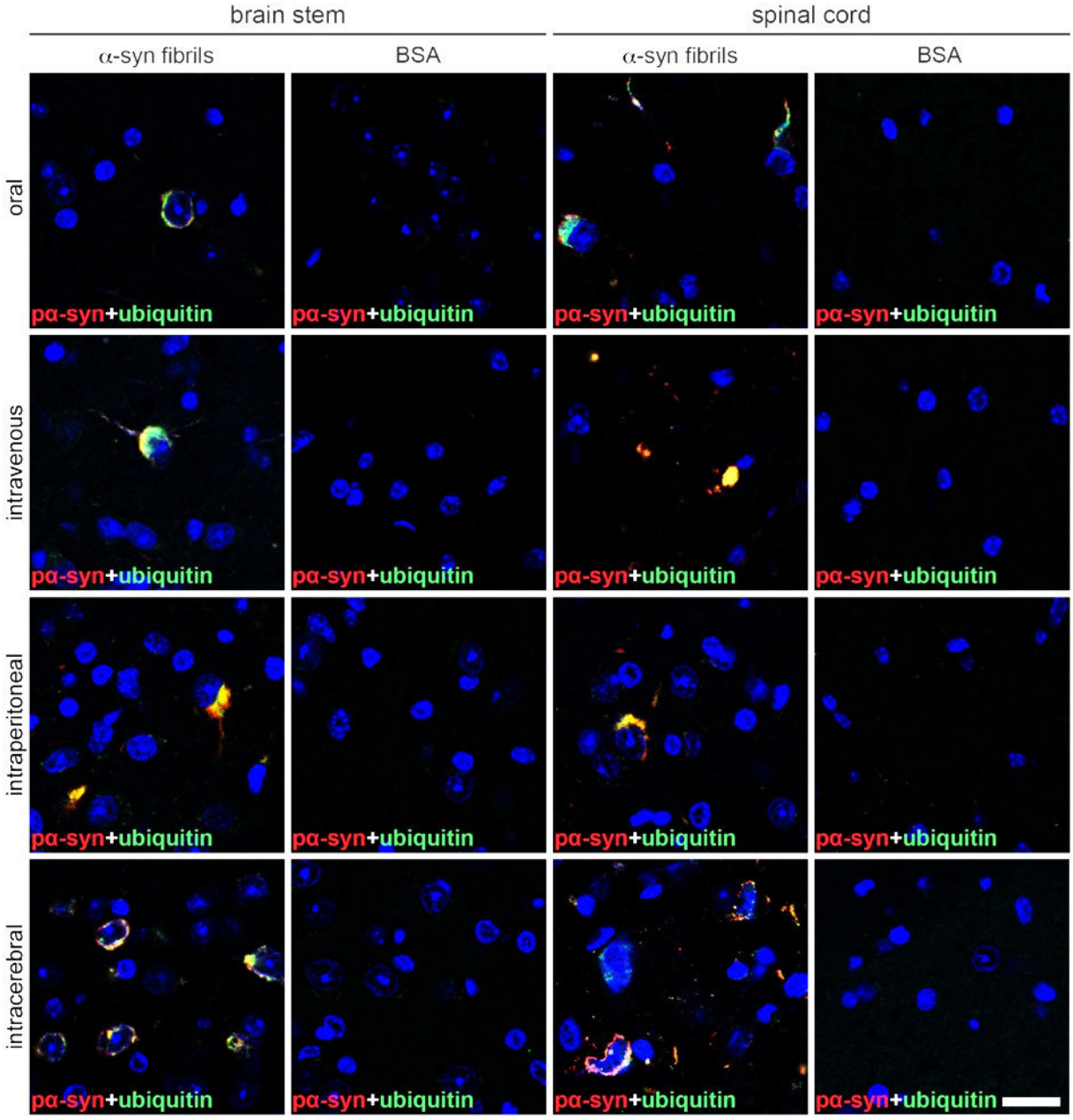

Figure 3.7: Aggregates of phosphorylated α-synuclein colocalize with ubiquitin in the CNS of inoculated TgM83$^{+/-}$ mice inoculated with α-synuclein fibrils. Immunofluorescence staining of brain stem and spinal cord tissue sections shows that phosphorylated α-synuclein (red), detected by the EP1536Y antibody, colocalizes with ubiquitin (green), detected by the MAB1510 antibody (shown are merged images). Colocalization (yellow) was detected in all

TgM83$^{+/-}$ mice inoculated with human α-synuclein fibrils, regardless of the inoculation route. In contrast, none of the BSA-challenged mice showed phosphorylated α-synuclein or ubiquitin protein deposits either in the brain stem nor in the spinal cord. Nuclear staining with DAPI is shown in blue. Scale bar = 20 µm. Published in Lohmann *et al.*, 2019.

Correlating closely with the ubiquitination of phosphorylated α-synuclein, Lewy bodies have also been shown to include the ubiquitin-binding protein p62 (Sequestome-1), which is normally involved in the proteasomal degradation of ubiquitinated proteins through activation of autophagy-mediated clearance, a process that seems to be inhibited in inclusion bodies (Kuusisto, Salminen and Alafuzoff, 2001; Watanabe *et al.*, 2012; Sato *et al.*, 2018). Given the ubiquitination of phosphorylated α-synuclein, validation of pathological α-synuclein after fibril inoculation was shown by immunofluorescence staining for phosphorylated α-synuclein (pSyn#64) and p62 (18420-1 AP). Double-staining of brain stem and spinal cord sections confirmed co-localization of phosphorylated α-synuclein and p62 in the brains of diseased mice. Neither deposits of phosphorylated α-synuclein nor p62 were detected in BSA control mice (Figure 3.8).

Thus, co-localization of phosphorylated α-synuclein with ubiquitin or p62 indicates an aberrant protein homeostasis in the CNS of TgM83$^{+/-}$ mice challenged intracerebrally, intravenously, intraperitoneally, or orally with human α-synuclein fibrils.

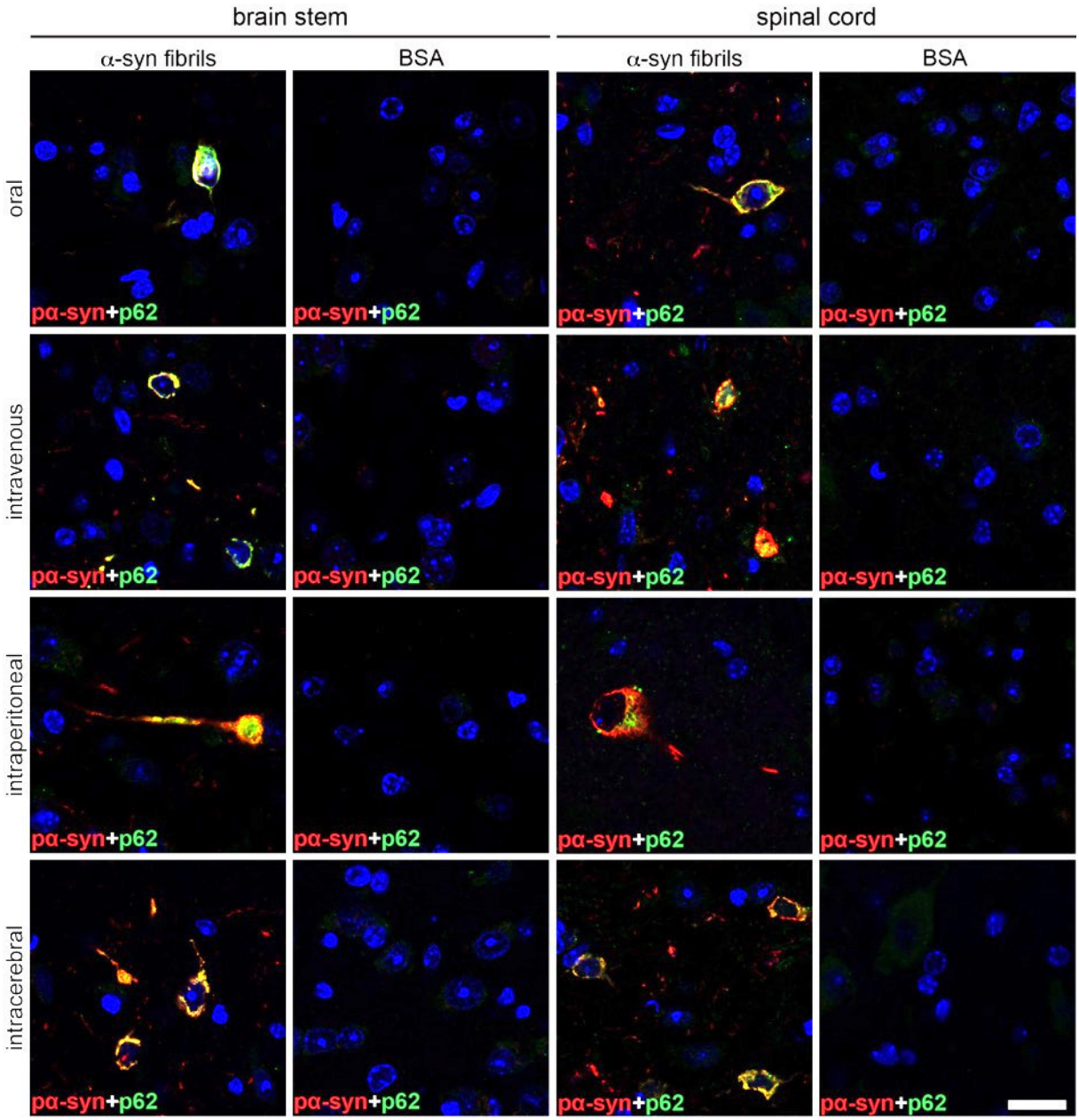

Figure 3.8: Aggregates of phosphorylated α-synuclein colocalize with p62 in the CNS of inoculated TgM83$^{+/-}$ mice inoculated with α-synuclein fibrils. Immunofluorescence staining of brain stem and spinal cord tissue sections shows that phosphorylated α-synuclein (red), detected by the pSyn#64 antibody, colocalizes with p62 (sequestome-1, green), detected by the 18420-1 AP antibody (shown are merged images). Colocalization (yellow) was detected in all TgM83$^{+/-}$ mice inoculated with human α-synuclein fibrils, regardless of the route. In contrast, none of the BSA-challenged mice showed phosphorylated α-synuclein or p62-tagged protein deposits, either in the brain stem nor in the spinal cord. Nuclear staining with DAPI is shown in blue. Scale bar = 20 µm. Published in Lohmann *et al.*, 2019.

3.1.6 Pathological α-synuclein induces neuroinflammation in the brains of diseased mice

The progression of neurodegeneration in synucleinopathies is often indicated by α-synuclein pathology, which is accompanied by increased astrogliosis and microgliosis (Zhang *et al.*, 2005; Breid *et al.*, 2016; Duffy *et al.*, 2018). Therefore, brain stem sections of TgM83$^{+/-}$ mice inoculated intracerebrally, intravenously, intraperitoneally, or orally were analyzed by immunofluorescence co-staining of phosphorylated α-synuclein (pSyn#64), and either ionized calcium-binding adaptor molecule-1 (Iba1) for microglia detection, or glial fibrillary acidic protein (GFAP) for detection of reactive astrocytes (Figure 3.9a). Quantification of the relative area occupied by microglia in close proximity to pathological α-synuclein revealed a significant increase in microgliosis after human α-synuclein fibril challenge in all diseased mice compared to BSA-challenged control mice (mean % ± SD; $p \leq 0.001$; Figure 3.9b). Area analysis of astrocytes in close proximity to pathological α-synuclein also showed a significant increase in astrogliosis in all diseased mice compared to healthy, BSA-challenged control animals (mean % ± SD; $p \leq 0.05$; Figure 3.9c).

In conclusion, neuroinflammation indicated by microgliosis and astrogliosis was significantly induced after intracerebral, intravenous, intraperitoneal, and oral challenge with α-synuclein fibrils.

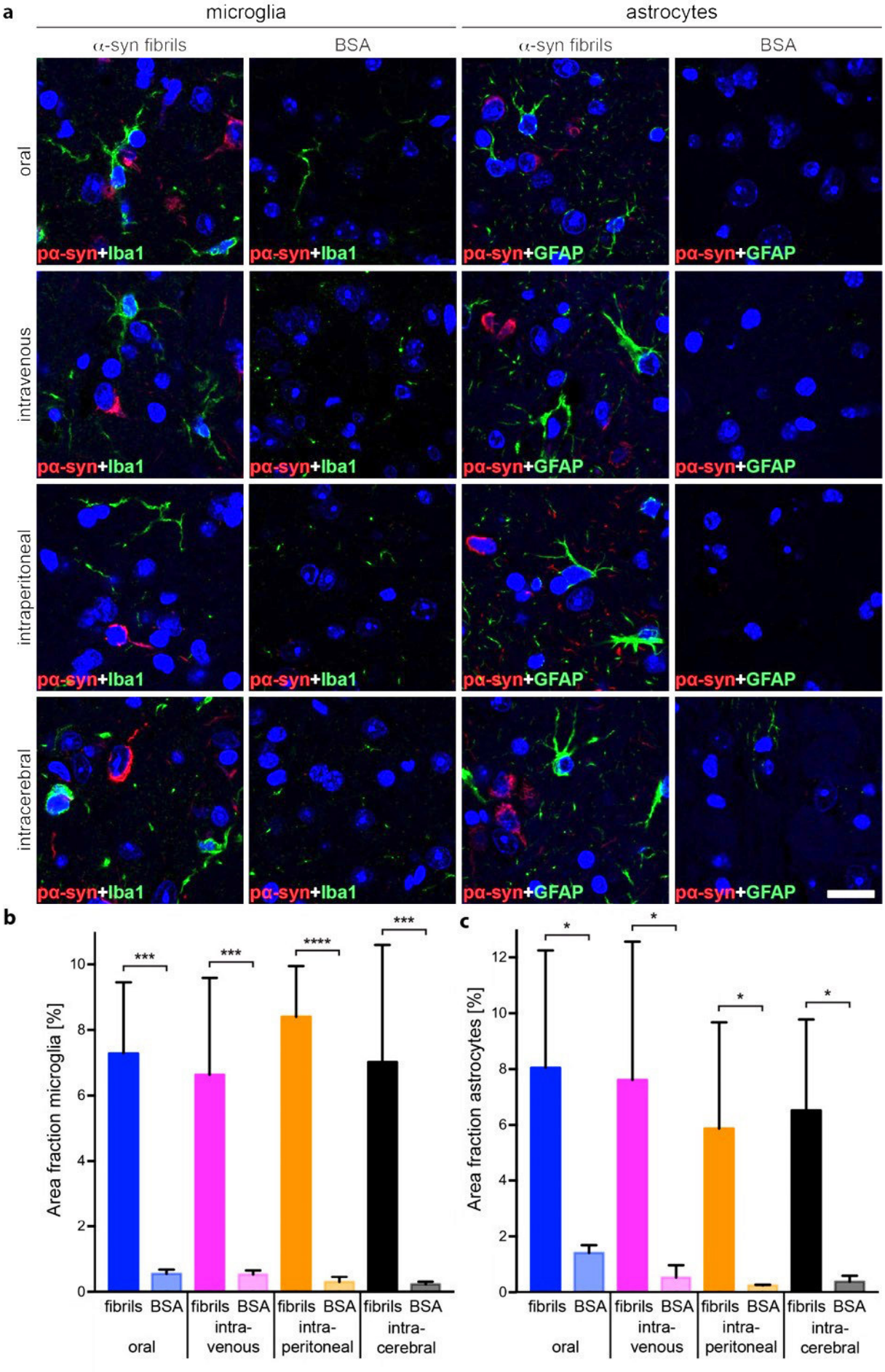
a
microglia
astrocytes
α-syn fibrils
BSA
α-syn fibrils
BSA
oral
intravenous
intraperitoneal
intracerebral
pα-syn+Iba1
pα-syn+GFAP
b
Area fraction microglia [%]
c
Area fraction astrocytes [%]
fibrils
BSA
oral
intra-venous
intra-peritoneal
intra-cerebral

Figure 3.9: Astrogliosis and microgliosis was significantly increased in TgM83$^{+/-}$ mice inoculated with human α-synuclein fibrils. Immunofluorescence staining of brain stem tissue sections of TgM83$^{+/-}$ mice challenged with α-synuclein fibrils shows that phosphorylated α-synuclein deposits (red), detected with the pSyn#64 antibody, were frequently surrounded by microglia (green), detected with the Iba-1 antibody, and astroglia (green), detected with the GFAP antibody. In contrast, none of the BSA-challenged mice showed deposits of phosphorylated α-synuclein or reactive astrocytes and microglia (a). Quantification of the brain stem of challenged TgM83$^{+/-}$ mice, positive for Iba-1 (b) or GFAP (c) after immunostaining reveals that microgliosis and astrogliosis were significantly induced in α-synuclein challenged animals regardless of the inoculation route compared to BSA-challenged animals. Data shown as mean % ± SD. One-way ANOVA followed by Holm-Šídák test (P: * ≤ 0.05, *** ≤ 0.001, **** ≤ 0.0001). n = 3–4/group. N = 4. Nuclear staining with DAPI is shown in blue. Scale bar = 20 µm. Published in Lohmann *et al.*, 2019.

3.2 MCAO study

The correlation between focal cerebral ischemia and α-synuclein aggregation is mostly unclear. This thesis aims to uncover whether the cellular response in post-stroke tissue triggers a cascade, which could induce aggregation of α-synuclein and cause the loss of dopaminergic neurons in the SN, and thus lead to PD (Spillantini *et al.*, 1997; A E Lang and Lozano, 1998; Anthony E. Lang and Lozano, 1998). Therefore, hemizygous TgM83$^{+/-}$ mice overexpressing the A53T mutant of human α-synuclein (Giasson *et al.*, 2002) were either subjected to 30 min of middle cerebral artery occlusion (MCAO) or to a negative-control sham surgery. Mice were monitored for signs of disease, weight loss, and behavioral impairment until they were sacrificed at 14, 30, 90, 180, and 360 days post surgery (dps). Ipsi- and contralateral brain hemispheres were analyzed for neuroinflammation, neurodegeneration, and pathological α-synuclein by immunohistochemical and biochemical methods.

3.2.1 MCAO-treated mice display motor deficits

Following the MCAO or sham surgery, TgM83$^{+/-}$ mice were monitored weekly for signs of malaise and disease, using a neurological scoring system and bodyweight. None of the treated mice showed any signs indicative of impaired health or neurological disease, such as reduced grooming, impaired wound healing, dyspnea, impaired movement, paralysis, or kyphosis. The only neurological abnormality mice showed after MCAO, was circling towards the left direction due to a mild hemiparesis. Also, weight gain in TgM83$^{+/-}$ mice subjected to surgery appeared to be normal. Female MCAO- and sham-treated control mice constantly gained bodyweight from 19.8 ± 1.0 g up to 29.3 ± 3.0 g over the duration of the experiment time of 360 days, indicating that they were healthy animals (Figure 3.10).

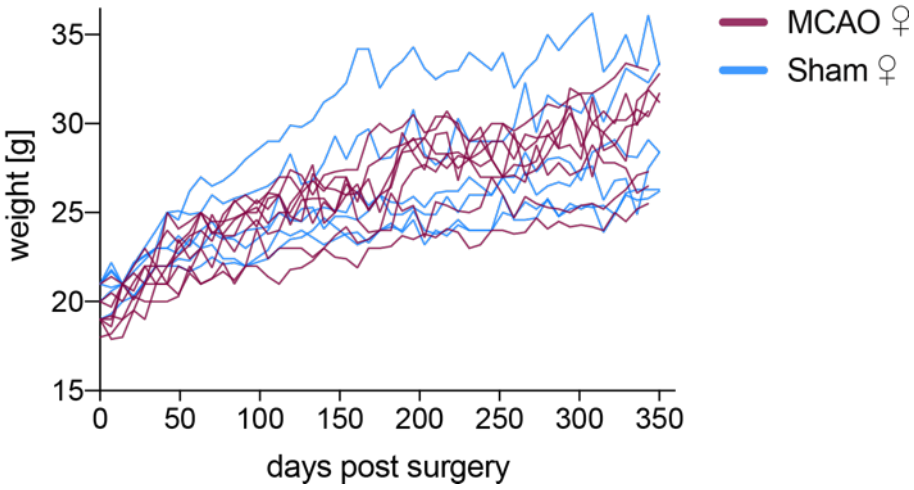

Figure 3.10: MCAO-treated TgM83$^{+/-}$ mice gain weight. Female animals subjected to MCAO (n=8, Indian red lines) as well as female sham animals (n=6, blue lines) remained healthy and continuously gained bodyweight over the maximum time of 360 days.

Behavioral assessment of MCAO- and sham-treated TgM83$^{+/-}$ mice at 90, 180, and 360 dps was performed using the rotarod test. This performance test reveals changes in the ability for motor-skill learning and coordination, and thus provides information on motor impairment (Buitrago et al., 2004). Mice were placed on an accelerating rotarod treadmill and the latency to fall was recorded. Sham-treated control mice displayed a similar latency to fall at all three timepoints, with an overall mean of 197 ± 13 s. Mice 90 days after the MCAO also displayed a similar level of motor behavior as the sham-treated mice, with a latency to fall after 219 ± 21 s. At 180 dps, a significant effect of the MCAO on the motor behavior was observed, as MCAO-treated animals displayed a significantly decreased latency to fall (153 ± 17 s; p = 0.024), compared to 90 dps. The level of motor impairment was further increased at 360 days after the MCAO. At this timepoint, the latency to fall was significantly elevated in MCAO-treated animals, compared to the early 90 dps timepoint (219 ± 21 s; p = 0.002), and also compared to the control group 360 days after the sham surgery (205 ± 20; p = 0.007; data not shown), excluding an age-dependent reduction of motor performance (Figure 3.11).

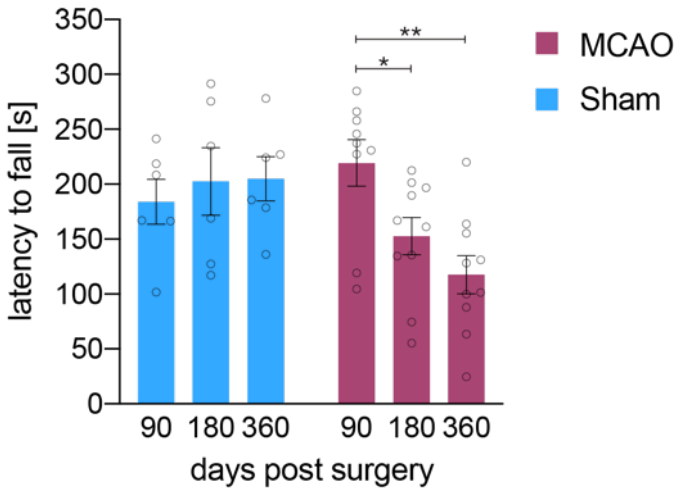

Figure 3.11: Middle cerebral artery occlusion in TgM83$^{+/-}$ leads to behavioral deficits. Sham- and MCAO-treated mice were tested for motor impairment using a rotarod at 90, 180, and 360 days post surgery. TgM83$^{+/-}$ mice that underwent 30 min MCAO (Indian red) showed significantly reduced motor skills at 180 and 360 days post surgery compared to 90 days post surgery. In contrast, sham-treated control animals (blue) did not show behavioral deficits over time. Data shown as mean ± SEM. Two-way ANOVA followed by Tukey post-hoc test (P: * ≤ 0.05, ** ≤ 0.01). n = 6–10/group.

3.2.2 MCAO-treated mice display neuronal loss

The striatum was the most affected brain region after transient MCAO and the center of the ischemic core region of the lesion. The total ischemic region ranged from bregma +1.20 mm to bregma –2.10 mm. There, neurons are the most sensitive cell types to be

affected by ischemia (Endres et al., 1998; Buscemi et al., 2019). Therefore, coronal sections at bregma 0.14 mm and bregma –1.22 mm of TgM83$^{+/-}$ mice subjected to MCAO were stained for neurons, using the NeuN antibody (MAB377), which recognizes the specific neuron-binding protein, and additional counterstaining with hematoxylin as a nuclear marker. Immunostaining visualized the neuronal population in the lesion area of TgM83$^{+/-}$ mice 14 days after the MCAO (Figure 3.12). Less neuronal staining was present in the ipsilateral hemisphere after MCAO compared to the contralateral hemisphere. Hence, the ischemic core region corresponds to the infarct volume, as it is characterized by the loss of vulnerable neurons. Due to the specific neuronal degeneration in the ipsilateral ischemic region, it can be concluded that the MCAO surgery successful induced a focal cerebral ischemia.

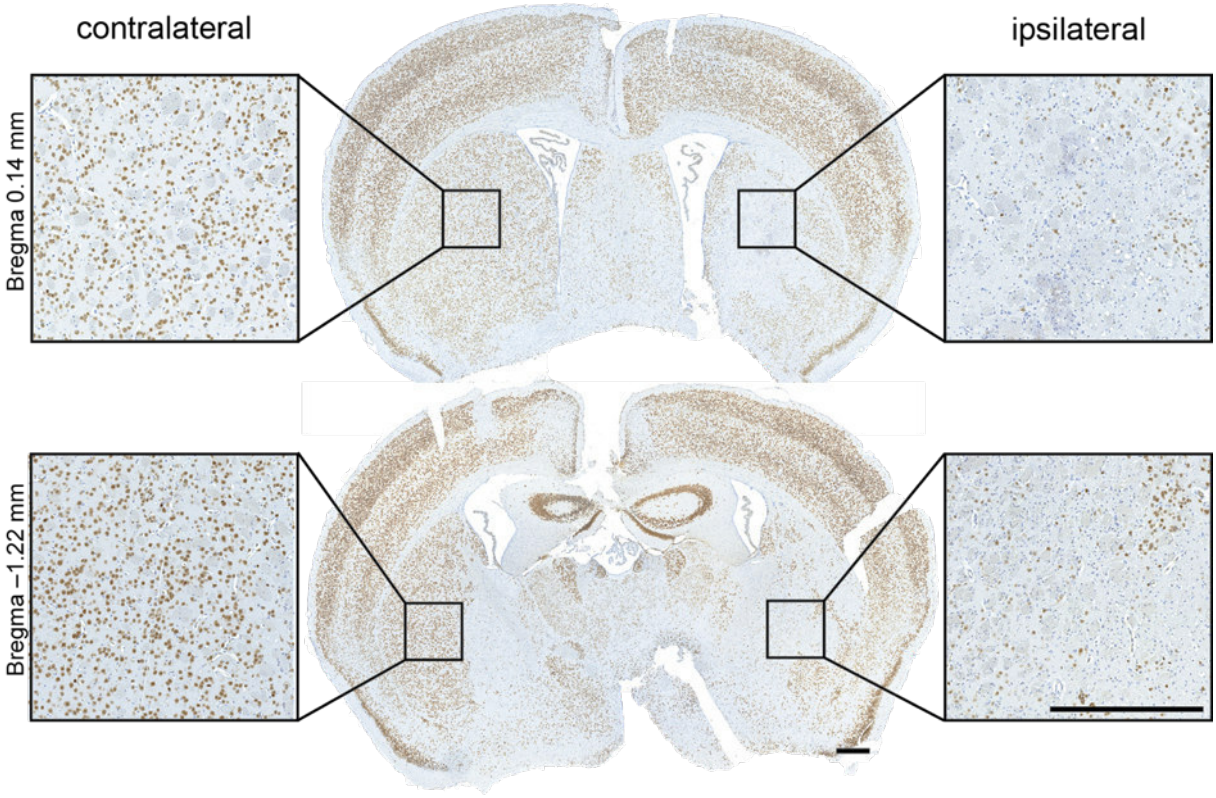

Figure 3.12: Immunohistochemical staining shows ipsilateral neuronal loss in TgM83$^{+/-}$ mice after MCAO. Neurons in the ischemic brains were detected by the MAB377 antibody, recognizing the specific neuron-binding protein NeuN. Brain sections at bregma 0.14 mm and bregma –1.22 mm of TgM83$^{+/-}$ mice subjected to MCAO showed ipsilateral neuronal degeneration in the ischemic core and peri-infarct region. Scale bar = 500 µm.

3.2.3 MCAO-induced neuroinflammation

The neurodegeneration in ischemic tissue is accompanied by an early induction of microgliosis and astrogliosis (Iadecola and Anrather, 2011; Kuric and Ruscher, 2014). In synucleinopathies on the other hand, an increased neuroinflammation is due to the progression of neurodegeneration over time (Zhang et al., 2005; Breid et al., 2016). As a proof of a valid ischemia model, and to investigate the progression of

neuroinflammation over time, the stroke lesion area, ranging from bregma +1.20 mm to bregma −2.10 mm was analyzed in MCAO- and sham-treated TgM83$^{+/-}$ mice. Therefore, 12 brain sections throughout the lesion area were stained for microglia, using the ionized calcium-binding adaptor molecule-1 (Iba-1) and an additional counterstaining with hematoxylin as a nuclear marker. Immunostaining visualized microglia in the acute stroke tissue of ipsi- and contralateral brain hemispheres of MCAO- and sham-treated TgM83$^{+/-}$ mice over a time of 360 dps (Figure 3.13a). Quantification of relative area occupied by microglia revealed an induction of microgliosis in the ipsilateral hemisphere of MCAO-treated mice. A significantly increased microgliosis was detected at 14 dps in ipsilateral MCAO brains (3.7 ± 2.6%; $p < 0.0001$), compared to the contralateral hemisphere (0.8 ± 0.4%), as well as to the ipsi- (0.8 ± 0.4%) and contralateral sham controls (0.6 ± 0.3%). In ipsilateral MCAO tissue 30 dps microglia were still significant increased (2.9 ± 2.6 %; $p < 0.0001$) compared to the contralateral hemisphere (0.9 ± 0.5%) and to ipsi- (1.3 ± 0.9%) and contralateral sham control brains (0.9 ± 0.4%), although a significant decrease compared to the ipsilateral MCAO hemisphere at 14 dps was displayed ($p = 0.007$). At 90 dps ipsilateral MCAO tissue displayed significant increased microgliosis (1.9 ± 1.6%; $p < 0.0001$) compared to sham controls (ipsi: 0.5 ± 0.4%; contra: 0.4 ± 0.4%). In contrast, no significant difference was detected within the MCAO- and sham-treated hemispheres at 180 dps. A significant reduction in microgliosis in the ipsilateral stroke lesion area compared to 14 dps was also observed at 90 (1.9 ± 1.6%), 180 (1.6 ± 0.7%), and 360 dps (2.1 ± 0.7%; $p < 0.0001$), although at 360 dps a trend, that the area fraction of microglia seems to be increasing again was visible. Additionally, ipsilateral MCAO tissue shows a significant increase in microgliosis (2.1 ± 0.7%; $p < 0.0001$) compared to the ipsi- (0.6 ± 0.4%) and contralateral sham controls (0.6 ± 0.3%) at 360 dps (Figure 3.13b).

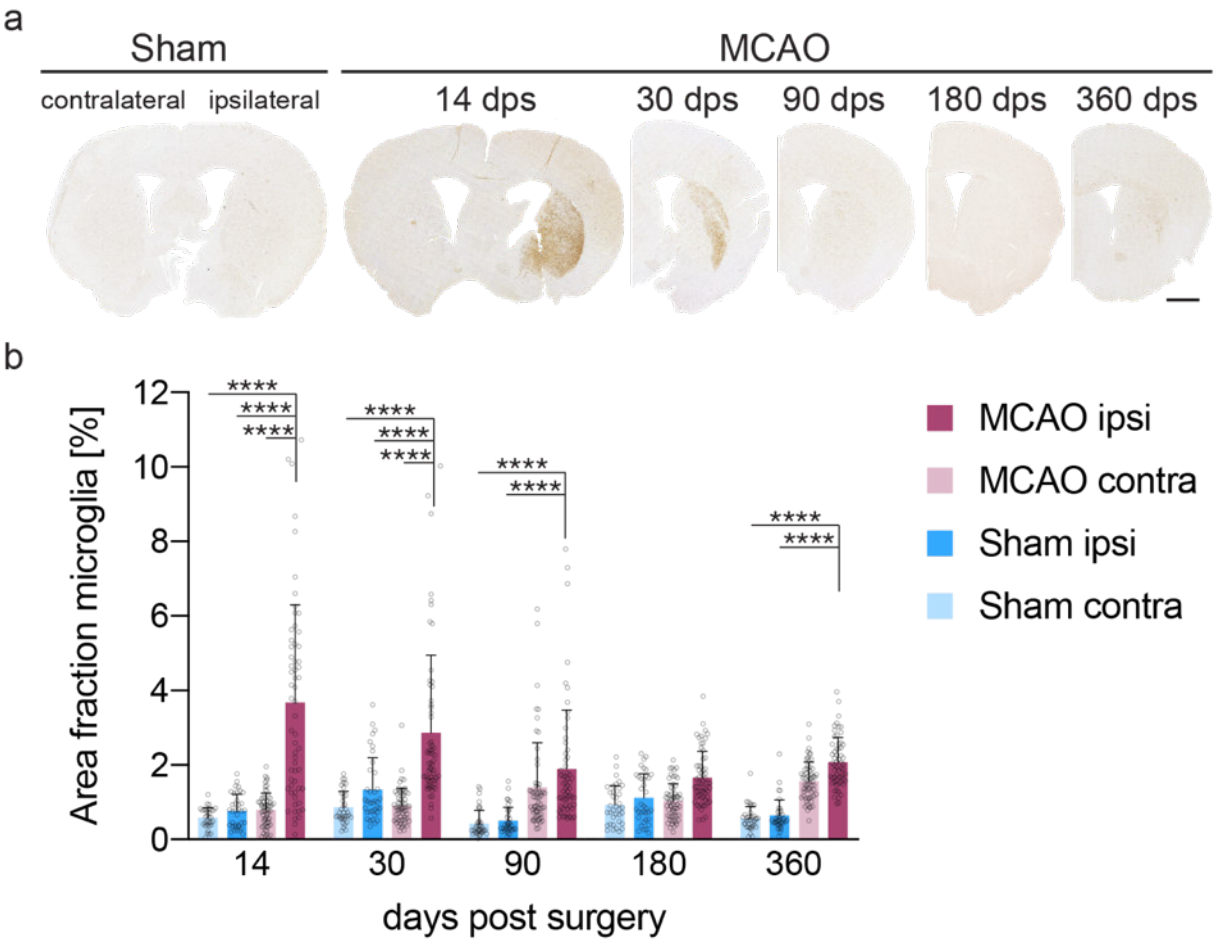

Figure 3.13: Immunhistochemical analysis shows induced ipsilateral microgliosis in TgM83$^{+/-}$ mice after MCAO. In MCAO- and sham-treated mice microglia were detected by the Iba-1 antibody within the stroke lesion area, ranging from bregma +1.20 mm to bregma –2.10 mm (a). Quantification of ipsilateral (ipsi) and contralateral (contra) hemispheres of TgM83$^{+/-}$ mice, revealed a significant ipsilaterally induced microgliosis in mice subjected to MCAO (dark Indian red), when compared to the ipsi- (dark blue) and contralateral (light blue) hemispheres of sham-treated animals. Significantly increased microgliosis was present ipsilaterally in MCAO mice 14, 30, 90, and 360 days post surgery (dps) (b). Data shown as mean % ± SD. Two-way ANOVA followed by Tukey post-hoc test (P: **** < 0.0001). n = 3-5/group. N = 12. Scale bar = 1000 µm.

Next to microgliosis, TgM83$^{+/-}$ mice were also analyzed for astrogliosis as a marker for induced ischemia and the progression of neurodegeneration over time. Therefore, six sections of the lesion area, ranging from bregma +1.20 mm to bregma –2.10 mm were stained for glial fibrillary acidic protein (GFAP) for detection of reactive astrocytes and additionally counterstained with hematoxylin as a nuclear marker. Immunostaining revealed an increase in staining for astrocytes in the ipsi- and contralateral brain hemispheres of MCAO- and sham-treated TgM83$^{+/-}$ mice over a time of 360 dps (Figure 3.14a). Quantification of relative area fraction of astrocytes revealed an induction of astrogliosis in the ipsilateral hemisphere of MCAO-treated mice. At 14 dps a significantly increased astrogliosis was detected in the ipsilateral MCAO-treated hemisphere (13.6 ± 7.7%; $p < 0.0001$) compared to the contralateral hemisphere (1.1 ± 1.4%), as well as to the ipsi- (2.3 ± 1.2%) and contralateral hemispheres of sham

controls (1.6 ± 1.9%). Astrogliosis in ipsilateral MCAO tissue was still significantly increased after 30 days (8.5 ± 5.9%; $p < 0.0001$) compared to the contralateral tissue (2.1 ± 2.3%) and to ipsi- (1.9 ± 1.4%) and contralateral (1.0 ± 1.0%) tissue of sham control brains. No significant difference in astroglia was detected at 90 dps within the MCAO- and sham-treated hemispheres. At 180 days after the MCAO, a significant ipsilateral increase in astroglia was detected (5.6 ± 5.9%) when compared to the contralateral side (2.2 ± 1.7%; $p = 0.0184$) and the ipsi- (0.9 ± 0.9%; $p = 0.0006$) and contralateral (0.4 ± 0.5%; $p < 0.0001$) side of sham control mice. Ultimately, a significant increase in microgliosis was detected in the ipsilateral MCAO hemisphere (6.8 ± 5.0%) compared to the contralateral hemisphere (3.3 ± 2.2%, $p = 0.0110$) and both hemispheres of sham control mice (ipsi: 0.8 ± 0.7%; contra: 0.5 ± 0.6%; $p < 0.0001$) at 360 dps (Figure 3.14b).

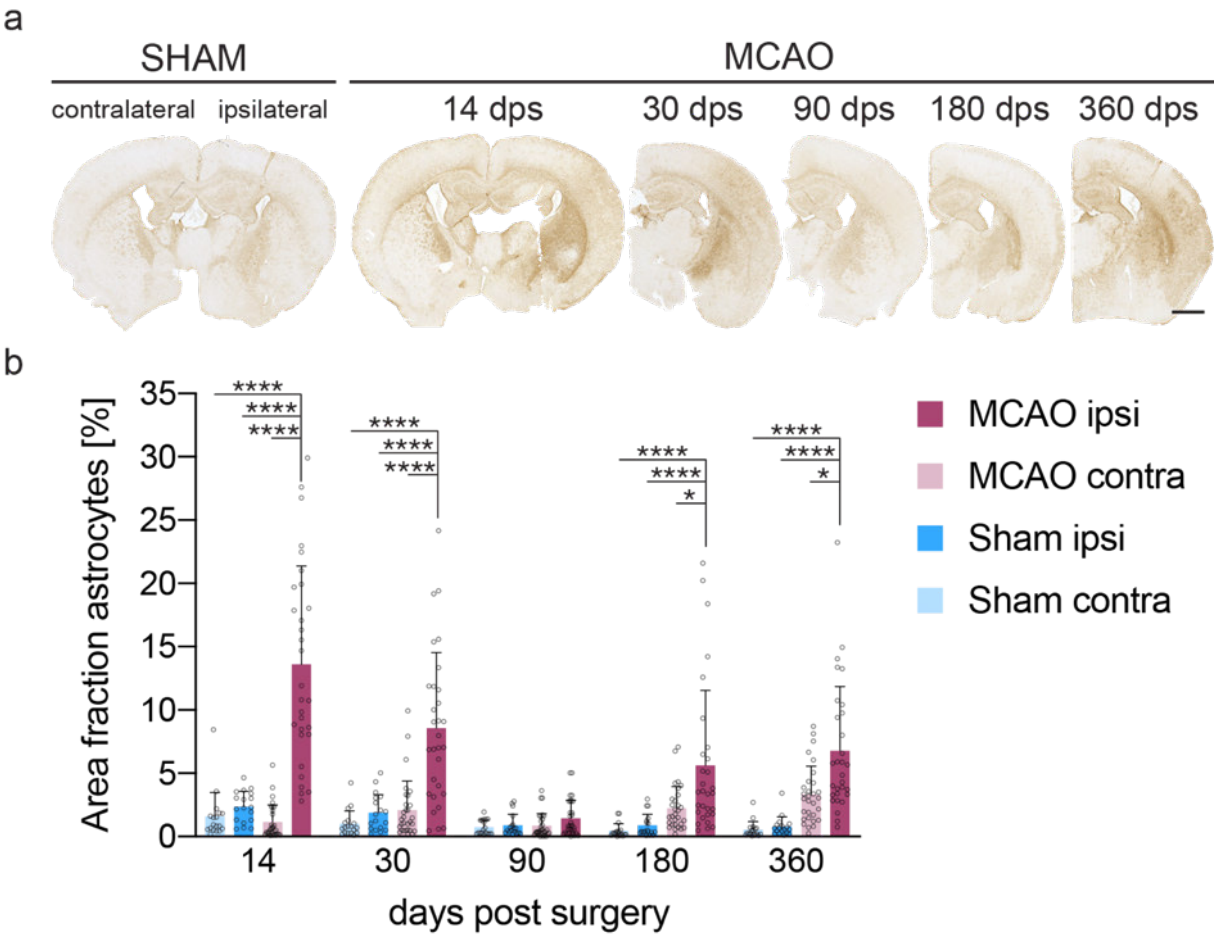

Figure 3.14: Immunhistochemical analysis shows induced ipsilateral astrogliosis in TgM83$^{+/-}$ mice after MCAO. In MCAO- and sham-treated mice astroglia were detected by the GFAP antibody within the stroke lesion area, ranging from bregma +1.20 mm to bregma –2.10 mm (a). Quantification of ipsilateral (ipsi) and contralateral (contra) hemispheres of TgM83$^{+/-}$ mice, revealed a significant ipsilaterally induced astrogliosis in mice subjected to MCAO (dark Indian red) when compared to ipsi- (dark blue) and contralateral (light blue) sham animals. Significantly increased astrogliosis was present ipsilaterally in MCAO mice at 14, 30, 180, and 360 days post surgery (b). Data shown as mean % ± SD. Two-way ANOVA followed by Tukey post-hoc test (P: * < 0.05, **** < 0.0001). n = 3-5/group. N = 6. Scale bar = 1000 µm.

Additionally, astrogliosis in the ipsilateral MCAO hemisphere of TgM83$^{+/-}$ mice was significantly reduced for later time points, when compared to 14 dps ($p < 0.0001$; data not shown). Although the data showed that astrogliosis in ipsilateral stroke tissue was significantly increased at 14 dps (13.6 ± 7.7%) astrogliosis is decreasing in the lesion area for up to 90 dps (1.4 ± 1.4%). Onwards from 90 dps astrogliosis in the ipsilateral lesion area was significantly increased again, up to 5.6 ± 5.9% at 180 dps ($p = 0.0004$; data not shown), and 6.8 ± 5.0% area fraction of astroglia ($p < 0.0001$; data not shown) at 360 dps.

Generally, 30 min of MCAO induced a significant, acute, and early neuroinflammation in the ipsilateral brain hemisphere of TgM83$^{+/-}$ mice. Additionally, a decrease in neuroinflammation was observed in the lesion area for time points greater than 14 dps and lasting for up to 90 or 180 dps. At 360 dps, a renewed increase in neuroinflammation was detected, as the number of microglia and astrocytes was increased again in MCAO-treated animals.

3.2.4 MCAO leads to a loss of dopaminergic neurons

To determine if a stroke can induce PD, MCAO-treated mice were analyzed for a loss of dopaminergic neurons in the substantia nigra (SN), which is one of the hallmarks of PD (Hirsch, Graybiel and Agid, 1988; Petrucelli *et al.*, 2002). Therefore, dopaminergic neurons in four SN sections per TgM83$^{+/-}$ mouse were immunostained, using the ab152 antibody, recognizing tyrosine hydroxylase (TH). Nuclei were counterstained with hematoxylin. Immunostaining visualized dopaminergic neurons in the SN of ipsi- and contralateral brain hemispheres of MCAO- and sham-treated TgM83$^{+/-}$ mice over a period of 360 days (Figure 3.15a). No significant loss of dopaminergic neurons was detected at 14, 30, 90, and at 180 dps, as MCAO- and sham-treated mice displayed a similar number of dopaminergic neurons with 107.8 ± 13.3 TH^{+} cells in both brain hemispheres. In contrast, degeneration of dopaminergic neurons was detected in the ipsilateral hemisphere of MCAO-treated animals at 360 dps. With 74.45 ± 27.9 TH^{+} cells the number of dopaminergic neurons was significantly reduced in the ipsilateral hemisphere of MCAO-treated mice when compared to the contralateral hemisphere with 119.5 ± 47 cells ($p = 0.0047$), and the ipsi- (124.8 ± 28.7 cells; $p = 0.0004$) and contralateral hemispheres (117.9 ± 29.6 cells; $p = 0.0024$) of sham-treated control mice (Figure 3.15b).

In conclusion, MCAO with a 30 min ischemia leads to a significant loss of dopaminergic neurons in the ipsilateral brain hemisphere of TgM83$^{+/-}$ mice within 360 dps.

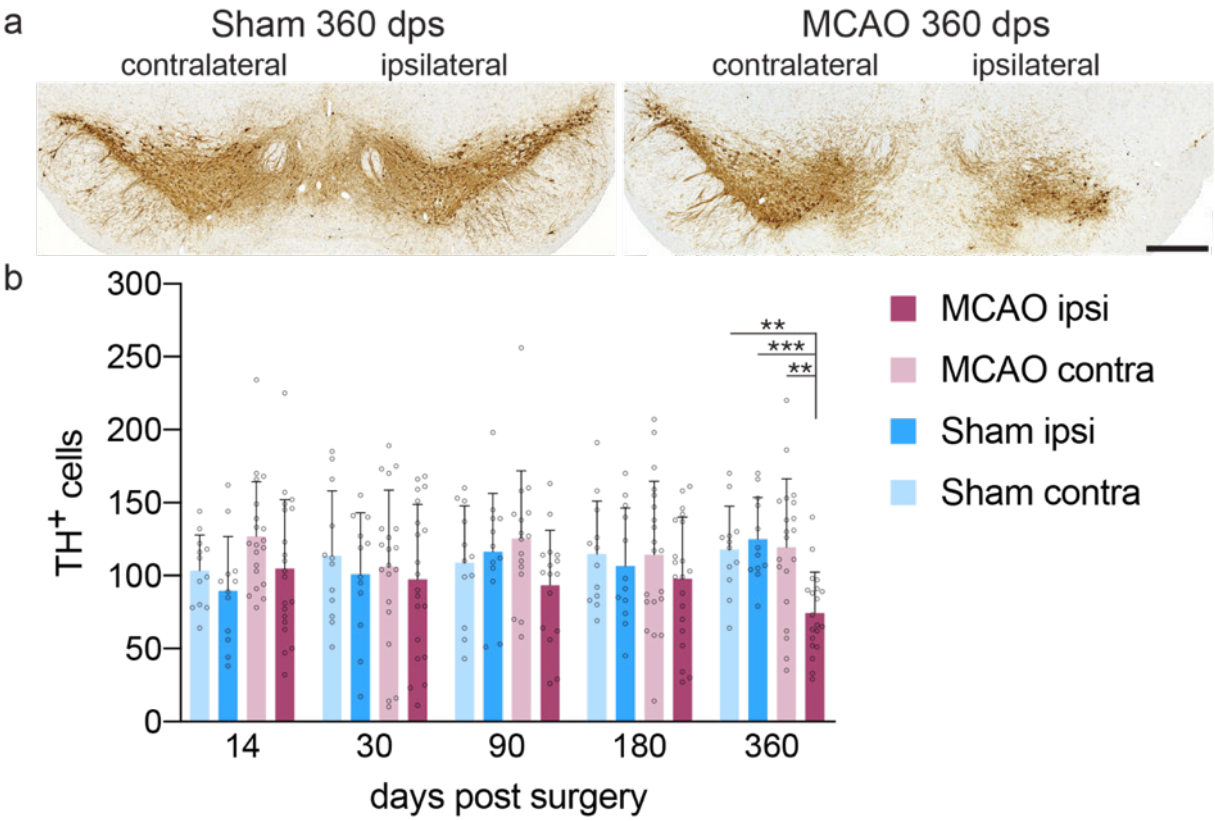

Figure 3.15: Immunhistochemical analysis shows ipsilateral loss of dopaminergic neurons in TgM83$^{+/-}$ mice at 360 days after MCAO. In the substantia nigra of MCAO- and sham-treated mice dopaminergic neurons were detected with an antibody against TH (a). Quantification of TH^{+} cells in the ipsilateral (ipsi) and contralateral (contra) area of the substantia nigra of TgM83$^{+/-}$ mice, revealed significant loss of dopaminergic neurons in its ipsilateral part of mice that had been subjected to an MCAO-treatment (dark Indian red) when compared to the contralateral (light Indian red) or the sham-treated control animals (dark and light blue) at 360 days post surgery (b). Data shown as mean TH^{+} cell numbers ± SD. Two-way ANOVA followed by Tukey post-hoc test (P: ** < 0.01, *** < 0.001). n = 3-5/group. N = 4. Scale bar = 500 µm.

3.2.5 MCAO causes α-synuclein to aggregate

Since a significant loss of dopaminergic neurons in the SN was observed at 360 dps, the correlation between MCAO and PD was further investigated. To this end, mice subjected to MCAO were examined for an accumulation of aggregated α-synuclein in their CNS, which is another hallmark of PD (Spillantini *et al.*, 1997; Baba *et al.*, 1998). Thus, a homogeneous time resolved fluorescence technology (FRET) assay was performed with brain homogenates of MCAO- and sham-treated TgM83$^{+/-}$ mice to quantify the amount of α-synuclein aggregates in each brain hemisphere (Figure 3.16). No difference was observed between all four groups at 14 dps. At 30 dps, both brain hemispheres of MCAO-treated animals showed a significantly elevated amount of aggregated α-synuclein when compared to sham-treated control mice. The ipsilateral hemisphere of MCAO-treated mice (636.73 ± 14.6) showed a significantly increased amount of aggregated α-synuclein when compared to contralateral (614.2 ± 20.7; p = 0.0146), and ipsi- and contralateral (508.9 ± 6.6; 503.4 ± 6.7; p < 0.0001) sham-treated mice. A significant increase was also measured in MCAO-treated (718.9 ±

13.0) mice when compared to sham-treated mice (ipsi: 508.4 ± 7.1; contra: 512.4 ± 6.5; $p < 0.0001$) treated mice at 90 dps, and at 180 dps (MCAO ipsi: 815.2 ± 12.3; sham: ipsi: 513.6 ± 3.9; contra: 517.1 ± 4.6; $p < 0.0001$). At 360 dps, the level of aggregated α-synuclein in the ipsilateral hemisphere of MCAO-treated mice (1043.3 ± 13.3, $p < 0.0001$) was significantly increased when compared to the contralateral hemisphere (1011.1 ± 8.5), and both hemispheres of control mice (520.7 ± 7.6).

Thus, the amount of aggregated α-synuclein in brain homogenates prepared from ipsi- (512.5 ± 7.8) and contralateral (512.8 ± 9.0) brain hemispheres of sham-treated control mice remained similarly low over 360 days, while the level of aggregated α-synuclein in the brains of mice subjected to MCAO increased significantly over time.

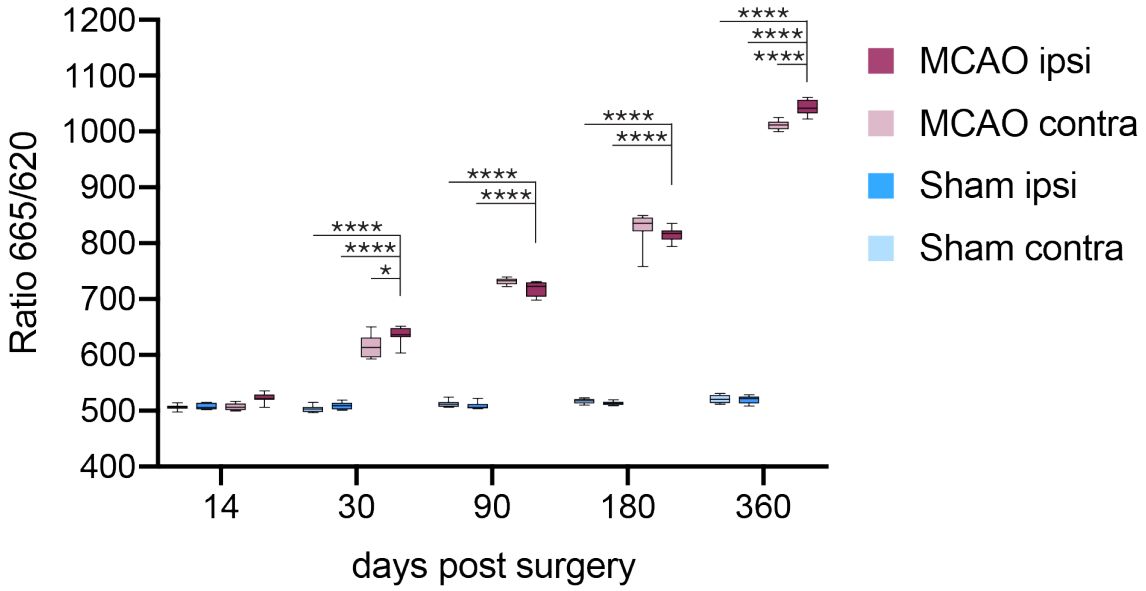

Figure 3.16: The amount of aggregated α-synuclein was increased in the brains of TgM83$^{+/-}$ mice after MCAO. The amount of aggregated α-synuclein was quantified in brain homogenates prepared from the ipsilateral (ipsi, dark color) and contralateral (contra, light color) brain hemispheres of TgM83$^{+/-}$ mice subjected to MCAO- (Indian red) or sham-treated animals (blue) using FRET assay. Significantly increased amounts of aggregated α-synuclein were detected in both brain hemispheres of mice subjected to MCAO at 30, 90, 180, and 360 days post surgery when compared to the sham controls. Data shown as whiskers from minimum to maximum with the additional horizontal line in the box representing the median. Two-way ANOVA followed by Tukey post-hoc test (P: * < 0.05, **** < 0.0001). n = 3/group. N = 3.

4 Discussion

4.1 Peripheral challenge study

This study successfully showed the onset of neurological disease after a single challenge of TgM83$^{+/-}$ mice with human recombinant α-synuclein fibrils along four different routes. Several characteristic traits of synucleinopathies were identified. Among these were inclusions of phosphorylated α-synuclein in the soma and neurites of neurons, colocalization of phosphorylated α-synuclein with ubiquitin and p62, as well as the presence of specific oligomeric and fibrillar conformers of pathologic α-synuclein, along with neuroinflammation as evidenced by astrogliosis and microgliosis, and the development of motor impairment. All these pathologic changes showed that α-synuclein prionoids can invaded the CNS and cause disease, not only after intracerebral and intraperitoneal, but also after a single intravenous and oral challenge of α-synuclein fibrils.

Both oral and intravenous transmission of prions are known to cause clinical prion disease (Hunter *et al.*, 2002; Huang and MacPherson, 2004). Moreover, several studies have shown that intracerebral challenge of WT and Tg mice with recombinant α-synuclein fibrils induce prion-like propagation of phosphorylated α-synuclein pathology, ultimately causing CNS disease (Kelvin C. Luk *et al.*, 2012; Masuda-Suzukake *et al.*, 2013; Rutherford *et al.*, 2017). Additionally, transmission from the periphery to the CNS was verified via intraperitoneal transmission of α-synuclein fibrils (Breid *et al.*, 2016; Sargent *et al.*, 2017). In this study, both types of transmission, intracerebrally and intraperitoneally injections were used as a control for the infectivity of the produced recombinant α-synuclein fibrils. Findings of pathological α-synuclein in the myenteric and submucosal plexuses of the gastrointestinal wall in PD patients suggest the existence of a gut-to-brain propagation of pathological α-synuclein via peripheral nerves (Holmqvist *et al.*, 2014; Manfredsson *et al.*, 2018). To gain further insights into the prion-like behavior of α-synuclein, this work investigated the propensity of α-synuclein fibrils to induce a synucleinopathy after oral challenge. Furthermore, systemic challenge after a single intravenous injection of recombinant human α-synuclein fibrils in TgM83$^{+/-}$ mice was investigated.

4.1.1 Intracerebral injection of α-synuclein fibrils causes neurological disease

Several transmission studies have been published over the last decade, of which most primarily focused on intracerebral transmission and later also on peripheral transmission. Injection of α-synuclein fibrils into different brain regions, such as the striatum, hippocampus, and SN, as well as intramuscular injection into the femoris or

gastrocnemius muscle, and intragastric and intraperitoneal injections successfully seeded the aggregation of endogenous α-synuclein causing central and peripheral spreading of α-synuclein and neuropathology (Kelvin C Luk *et al.*, 2012; Masuda-Suzukake *et al.*, 2013; Sacino, Brooks, Thomas, McKinney, Lee, *et al.*, 2014; Breid *et al.*, 2016). Even though an aggregation of α-synuclein was observed in all studies, the severity of neuropathology and the propagation of pathologic α-synuclein throughout the brain differed, and a loss of dopaminergic neurons or motor impairment was not seen in all studies. These different outcomes likely originate in different experimental setups, starting from α-synuclein fibril preparation, resulting in various protein conformations and therefore in various seeding properties. Some studies used recombinant mouse α-synuclein fibrils, whereas others used human α-synuclein fibrils. In a WT mouse model, mouse α-synuclein fibrils are shown to be more effective in spreading and showing a rapid-onset of disease phenotypes compared to human fibrils (Kelvin C Luk *et al.*, 2012). In contrast, human α-synuclein fibrils are more pathogenic than mouse α-synuclein fibrils in Tg mouse models overexpressing specific mutant human forms of α-synuclein such as the TgM83$^{+/-}$ mouse model (Sacino, Brooks, Thomas, McKinney, McGarvey, *et al.*, 2014). Even pathogenic human α-synuclein can come in different oligomeric or fibrillar forms, and have several protein modifications caused by deletion or mutation of various amino acids (Rutherford *et al.*, 2017). For fibril formation, aggregation of recombinant α-synuclein is mostly done by shaking at 37 ˚C but protocols differ in duration of the shaking, which can range from 3 to 7 days, possibly resulting in intermediates with different conformations, affecting the toxicity and propagation properties of the respective prepared fibril (Winner *et al.*, 2011). Additionally, fibrils are mostly sonicated to obtain fibrils with a length under 100 nm, as these transmit more easily than larger fibrils, and therefore lead to a rapid disease onset (Tarutani *et al.*, 2016). Finally, bacterial endotoxins should be removed from the prepared recombinant α-synuclein fibrils, as these likely enhance inflammation and indirectly affect the propagation properties of α-synuclein, and may even result in structurally distinct α-synuclein fibril strains (Gao *et al.*, 2011; C. Kim *et al.*, 2016).

In this thesis, the Tg mouse line TgM83$^{+/-}$, overexpressing human α-synuclein was used, and thus, recombinant human WT α-synuclein preformed fibrils were prepared for inoculation. It was shown in previous studies that transmission of human α-synuclein fibrils to Tg mice recruits endogenous monomeric human α-synuclein, carrying the familial A53T mutation, which is overexpressed in TgM83$^{+/-}$ mice. Human α-synuclein preformed fibrils seed the aggregation of α-synuclein, leading to a rapid onset of a synucleinopathy (Bétemps *et al.*, 2014; Sargent *et al.*, 2017). As the aim of this study was to investigate different routes of neuroinvasion of α-synuclein from the periphery, regarding transmission and synucleinopathy onset, WT α-synuclein fibrils were used. These were assembled by agitation at 37 ˚C for 7 days, resulting in larger α-synuclein species, including protofibrils and fibrils. The following sonication step resulted in α-synuclein preformed fibrils with a majority fibril length of 25 nm to 70 nm (Figure 3.1), possessing a well-suited fibril length for cell-to-cell transmission and a

rapid disease onset (Tarutani *et al.*, 2016). An endotoxin removal kit ensured low levels of endotoxins in the prepared α-synuclein fibrils (>0.01 EU/ mL), so that an effect on neuropathology by endotoxins could be excluded, resulting in potent recombinant human WT α-synuclein preformed fibrils.

The amount of inoculum used in intracerebral transmission studies in mice varies considerably, with some studies reporting the use of 2 *µ*g and others of up to 25 *µ*g of α-synuclein fibrils (Kelvin C Luk *et al.*, 2012; Bétemps *et al.*, 2014). Aggregation of α-synuclein with subsequent CNS disease could be induced upon intracerebral injection of 4 *µ*g, whereas 2 *µ*g of preformed α-synuclein fibrils failed to cause aggregation and disease (Sacino, Mieu Brooks, McGarvey, McKinney, Thomas, Levites, *et al.*, 2014; Sacino, Mieu Brooks, Shaw, Golde, Giasson, McKinney, *et al.*, 2014). In primary cultured neurons a dose-dependency between the amount of inoculated α-synuclein fibrils and the pathological outcome was observed (Volpicelli-Daley, Luk and Lee, 2014). However, in mice a dose-dependency upon intramuscular injection was not observed, as mice injected with 2 *µ*g, 5 *µ*g, and 10 *µ*g preformed fibrils had similar mean survival times until disease onset, and also did not show a major difference in α-synuclein aggregation and spreading, suggesting that for intramuscular injections the highest infectious dose was already reached using 2 *µ*g preformed fibrils (Sorrentino *et al.*, 2018). In previous studies a single intraperitoneal injection with 50 *µ*g of human α-synuclein fibrils was sufficient to cause CNS disease in TgM83$^{+/-}$ mice (Breid *et al.*, 2016). Based on that, a concentration of 50 *µ*g α-synuclein fibrils was chosen as inoculum for intraperitoneal, intravenous, intracerebral, and oral challenge. To further evaluate parameters of neuropathology a lower dose of 10 *µ*g fibrils was used for intracerebral challenge of an additional mouse cohort, as this is the commonly used amount for intracerebral challenge. Since 50 *µ*g of α-synuclein fibrils may be extremely diluted upon arrival in the stomach, a high-level dose of 500 *µ*g fibrils was used for oral challenge of an additional cohort as well. According to *Sorrentino et al.*, in this study a dose-dependence upon intracerebral injection of 10 *µ*g and 50 *µ*g preformed α-synuclein fibrils was not observed (Sorrentino *et al.*, 2018). The mean survival times within these two groups just differed in 23 days, until α-synuclein aggregation caused CNS disease (Figure 3.1, Table 7). Additionally, similar amounts of aggregated α-synuclein were detected in the brains and spinal cords of injected mice, also displaying a comparable spreading pattern throughout the CNS (Figure 3.2).

The distribution of α-synuclein and onset of neuropathology also depends on the injection sites, as injection of α-synuclein fibrils into the striatum was shown to cause faster disease onset compared to injections into the SN (Masuda-Suzukake *et al.*, 2014). Additionally, bilateral injection into the brain causes faster propagation of α-synuclein throughout the brain, even though the same total amount of fibrils is injected. Unilateral injected fibrils not only propagate caudal to rostral, but also from ipsilateral to contralateral sites, resulting in a different pathology in the contralateral

site compared to the injected site (Masuda-Suzukake *et al.*, 2013). Bilaterally injected fibrils on the other hand, are already distributed between the two hemispheres upon injection, causing faster disease onset (Sacino, Mieu Brooks, Shaw, Golde, Giasson, McKinney, *et al.*, 2014). These studies show that α-synuclein prionoids propagate over long distances via trans-synaptic pathways and axonal transport of interconnected areas in a spatiotemporal pattern throughout the brain. Pathological α-synuclein is able to transmit from cell-to-cell within the basal ganglia, causing neuropathology not only in the striatum, but also in the dopaminoceptive regions, which are connected via dopaminergic projections with the striatum, such as the SN, amygdala, and parts of the cortex, causing pathology throughout the brain (David Smith and Paul Bolam, 1990; Gibb, 1997).

According to the spatiotemporal spreading pattern, intrastriatal injection of α-synuclein fibrils in this work also resulted in propagation along the anatomical connected brain areas, causing neuropathology in the SN, amygdala, thalamus, and the neocortex (Figure 3.5). Additionally, neuropathology was observed in hippocampal regions after intrastriatal and oral but not after intraperitoneal or intravenous transmission of α-synuclein fibrils (Figure 3.4). Severe hippocampal pathology was observed after intrastriatal injection, as the striatum and hippocampus are connected via dopaminergic projections, enhancing α-synuclein spreading and toxicity along interconnected regions. In contrast, hippocampal injection of α-synuclein fibrils have been reported not to spread along these or other connections to the striatum, as no phosphorylated α-synuclein was detected there within 4 months after injection (Sacino, Mieu Brooks, Shaw, Golde, Giasson, McKinney, *et al.*, 2014). The majority of endogenous α-synuclein is expressed in the hippocampal formation of mice, therefore the hippocampus seems to be a perfect region to seed polymerization of α-synuclein fibrils (Thul and Lindskog, 2018). In line with this, elevated expression levels of α-synuclein have been detected in the human hippocampus of PD and LBD patients (Camicioli *et al.*, 2003; Apostolova *et al.*, 2010). Additionally, native α-synuclein regulates dendritic maturation of adult neurogenesis in the hippocampus, and an impairment of neurogenesis was observed in the dentate gyrus of PD patients (Höglinger *et al.*, 2004; Winner *et al.*, 2012). In the present study, oral and intracerebral challenge lead to severe pathology in the dentate gyrus, and only to moderate pathology in the hippocampal regions CA1 and CA3, suggesting that the hippocampus and, especially, the dentate gyrus are selectively vulnerable to α-synuclein pathology (Henderson *et al.*, 2019).

4.1.2 Transmission of α-synuclein via peripheral routes causes pathology and neurological disease

Corresponding to Braak's stages observation, LB pathology seem to spread retrogradely in patients with sporadic PD, which lead to the gut-to-brain dual-hit hypothesis, which has been investigated in various animal models (Heiko Braak *et al.*,

2003). A body-to-brain propagation was observed after injection of α-synuclein fibrils into the body of mice, such as into the gastric wall, the peritoneal cavity, hind limb muscles, and the urogenital tract, and is believed to happen retrogradely via the vagus nerve to the dorsal motor nucleus of the vagus nerve, resulting in neuropathology and CNS disease (Sacino, Brooks, Thomas, McKinney, Lee, *et al.*, 2014; Ayers *et al.*, 2017; Manfredsson *et al.*, 2018; Ding *et al.*, 2020). This route of propagation was further highlighted by vagotomy, were the vagal nerves were severed bilaterally, after which fibrils injected into the gastric wall were not capable to propagate to the brain and to induce any neuropathology (Uemura *et al.*, 2018; Kim *et al.*, 2019). In this study, intraperitoneal transmission resulted in 100% infection rate, causing CNS disease 202 ± 35 days after injection (Table 7). This result is comparable with a previous study from this lab, in which intraperitoneal injection with 50 μg fibrils caused neuropathology 229 ± 17 days post injection in TgM83$^{+/-}$ mice (Breid *et al.*, 2016). In both studies, pathological α-synuclein was detected in the motor cortex, the striatum, the hypothalamus, the amygdala, the brain stem, and the spinal cord and thus, throughout the CNS. In this study, intraperitoneal injection presented mild pathology in rostral brain regions, such as cortical regions, striatum, hypothalamus and thalamus, and moderate pathology in caudal brain regions, such as the midbrain and brain stem. This distribution pattern has been obtained by immuno-histochemistry for p-α-synuclein (Figure 3.5), and is in accordance with previous results (Breid *et al.*, 2016). Additionally, neuroinflammation was detected upon disease onset, as astrogliosis and microgliosis were significantly induced (Figure 3.9). The other peripheral route used in this thesis caused disease in two out of eight TgM83$^{+/-}$ mice at day 220 and 350 after oral transmission of 50 μg α-synuclein fibrils. A higher dose of 500 μg α-synuclein fibrils via oral gavage caused disease in 50% of the challenged mice, within 384 ± 131 days (Table 7). Although oral challenge presented a lower and slower infection rate, severe pathology in caudal parts of the brain was detected by immunohistochemistry for p-α-synuclein and biochemical analysis of insoluble oligomeric p-α-synuclein (Figure 3.4, Figure 3.3). Deposits of pathological α-synuclein in the brain and spinal cord were colocalized with markers for p62 and ubiquitin, presented conformer specific aggregates, and induced neuroinflammation throughout the CNS in all diseased mice (Figure 3.6, Figure 3.7, Figure 3.8). This work therefore shows for the first time that orally transmitted α-synuclein fibrils are able to cross the gastrointestinal wall and neuroinvade the CNS, ultimately causing motor symptoms and disease.

A previous study challenged WT mice orally with 400 μg human α-synuclein fibrils every two weeks for two months, but failed to detect any pathological α-synuclein in the CNS 6 and 14 months after challenge (Masuda-Suzukake *et al.*, 2014). Challenging WT mice with human α-synuclein would not result in potent seeding of α-synuclein aggregation, even if α-synuclein fibrils would have crossed the gastrointestinal tract, as only transgenic modified mice are able to express human α-synuclein, but not WT mice. In other studies, investigating the gut-to-brain

hypothesis, α-synuclein fibrils were directly injected into the intestinal wall of the stomach or into the gut wall of the duodenum (Manfredsson *et al.*, 2018; Van Den Berge *et al.*, 2019b). Injection of 48 *µ*g mouse α-synuclein fibrils into the stomach wall of WT mice resulted in pathology in the brain stem 12 months post injection, but failed to induce neurodegeneration (Uemura *et al.*, 2018). In 2019, Kim and colleagues showed that a total amount of 25 *µ*g mouse α-synuclein fibrils injected at two sites in the upper duodenum and at two sites in the pyloric stomach of WT mice, caused pathology and loss of dopaminergic neurons 10 months post injection (Kim *et al.*, 2019). Even though these studies showed that gut-to-brain propagation of α-synuclein can cause neurological disease within 12 months, similar amounts of α-synuclein fibrils to those used in this thesis, were directly injected into the gastrointestinal wall. The stomach and duodenum are directly connected to the vagus nerve via the myenteric and submucosal plexus in the gastrointestinal wall, giving an interplay between the ENS and CNS by the vagus and pelvic nerves via sympathetic pathways, resulting in normal trans-synaptical propagation of α-synuclein via the vagus nerve to the dorsal motor nucleus of the vagus nerve (Hawkes, Del Tredici and Braak, 2007; Furness, 2012). In contrast, orally transmitted α-synuclein fibrils as in the present study, probably first need to cross the epithelial lining of the gastrointestinal wall, to then propagate along the pyloric stomach and duodenum, until they reach the enteric plexus, to finally spread retrogradely via the vagal nerve to the brain (H. Braak *et al.*, 2003). Additionally, given that the amount of fibrils is extremely reduced in the gastrointestinal tract, partly due to digestion by different enzymes and the highly acidic environment and because of their excretion in feces, resulting in a much lower infectious dose, it is striking that not only the high dose of 500 *µ*g fibrils but also the lower dose of 50 *µ*g α-synuclein fibrils resulted in disease onset within 12 months. However, the exact mechanism how α-synuclein propagates from the stomach to the CNS has still to be investigated.

The difference in the pathology pattern on disease onset between the two peripheral routes used in this thesis may be based upon different α-synuclein strains. Similar to prions, where different prion strains cause a variety of clinical phenotypes of prion disease, there is growing evidence that there may be different strains of α-synuclein with different conformers and therefore biophysical properties. The different structures of α-synuclein strains cause different levels of toxicity, different seeding properties and propagation patterns, resulting in specific phenotypes of synucleinopathies (Bousset *et al.*, 2013; Peelaerts *et al.*, 2015b). There are different α-synuclein strains in different cell types, suggesting an effect of the intracellular environment on α-synuclein strain generation. Pathological α-synuclein accumulation in oligodendrocytes presents a glial cytoplasmic inclusions (GCI)-like strain, as it is seen in multiple system atrophy (MSA). This GCI-like strain shows a more compact structure and is 1,000-fold more potent in seeding aggregation, even maintaining this seeding activity when propagated into neurons, than α-synuclein that is aggregated in neurons, presented as LB's (Peng *et al.*, 2018). Given that the cellular milieu of the gastrointestinal tract varies from the one

of the peritoneum, α-synuclein may be taken up by different cell types, causing accumulation of gut-specific α-synuclein strains. These strains may own different propagation and seeding properties, thus, oral transmission may favor a gut-specific α-synuclein strain, resulting in hippocampal invasion of pathological α-synuclein only after oral, but not after intraperitoneal transmission.

4.1.3 Intravenous transmission causes neuropathology and neurological disease

In familial PD patients, α-synuclein was not only detected in the CNS and gastrointestinal tract, but also in the blood. The multiplication of the *SNCA* gene doubles the amount of α-synuclein in the blood, with more than 99% of α-synuclein specifically found in red blood cells (Miller *et al.*, 2004; Barbour *et al.*, 2008). Additionally, it was shown, that the presence of native α-synuclein increases the permeability of the blood brain barrier, enabling neuroinvasion of pathogens from the blood to the brain (Jangula and Murphy, 2013). Based on these data, the prion-like behavior of α-synuclein in regard of transmission via the hematogenous route, as it is known to transmit prion diseases via blood-transfusion resulting in neuroinvasion (Hunter *et al.*, 2002; Llewelyn *et al.*, 2004), was investigated here. To evaluate the prion-like character of α-synuclein, TgM83$^{+/-}$ mice were intravenously injected with 50 µg α-synuclein fibrils. This work is the first time, that a single systemic administration resulted in full transmission in 10 out of 10 animals at 208 ± 20 dpi, including neuropathology and signs of neurological disease (Figure 3.1, Figure 3.2, Figure 3.6). This shows that α-synuclein fibrils are able to cross the blood brain barrier and to seed propagation of pathological α-synuclein throughout the CNS.

Previous studies obtained similar results, although they used a rat model and performed repeated injections of fluorescent labeled α-synuclein fibrils, with 10 µg every 2 weeks over 4 months, resulting in a total amount of 80 µg (Peelaerts *et al.*, 2015b). In another study, intravenous injection of 20 µg mouse α-synuclein fibrils into 2-months-old homozygous TgM83$^{+/+}$ mice resulted in neuroinvasion and pathology in the CNS of all 5 mice, at 120 dpi (Ayers *et al.*, 2017). In contrast to our findings, none of the challenged homozygous mice showed motor impairment or signs of disease. A possible reason may be the reduced time period of the experiment, which was necessary to rule out a spontaneous onset of motor impairment, which homozygous TgM83$^{+/+}$ mice develop from 8 months of age on (Giasson *et al.*, 2002). Additionally, not human but mouse α-synuclein fibrils were used, and although these fibrils were sonicated, the polymers imaged via electron microscopy had a length of about 150 nm, and were, thus, twice the size of the fibrils used in the studies described here. These bigger fibrils may take longer to penetrate cells and the blood brain barrier, and may be taken up and degraded by immune cells, the UPS, and the ALP after crossing the blood brain barrier, causing a different disease onset due to a temporal clearance

pattern. Therefore, these fibrils may be too big to be potent enough to not only cause neuropathology, but also signs of neurological disease within that shorter experiment.

4.1.4 Prion-like character of α-synuclein

However, systematic administration of infectious prions had been reported to cause replication in non-nervous tissue and uptake via various nerve endings in lymphoid organs (Aguzzi, Sigurdson and Heikenwaelder, 2008; McCulloch *et al.*, 2011). Findings about the behavior of pathogenic α-synuclein regarding uptake from the bloodstream are still limited. In patients with LB disorders, pathological α-synuclein was not only found in the CNS, ENS, and the blood, but also in other organs (Beach *et al.*, 2010). Additionally, a recent study showed that α-synuclein fibrils injected into the gastrointestinal tract of rats, not only propagated within the ENS and CNS, but also propagated to the heart. Pathological α-synuclein was even observed in the heart at an earlier timepoint compared to the SN (Van Den Berge *et al.*, 2019).

My findings, of α-synuclein being able to cross the blood brain barrier, together with the evidence of α-synuclein being observed in various organs, promotes the hypothesis of α-synuclein uptake from the bloodstream via nerve endings into organs, and therefore a prion-like hypothesis for the propagation of α-synuclein. Even though transmission of synucleinopathies via blood-transfusion has not been reported yet, the unknown incubation time until disease onset needs to be considered. Based on LB's that were found in peripheral organs of patients up to 20 years prior to their PD diagnosis (Stokholm *et al.*, 2016), peripheral transmission of pathological α-synuclein may cause PD after several decades. A similar extended incubation time is also known for human prion diseases, such as up to 40 years incubation time for Creutzfeldt-Jakob disease prions (Rudge *et al.*, 2015). Considering that PD is the second most common neurodegenerative disease with increasing age as the major risk factor, it is complicated to observe and track possible transmission cases, and to distinguish them clearly from familial or idiopathic cases of PD.

4.2 MCAO study

Besides the propagation and disease-causing accumulation of transmitted α-synuclein via different routes, this thesis aimed to investigate as well the effect of focal cerebral ischemia on α-synuclein aggregation. This study confirmed that even a mild MCAO-induced ischemic injury leads to behavioral deficits and neuronal loss in the ischemic core over time, to a loss of dopaminergic neurons, accompanied by an increased level of aggregated α-synuclein. Thus, mice subjected to a mild cerebral ischemia developed motor deficits and neuropathology resembling PD.

4.2.1 Mild MCAO causes motor deficits and neurodegeneration

Since the majority of ischemic strokes in patients occur in the area around the middle cerebral artery, many animal models mimicking strokes in this area have been developed over time (Mohr, Lazar and Marshall, 2011). Focal cerebral stroke models in animals vary from permanent stroke, by e.g. photo-thrombosis, embolic stroke, or intraluminal permanent suture of arteries, up to transient stroke, by middle cerebral artery occlusion (MCAO) (Lee *et al.*, 2007; Wells *et al.*, 2012; Zhang *et al.*, 2015; Sommer, 2017). The transient MCAO model is a highly studied and established model, resulting in an ischemic core and penumbra region similar to human cerebral stroke. The ischemic impact can be determined by the duration of occlusion, leading to a mild (up to 30 min), moderate (30 - 90 min) or severe (from 90 min on) insult of the tissue and thus, to a proportional increase in infarct size (Maeda, Hata and Hossmann, 1999; McColl *et al.*, 2004; Howells *et al.*, 2010). Because the duration time of ischemia, and the following reperfusion time are highly controllable and reproducible, transient MCAO was used in this thesis to model cerebral ischemia. Occlusion of the MCA, one of the largest arteries in the brain follows a stereotypical progression in a rodent model by first affecting the striatum, followed by the hypothalamus and cerebral cortices. A lesion of the striatum results in altered coordination of motor and cognitive behavior, resulting in hemiparesis, and a lesion of the hypothalamus affects homeostatic mechanisms and hormone release. The affected cerebral cortices are the temporal cortex, leading to impaired hearing and communication, the parietal cortex, resulting in altered sensory processing of sounds, touch and movement, and the occipital cortex, which exhibits most regions of the visual cortex, leading to impaired visual processing (Zülch, 1981; Garcia, Liu and Ho, 1995; Popp *et al.*, 2009). All these impairments manifest as defined symptoms of human cerebral stroke: contralateral paresis and sensory loss in face, arms, and legs, anosognosia, spatial neglect, and hemi-sensory impaired vision (Rehme and Grefkes, 2013; Vossel *et al.*, 2013; Boes *et al.*, 2015).

In this thesis, a mild MCAO with a 30 min ischemia was performed in 6 to 8-week-old TgM83$^{+/-}$ mice. The natural reperfusion, induced upon removal of the silicon coated nylon filament was stopped at 14, 30, 90, 180, or 360 days post surgery (dps), by sacrificing the animals. Within 360 days post ischemia, MCAO- and sham-treated

control animals constantly gained weight suggesting a good general condition (Figure 3.10). At 180 and 360 dps significant behavioral deficits were observed by the rotarod performance test in animals following a mild ischemia (Figure 3.11). The animals circled towards the left direction for a short period of time after the surgery. However, no other signs of impaired general health condition were monitored over the time period of this experiment. Due to the striatum being the most affected brain region after MCAO, the motor impairment of circling towards the left direction can be explained by a mild hemiparesis. Hemisphere impairment is affecting the function of the contralateral, in this case the left front limbs of the mice following occlusion of the right MCA. An additional reason may be contralateral vision loss, which requires the mice to circle, to get a complete picture of their surroundings. Thus, circling towards the contralateral site can be used as a basic score for success of the stroke-modeling surgery (Longa *et al.*, 1989; Engel *et al.*, 2010). Additionally, the successfully induced cerebral ischemia was verified by NeuN staining of the ipsilateral neuronal loss (Figure 3.12). Since neurons are particularly vulnerable to ischemia, neuronal damage follows a spatiotemporal pattern resulting in an early observable lesion core. Additional confirmation of the induced ischemia was an increased neuroinflammation in the ischemic core. The amount of activated microglia and astroglia were significantly increased, especially in the ipsilateral striatal and thalamic regions within the first 30 days of reperfusion (Figure 3.13, Figure 3.14). Alteration of these confirmed regions can lead to motor impairment, that may result in circling towards the contralateral site, as these striatal regions are the first regions to be affected by MCAO and responsible for motor symptoms (Endres *et al.*, 1998).

4.2.2 MCAO causes neuroinflammation

It was previously shown that 30 min MCAO induces neuroinflammation with astrocytes slowly surrounding the periphery of the lesion along the infarct area after 48 h, and a manifestation of a glial scar at 7 dps (Wanner *et al.*, 2013; Buscemi *et al.*, 2019). In contrast, activated microglia have been described to invade the ischemic core region much faster, with an induced microgliosis at 3 h of reperfusion. Activated microglia were even detected in brain regions where no neuronal degeneration had happened yet, as microglia seem to respond to reduced and lost signals originating from injured neurons (Ransohoff and Cardona, 2010; Buscemi *et al.*, 2019). In this thesis, increased neuroinflammation was verified at the earlier time points. Microgliosis was significantly increased in the ipsilateral site 14, 30, and 90 d after the MCAO. However, after 180 dps no significant increase in microgliosis was detected anymore. Interestingly, at 360 dps microgliosis was significantly increased again (Figure 3.13). Similar to the behavior of activated microglia, significantly increased numbers of astrocytes were detected in the ipsilateral side 14 and 30 d after MCAO, again being reduced at 30 dps compared to 14 dps. No significant difference was detected at 90 dps. Although the numbers of astrocytes were reduced to a minimum at 90 dps, significantly increased astrogliosis was detected again at 180 and 360 dps (Figure 3.14). This time-dependent

change in neuroinflammation could explain possible microenvironmental changes in the brain. Additionally, it was previously shown that cerebral ischemia leads to inflammation not only in the lesion core but also in interconnected areas, such as the SN over time (Block, Dihné and Loos, 2005; Rodriguez-Grande *et al.*, 2013).

4.2.3 MCAO causes loss of dopaminergic neurons and neuropathology

One of the hallmarks of PD is loss of dopaminergic neurons (Hirsch, Graybiel and Agid, 1988; Petrucelli *et al.*, 2002). To evaluate if cerebral ischemia may cause PD, and because we detected increased inflammation, also in the interconnected SN, the loss of dopaminergic neurons was investigated. No significant differences were detected in the number of dopaminergic neurons comparing MCAO- and sham-treated controls for up to 180 d. At 360 dps the ipsilateral hemisphere of MCAO-treated mice showed a significant reduction of dopaminergic neurons (Figure 3.15). As dopaminergic neurons are vulnerable to oxidative stress (Morató *et al.*, 2014) and the striatum is directly connected with the SN via GABAergic projections, it was shown before that lesion of the striatum causes significant loss of dopaminergic neurons in the SN (Burke *et al.*, 1992; Mao *et al.*, 2017; Zhong *et al.*, 2019). Most of these studies used a severe (120 min) or permanent form of MCAO and shorter reperfusion times (48 h). Since here a significant reduction of dopaminergic neurons was only detected at 360 dps, the latest time point, loss of dopaminergic neurons may not be a result of direct impact of the cerebral ischemia, but due to the toxicity of α-synuclein aggregation (Feany and Bender, 2000; Masliah *et al.*, 2000a; Lee *et al.*, 2002; Hoban *et al.*, 2020). Cerebral ischemia not only leads to neuroinflammation and following neuronal degeneration but also to altered expression of various proteins (Li *et al.*, 1997).

Since another hallmark of PD are inclusion bodies consisting of aggregated α-synuclein (Spillantini *et al.*, 1997; Baba *et al.*, 1998), several studies investigated the effects of cerebral ischemia on altered expression of α-synuclein, mediating secondary brain damage. A population-based study performed a 3-year follow up, to evaluate risk of getting a stroke between PD and non-PD groups. They found out, that risk of getting an ischemic stroke was significantly increased in PD patients (Huang *et al.*, 2013). Since α-synuclein levels are upregulated in the red blood cells of PD patients, more studies investigated blood samples of ischemic stroke patients (Miller *et al.*, 2004; Barbour *et al.*, 2008). A significant higher level of oligomeric α-synuclein was found in red blood cells in PD patients, but also in ischemic stroke patients, compared to healthy subjects (Zhao *et al.*, 2016b). In addition, another study observed significantly higher levels of not only oligomeric α-synuclein, but also of hemoglobin-bound and S129 phosphorylated α-synuclein in patients with acute ischemic stroke (Wu *et al.*, 2019). In this thesis, the amount of aggregated α-synuclein in ipsi- and contralateral hemispheres of sham animals remained similar over all five timepoints, whereas the level of aggregated α-synuclein in mice subjected to MCAO significantly increased

over time. Thus, at 360 dps MCAO-treated mice displayed a significantly elevated amount of aggregated α-synuclein in comparison to sham-treated controls. This significant increase was observed in both, the ipsi- and contralateral hemisphere of mice subjected to MCAO (Figure 3.16).

In a previous study, aggregated α-synuclein was observed in neurons and even colocalized with ubiquitin, indicating mature LBs, when mice were subjected to a mild, 30 min MCAO and 72 h of reperfusion (Unal-Cevik *et al.*, 2011). Another study performed 90 min MCAO in mice, with a reperfusion time of max 7 days. They already observed a significantly increased nuclear level of cortical phosphorylation of α-synuclein, at 24 h of reperfusion. However, lacking these in their cytosolic levels, indicating nuclear translocation of α-synuclein and phospho-α-synuclein. They also performed 90 min MCAO with a reperfusion time of 4 months in α-syn$^{+/+}$ mice, and detected an ipsilateral increase in α-synuclein that resisted proteinase K treatment, and thus, proper α-synuclein aggregates (T. H. Kim *et al.*, 2016). Following a very mild MCAO (5 min) in gerbils α-synuclein levels started to increase 3 h after ischemia in the CA1 region of the hippocampus. A maximum level of α-synuclein expression was reached 1 day post ischemia, and decreased steadily over the course of 4 days (Yoon *et al.*, 2006). In contrast, permanent MCAO, without reperfusion caused a decrease in α-synuclein in the cerebral cortices of WT rats at 1 day of occlusion (Kang *et al.*, 2018). This was verified by glutamate treatment of hippocampal-derived cell line, leading to reduction of α-synuclein in a dose dependent manner (Koh, 2017). Since an ischemic event leads to oxygen deprivation, it impacts the microenvironment of the brain due to the ischemic infarct, initiating cell death and inflammation, resulting in loss of neurons, and activation and migration of microglia and astrocytes into the lesion core (Burda and Sofroniew, 2014; Feng et al., 2017). These immune cells express activation markers, produce cytokines and recruit lymphocytes. All the mechanisms are accompanied by an increased amount of reactive oxygen species (ROS), leading to ER stress, oxidative DNA damage and mitochondrial dysfunction, ultimately resulting in cell death (Lipton, 1999; Lo, Dalkara and Moskowitz, 2003; Sen et al., 2009; Xing et al., 2012; Lopez, Dempsey and Vemuganti, 2015; Zhao et al., 2016a). Additionally, abnormal α-synuclein enhances an inflammatory response not only via accumulation, but also via release of the aggregated protein into the extracellular space (Glass et al., 2010). Extracellular α-synuclein promotes microglia activation via the NF-κB pathway, by acting as an endogenous agonist for the Toll-like receptor 2, and may be a chemoattractant, promoting microglia migration (Park et al., 2008; Kim et al., 2013; Wang et al., 2015; Yun et al., 2018), ultimately inducing increased ROS release.

Reperfusion, the reoxygenation of the tissue, is responsible for the secondary neuronal injury. It leads to formation of additional elevated free radical levels, resulting in an increase of reactive oxygen and nitrogen species in the tissue, that enhances the ischemic effect (Lo, Dalkara and Moskowitz, 2003; Xing *et al.*, 2012; Lopez, Dempsey and Vemuganti, 2015; Zhao *et al.*, 2016a). Since no reperfusion occurs by permanent

MCAO, less ROS is present in the tissue, also reducing cellular changes that are known to mediate pathophysiological mechanisms in α-synuclein aggregation (Guardia-Laguarta *et al.*, 2014; Stefanovic *et al.*, 2014). By performing MCAO and the naturally occurring reperfusion, the increased levels of ROS lead to increased spreading of pathological α-synuclein within the brain, but also to increased accumulation (Musgrove *et al.*, 2019). In the presence of ROS all four methionine (met) residues of α-synuclein are oxidized to met sulfoxides (Glaser *et al.*, 2005; Zhu *et al.*, 2006; Lee and Gladyshev, 2011). This oxidation of α-synuclein reduces the binding affinity for biological membranes and also inhibits protein degradation by the 20S proteasome due to structural alteration (Maltsev *et al.*, 2013; Alvarez-Castelao *et al.*, 2014). Therefore, N- and C-terminal methionine oxidation via ROS enhances oligomerization of α-synuclein, resulting in inclusion bodies (Mirzaei *et al.*, 2006; Carmo-Gonçalves *et al.*, 2014).

In consistence with previous studies, an increase in aggregated α-synuclein in the brains of mice subjected to MCAO was observed. Although no alteration in aggregated α-synuclein was present at 14 dps, but afterwards, starting from 30 dps. In contrast, most previous studies only have a reperfusion time of 1 day up to 7 days, and no extended time periods. Most of them observed a significant upregulation of α-synuclein within the first 24 h of reperfusion, with a declining number over time. Due to ischemia and reperfusion, an early increase in ROS may lead to α-synuclein aggregation, but above all to an inflammatory response. Neuroinflammation not only reacts to the ischemic impact, but it also enhances clearing mechanism, such as protein degradation. Due to the significantly increased micro- and astrogliosis at 14 and 30 dps in the animal model studied in this thesis, clearing mechanism may be potent enough to reduce the amount of α-synuclein within the second week post MCAO, as other studies already observed a decline in aggregated α-synuclein after 1 day. However, the continuously recruited and activated immune cells also release ROS, which was previously reported to act as a mediator, linking inflammation and pathological α-synuclein in PD (Gao et al., 2008). Thus, increased amount of ROS triggers α-synuclein oligomerization via different mechanisms. At a later stage (90 dps), a decrease in neuroinflammation was observed, and thus a reduction in clearing mechanism of abnormal proteins. The abnormal α-synuclein may then polymerize more strongly into aggregates and recruit more and more native protein. Based on this, the significantly increased activation of astrocytes and microglia at the later time points may be due to the presence of aggregated α-synuclein at 360 dps, and therefore causing toxicity.

5 Conclusion and future perspectives

The findings presented in the first part of this thesis reveal that not only intracerebral and intraperitoneal injections, but also a single intravenous or oral challenge causes spreading of pathological α-synuclein to the CNS and neurological disease. Neurological disease in all Tg mice overexpressing human α-synuclein was observed after intracerebral, intraperitoneal, or intravenous challenge. In comparison to the previous routes, oral challenge resulted in a delayed onset of disease and a transmission rate of only 50% when challenged with 500 μg fibrils. A clear relation between occurrence of symptoms and severity of pathology was seen, as well as a clear induction of astrogliosis and microgliosis. All four inoculation routes resulted in a similar distribution of phosphorylated α-synuclein deposits in the CNS, although pathological α-synuclein only invaded the hippocampal regions after oral and intracerebral inoculation. Fibrillar and oligomeric α-synuclein as well as colocalization of phosphorylated α-synuclein with ubiquitin and p62 were detected, from which it can be concluded with certainty that all four inoculation routes resulted in LB-like pathological α-synuclein deposits in the CNS. These findings support the hypothesis that α-synuclein is a 'prion-like' protein, as misfolded α-synuclein and some prion proteins can cross the blood brain barrier upon intravenous injection. Additionally, α-synuclein can cross the gastrointestinal wall and invade the CNS after oral uptake and cause neuropathology as it was shown for some prion strains. However, how the pathological α-synuclein propagates to the CNS upon oral uptake need further investigation.

Epidemiological findings suggest that ischemic stroke increases the risk of subsequent PD. However, to date no animal model or mechanistic explanation exists that can proof this causal relation or can be used to study it. In the second part of this thesis a new mouse model was established to study this problem: MCAO in combination with a one-year follow up revealed a causal relation between mild cerebral ischemia and PD. Cerebral ischemia resulted in aggregation of α-synuclein and a concomitant loss of dopaminergic neurons in the SN, which subsequently results in PD. Mice displayed significant motor deficits and loss of dopaminergic neurons in the SN within a year after the MCAO. Additionally, neuroinflammation was significantly increased at early time points (14 and 30 dps) due to the infarct but also after a year. This late-stage astrogliosis and microgliosis were consistent with a significantly increased amount of aggregated α-synuclein. Thus, mice subjected to a mild MCAO developed neuropathology and motor deficits resembling PD within a year after treatment.

6 Bibliography

Abbott, A. (2010) 'Levodopa: The story so far', *Nature*. doi: 10.1038/466S6a.

Abeliovich, A. *et al.* (2000) 'Mice lacking α-synuclein display functional deficits in the nigrostriatal dopamine system', *Neuron*. doi: 10.1016/S0896-6273(00)80886-7.

Abeywardana, T. *et al.* (2013) 'Site-specific differences in proteasome-dependent degradation of monoubiquitinated α-synuclein.', *Chemistry & biology*, 20(10), pp. 1207–1213. doi: 10.1016/j.chembiol.2013.09.009.

Abounit, S. *et al.* (2016) 'Tunneling nanotubes spread fibrillar α-synuclein by intercellular trafficking of lysosomes', *The EMBO Journal*. doi: 10.15252/embj.201593411.

Aguzzi, A. and Polymenidou, M. (2004) 'Mammalian Prion Biology: One Century of Evolving Concepts', *Cell*. doi: 10.1016/S0092-8674(03)01031-6.

Aguzzi, A., Sigurdson, C. and Heikenwaelder, M. (2008) 'Molecular mechanisms of prion pathogenesis', *Annual Review of Pathology: Mechanisms of Disease*. doi: 10.1146/annurev.pathmechdis.3.121806.154326.

Ahn, S. *et al.* (2002) 'Src-dependent tyrosine phosphorylation regulates dynamin self-assembly and ligand-induced endocytosis of the epidermal growth factor receptor', *Journal of Biological Chemistry*. doi: 10.1074/jbc.M201499200.

Allaman, I., Bélanger, M. and Magistretti, P. J. (2011) 'Astrocyte-neuron metabolic relationships: For better and for worse', *Trends in Neurosciences*. doi: 10.1016/j.tins.2010.12.001.

Allen (2007) 'ALLEN Mouse Brain Atlas', *Gene Expression*. doi: 10.1038/nature05453.

Alvarez-Castelao, B. et al. (2014) 'Mechanism of cleavage of alpha-synuclein by the 20S proteasome and modulation of its degradation by the RedOx state of the N-terminal methionines', Biochimica et Biophysica Acta - Molecular Cell Research. doi: 10.1016/j.bbamcr.2013.11.018.

Anderson, J. P. *et al.* (2006) 'Phosphorylation of Ser-129 Is the Dominant Pathological Modification of α-Synuclein in Familial and Sporadic Lewy Body Disease', *Journal of Biological Chemistry* , 281(40), pp. 29739–29752. doi: 10.1074/jbc.M600933200.

Angelova, P. R. *et al.* (2016) 'Ca2+ is a key factor in α-synuclein-induced neurotoxicity', *Journal of Cell Science*. doi: 10.1242/jcs.180737.

Apostolova, L. G. *et al.* (2010) 'Hippocampal, caudate, and ventricular changes in Parkinson's disease with and without dementia', *Movement Disorders*. doi: 10.1002/mds.22799.

Appel-Cresswell, S. *et al.* (2013) 'Alpha-synuclein p.H50Q, a novel pathogenic mutation for Parkinson's disease', *Movement Disorders*. doi: 10.1002/mds.25421.

Ascherio, A. and Schwarzschild, M. A. (2016) 'The epidemiology of Parkinson's disease: risk factors and prevention', *The Lancet Neurology*. doi: 10.1016/S1474-4422(16)30230-7.

Aschoff, L. (1924) 'Das reticulo-endotheliale System', in *Ergebnisse der Inneren Medizin und Kinderheilkunde*. doi: 10.1007/978-3-642-90639-8_1.

Ayers, J. I. *et al.* (2017) 'Robust Central Nervous System Pathology in Transgenic Mice following Peripheral Injection of α-Synuclein Fibrils', *Journal of Virology*. doi: 10.1128/jvi.02095-16.

Baba, M. *et al.* (1998) 'Aggregation of alpha-synuclein in Lewy bodies of sporadic Parkinson's disease and dementia with Lewy bodies.', *The American journal of pathology*. United States, 152(4), pp. 879–884.

Barbour, R. *et al.* (2008) 'Red blood cells are the major source of alpha-synuclein in blood', *Neurodegenerative Diseases*. doi: 10.1159/000112832.

Bastide, M. F. *et al.* (2015) 'Pathophysiology of L-dopa-induced motor and non-motor complications in Parkinson's disease', *Progress in Neurobiology*. doi: 10.1016/j.pneurobio.2015.07.002.

Beach, T. G. *et al.* (2010) 'Multi-organ distribution of phosphorylated α-synuclein histopathology in subjects with Lewy body disorders', *Acta Neuropathologica*. doi: 10.1007/s00401-010-0664-3.

Becker, C., Jick, S. S. and Meier, C. R. (2010) 'Risk of stroke in patients with idiopathic Parkinson disease', *Parkinsonism and Related Disorders*. doi: 10.1016/j.parkreldis.2009.06.005.

Van Den Berge, N. *et al.* (2019a) 'Evidence for bidirectional and trans-synaptic parasympathetic and sympathetic propagation of alpha-synuclein in rats', *Acta Neuropathologica*. Springer Berlin Heidelberg, 138(4), pp. 535–550. doi: 10.1007/s00401-019-02040-w.

Van Den Berge, N. *et al.* (2019b) 'Evidence for bidirectional and trans-synaptic parasympathetic and sympathetic propagation of alpha-synuclein in rats', *Acta Neuropathologica*, 138(4), pp. 535–550. doi: 10.1007/s00401-019-02040-w.

Bergeron, M. *et al.* (2014) 'In vivo modulation of polo-like kinases supports a key role for PLK2 in Ser129 α-synuclein phosphorylation in mouse brain.', *Neuroscience*. United States, 256, pp. 72–82. doi: 10.1016/j.neuroscience.2013.09.061.

Bernis, M. E. *et al.* (2015) 'Prion-like propagation of human brain-derived alpha-synuclein in transgenic mice expressing human wild-type alpha-synuclein', *Acta neuropathologica communications*. doi: 10.1186/s40478-015-0254-7.

Betarbet, R. *et al.* (2000) 'Chronic systemic pesticide exposure reproduces features of Parkinson's disease', *Nature Neuroscience*. doi: 10.1038/81834.

Bétemps, D. *et al.* (2014) 'Alpha-synuclein spreading in M83 mice brain revealed by detection of pathological α-synuclein by enhanced ELISA', *Acta neuropathologica communications*. BioMed Central, 2, p. 29. doi: 10.1186/2051-5960-2-29.

Lo Bianco, C. *et al.* (2002) 'α-synucleinopathy and selective dopaminergic neuron loss in a rat lentiviral-based model of Parkinson's disease', *Proceedings of the National Academy of Sciences of the United States of America*. doi: 10.1073/pnas.152339799.

Block, F., Dihné, M. and Loos, M. (2005) 'Inflammation in areas of remote changes following focal brain lesion', *Progress in Neurobiology*. doi: 10.1016/j.pneurobio.2005.03.004.

Boes, A. D. *et al.* (2015) 'Network localization of neurological symptoms from focal brain lesions', *Brain*. doi: 10.1093/brain/awv228.

Bousset, L. *et al.* (2013) 'Structural and functional characterization of two alpha-synuclein strains', *Nature Communications*. doi: 10.1038/ncomms3575.

Braak, H. *et al.* (2003) 'Idiopathic Parkinson's disease: Possible routes by which vulnerable neuronal types may be subject to neuroinvasion by an unknown pathogen', *Journal of Neural Transmission*. doi: 10.1007/s00702-002-0808-2.

Braak, Heiko *et al.* (2003) 'Staging of brain pathology related to sporadic Parkinson's disease', *Neurobiology of Aging*. doi: 10.1016/S0197-4580(02)00065-9.

Braak, H. and Del Tredici, K. (2016) 'Potential pathways of abnormal tau and α-synuclein dissemination in sporadic Alzheimer's and Parkinson's diseases', *Cold Spring Harbor Perspectives in Biology*. doi: 10.1101/cshperspect.a023630.

Breid, S. *et al.* (2016) 'Neuroinvasion of α-Synuclein Prionoids after Intraperitoneal and Intraglossal Inoculation', *Journal of virology*. American Society for Microbiology, 90(20), pp. 9182–9193. doi: 10.1128/JVI.01399-16.

Brooks, A. I. *et al.* (1999) 'Paraquat elicited neurobehavioral syndrome caused by dopaminergic neuron loss', *Brain Research*. doi: 10.1016/S0006-8993(98)01192-5.

Buitrago, M. M. *et al.* (2004) 'Short and long-term motor skill learning in an accelerated rotarod training paradigm', *Neurobiology of Learning and Memory*. doi: 10.1016/j.nlm.2004.01.001.

Burai, R. *et al.* (2015) 'Elucidating the role of site-specific nitration of α-synuclein in the pathogenesis of Parkinson's disease via protein semisynthesis and mutagenesis', *Journal of the American Chemical Society*. doi: 10.1021/ja5131726.

Burda, J. E. and Sofroniew, M. V. (2014) 'Reactive gliosis and the multicellular response to CNS damage and disease', *Neuron*. doi: 10.1016/j.neuron.2013.12.034.

Burke, R. E. *et al.* (1992) 'Neonatal hypoxic-ischemic or excitotoxic striatal injury results in a decreased adult number of substantia nigra neurons', *Neuroscience*. doi: 10.1016/0306-4522(92)90447-A.

Burré, J. *et al.* (2010) 'α-Synuclein promotes SNARE-complex assembly in vivo and in vitro', *Science*, 329(5999), pp. 1663–1667. doi: 10.1126/science.1195227.

Burré, J., Sharma, M. and Südhof, T. C. (2014) 'α-Synuclein assembles into higher-order multimers upon membrane binding to promote SNARE complex formation', *Proceedings of the National Academy of Sciences of the United States of America*. doi: 10.1073/pnas.1416598111.

Buscemi, L. *et al.* (2019) 'Spatio-temporal overview of neuroinflammation in an experimental mouse stroke model', *Scientific Reports*. doi: 10.1038/s41598-018-36598-4.

Camicioli, R. *et al.* (2003) 'Parkinson's disease is associated with hippocampal atrophy', *Movement Disorders*. doi: 10.1002/mds.10444.

Campbell, B. C. *et al.* (2001) 'The solubility of alpha-synuclein in multiple system atrophy differs from that of dementia with Lewy bodies and Parkinson's disease.', *Journal of neurochemistry*. England, 76(1), pp. 87–96. doi: 10.1046/j.1471-4159.2001.00021.x.

Carmo-Gonçalves, P. *et al.* (2014) 'UV-induced selective oxidation of Met5 to Met-sulfoxide leads to the formation of neurotoxic fibril-incompetent α-synuclein oligomers', *Amyloid*. doi: 10.3109/13506129.2014.912208.

Chan, D. K. Y. *et al.* (2017) 'Mini-review on initiatives to interfere with the propagation and clearance of alpha-synuclein in Parkinson's disease', *Translational Neurodegeneration*. doi: 10.1186/s40035-017-0104-6.

Chandra, S. *et al.* (2003) 'A broken α-helix in folded α-synuclein', *Journal of Biological Chemistry*. doi: 10.1074/jbc.M213128200.

Chau, K.-Y. *et al.* (2009) 'Relationship between alpha synuclein phosphorylation, proteasomal inhibition and cell death: relevance to Parkinson's disease pathogenesis.', *Journal of neurochemistry*. England, 110(3), pp. 1005–1013. doi: 10.1111/j.1471-4159.2009.06191.x.

Chavarría, C. and Souza, J. M. (2013) 'Oxidation and nitration of α-synuclein and their implications in neurodegenerative diseases.', *Archives of biochemistry and biophysics*. United States, 533(1–2), pp. 25–32. doi: 10.1016/j.abb.2013.02.009.

Chen, L. *et al.* (2007) 'Oligomeric α-synuclein inhibits tubulin polymerization', *Biochemical and Biophysical Research Communications*. doi: 10.1016/j.bbrc.2007.02.163.

Chiueh, C. C. *et al.* (1984) 'Neurochemical and behavioral effects of 1-methyl-4-phenyl-1,2,3-tetrahydropyridine (MPTP) in rat, guinea pig, and monkey', *Psychopharmacology Bulletin*.

Choi, B. K. *et al.* (2013) 'Large α-synuclein oligomers inhibit neuronal SNARE-mediated vesicle docking', *Proceedings of the National Academy of Sciences of the United States of America*. doi: 10.1073/pnas.1218424110.

Chung, C. Y. *et al.* (2005) 'Cell type-specific gene expression of midbrain dopaminergic neurons reveals molecules involved in their vulnerability and protection', *Human Molecular Genetics*. doi: 10.1093/hmg/ddi178.

Chutna, O. *et al.* (2014) 'The small GTPase Rab11 co-localizes with α-synuclein in intracellular inclusions and modulates its aggregation, secretion and toxicity', *Human molecular genetics*. doi: 10.1093/hmg/ddu391.

Ciechanover, A. (2006) 'The ubiquitin proteolytic system: From a vague idea, through basic mechanisms, and onto human diseases and drug targeting', in *Neurology*. doi: 10.1212/01.wnl.0000192261.02023.b8.

Colla, E. *et al.* (2012) 'Accumulation of toxic α-synuclein oligomer within endoplasmic reticulum occurs in α-synucleinopathy in vivo', *Journal of Neuroscience*. doi: 10.1523/JNEUROSCI.5368-11.2012.

Collinge, J. and Clarke, A. R. (2007) 'A general model of prion strains and their pathogenicity', *Science*. doi: 10.1126/science.1138718.

Conn, K. J. *et al.* (2004) 'Identification of the protein disulfide isomerase family member PDIp in experimental Parkinson's disease and Lewy body pathology', *Brain Research*. doi: 10.1016/j.brainres.2004.07.026.

Conway, K. A., Harper, J. D. and Lansbury, P. T. (1998) 'Accelerated in vitro fibril formation by a mutant α-synuclein linked to early-onset Parkinson disease', *Nature Medicine*, 4(11), pp. 1318–1320. doi: 10.1038/3311.

Cremades, N. *et al.* (2012) 'Direct observation of the interconversion of normal and toxic forms of α-synuclein', *Cell*. doi: 10.1016/j.cell.2012.03.037.

Crowther, R. A. *et al.* (1998) 'Synthetic filaments assembled from C-terminally truncated α-synuclein', *FEBS Letters*. doi: 10.1016/S0014-5793(98)01146-6.

Cuervo, A. M. *et al.* (2004) 'Impaired degradation of mutant alpha-synuclein by chaperone-mediated autophagy.', *Science (New York, N.Y.)*. United States, 305(5688), pp. 1292–1295. doi: 10.1126/science.1101738.

Danielson, S. R. *et al.* (2009) 'Preferentially increased nitration of alpha-synuclein at tyrosine-39 in a cellular oxidative model of Parkinson's disease.', *Analytical chemistry*, 81(18), pp. 7823–7828. doi: 10.1021/ac901176t.

Danzer, K. M. *et al.* (2007) 'Different species of α-synuclein oligomers induce calcium influx and seeding', *Journal of Neuroscience*. doi: 10.1523/JNEUROSCI.2617-07.2007.

Danzer, K. M. *et al.* (2012) 'Exosomal cell-to-cell transmission of alpha synuclein oligomers', *Molecular Neurodegeneration*. doi: 10.1186/1750-1326-7-42.

Davalos, D. *et al.* (2005) 'ATP mediates rapid microglial response to local brain injury in vivo', *Nature Neuroscience*. doi: 10.1038/nn1472.

David Smith, A. and Paul Bolam, J. (1990) 'The neural network of the basal ganglia as revealed by the study of synaptic connections of identified neurones', *Trends in Neurosciences*. doi: 10.1016/0166-2236(90)90106-K.

Davidson, W. S. *et al.* (1998) 'Stabilization of α-Synuclein secondary structure upon binding to synthetic membranes', *Journal of Biological Chemistry*. doi: 10.1074/jbc.273.16.9443.

Desplats, P. *et al.* (2009) 'Inclusion formation and neuronal cell death through neuron-to-neuron transmission of α-synuclein', *Proceedings of the National Academy of Sciences of the United States of America*. doi: 10.1073/pnas.0903691106.

Dickson, D. W. (2007) 'Linking selective vulnerability to cell death mechanisms in Parkinson's disease', *American Journal of Pathology*. doi: 10.2353/ajpath.2007.061011.

Dimant, H. *et al.* (2014) 'Direct detection of alpha synuclein oligomers in vivo', *Acta Neuropathologica Communications*. doi: 10.1186/2051-5960-1-6.

Ding, X. *et al.* (2020) 'Propagation of Pathological α-Synuclein from the Urogenital Tract to the Brain Initiates MSA-like Syndrome', *iScience*. doi: 10.1016/j.isci.2020.101166.

Dorval, V. and Fraser, P. E. (2006) 'Small ubiquitin-like modifier (SUMO) modification of natively unfolded proteins tau and alpha-synuclein.', *The Journal of biological chemistry*. United States, 281(15), pp. 9919–9924. doi: 10.1074/jbc.M510127200.

Drolet, R. E. *et al.* (2009) 'Chronic rotenone exposure reproduces Parkinson's disease gastrointestinal neuropathology', *Neurobiology of Disease*. doi: 10.1016/j.nbd.2009.06.017.

Duda, J. E. *et al.* (2000) 'Widespread nitration of pathological inclusions in neurodegenerative synucleinopathies', *American Journal of Pathology*. doi: 10.1016/S0002-9440(10)64781-5.

Duffy, M. F. *et al.* (2018) 'Lewy body-like alpha-synuclein inclusions trigger reactive microgliosis prior to nigral degeneration', *Journal of neuroinflammation*. BioMed Central, 15(1), p. 129. doi: 10.1186/s12974-018-1171-z.

Ebrahimi-Fakhari, D. *et al.* (2011) 'Distinct roles in vivo for the ubiquitin-proteasome system and the autophagy-lysosomal pathway in the degradation of α-synuclein.', *The Journal of neuroscience : the official journal of the Society for Neuroscience*, 31(41), pp. 14508–14520. doi: 10.1523/JNEUROSCI.1560-11.2011.

Eliezer, D. *et al.* (2001) 'Conformational properties of α-synuclein in its free and lipid-associated states', *Journal of Molecular Biology*. doi: 10.1006/jmbi.2001.4538.

Ellis, C. E. *et al.* (2001) 'α-Synuclein Is Phosphorylated by Members of the Src Family of Protein-tyrosine Kinases', *Journal of Biological Chemistry*. doi: 10.1074/jbc.M010316200.

Emmanouilidou, E. *et al.* (2010) 'Cell-produced α-synuclein is secreted in a calcium-dependent manner by exosomes and impacts neuronal survival', *Journal of Neuroscience*. doi: 10.1523/JNEUROSCI.5699-09.2010.

Endres, M. *et al.* (1998) 'Attenuation of delayed neuronal death after mild focal ischemia in mice by inhibition of the caspase family', *Journal of Cerebral Blood Flow and Metabolism*. doi: 10.1097/00004647-199803000-00002.

Engel, O. *et al.* (2010) 'Modeling stroke in mice - Middle cerebral artery occlusion with the filament model', *Journal of Visualized Experiments*. doi: 10.3791/2423.

Fahn, S. and Cohen, G. (1992) 'The oxidant stress hypothesis in Parkinson's disease: Evidence supporting it', *Annals of Neurology*. doi: 10.1002/ana.410320616.

Farrer, M. *et al.* (2004) 'Comparison of Kindreds with Parkinsonism and α-Synuclein Genomic Multiplications', *Annals of Neurology*. doi: 10.1002/ana.10846.

Feany, M. B. and Bender, W. W. (2000) 'A Drosophila model of Parkinson's disease', *Nature*. doi: 10.1038/35006074.

Fellner, L. *et al.* (2013) 'Toll-like receptor 4 is required for α-synuclein dependent activation of microglia and astroglia', *GLIA*. doi: 10.1002/glia.22437.

Feng, Y. *et al.* (2017) 'Infiltration and persistence of lymphocytes during late-stage cerebral ischemia in middle cerebral artery occlusion and photothrombotic stroke models', *Journal of Neuroinflammation*. doi: 10.1186/s12974-017-1017-0.

Ferreira, S. A. and Romero-Ramos, M. (2018) 'Microglia response during Parkinson's disease: Alpha-synuclein intervention', *Frontiers in Cellular Neuroscience*. doi: 10.3389/fncel.2018.00247.

Foulds, P. G. *et al.* (2013) 'A longitudinal study on a-synuclein in blood plasma as a biomarker for Parkinson's disease', *Scientific Reports*. doi: 10.1038/srep02540.

Fujiwara, H. *et al.* (2002) 'A-Synuclein Is Phosphorylated in Synucleinopathy Lesions', *Nature Cell Biology*, 4(2), pp. 160–164. doi: 10.1038/ncb748.

Furness, J. B. (2012) 'The enteric nervous system and neurogastroenterology', *Nature Reviews Gastroenterology and Hepatology*. doi: 10.1038/nrgastro.2012.32.

Fusco, G. *et al.* (2014) 'Direct observation of the three regions in α-synuclein that determine its membrane-bound behaviour', *Nature Communications*. doi: 10.1038/ncomms4827.

Gao, H. M. *et al.* (2008) 'Neuroinflammation and oxidation/nitration of α-synuclein linked to dopaminergic neurodegeneration', *Journal of Neuroscience*. doi: 10.1523/JNEUROSCI.0143-07.2008.

Gao, H. M. *et al.* (2011) 'Neuroinflammation and α-synuclein dysfunction potentiate each other, driving chronic progression of neurodegeneration in a mouse model of Parkinson's disease', *Environmental Health Perspectives*. doi: 10.1289/ehp.1003013.

Garcia-Gracia, C. *et al.* (2013) 'The Prevalence of Stroke in Parkinson's Disease Is High: A Risk Factor Assessment (PD7.003)', *Neurology*, 80(7 Supplement), p. PD7.003 LP-PD7.003. Available at: http://n.neurology.org/content/80/7_Supplement/PD7.003.abstract.

Garcia, J. H., Liu, K. F. and Ho, K. L. (1995) 'Neuronal necrosis after middle cerebral artery occlusion in wistar rats progresses at different time intervals in the caudoputamen and the cortex', *Stroke*. doi: 10.1161/01.str.26.4.636.

George, J. M. (2002) 'The synucleins', *Genome Biology*. doi: 10.1186/gb-2001-3-1-reviews3002.

Giasson, B. I. *et al.* (1999) 'Mutant and Wild Type Human α-Synucleins Assemble into Elongated Filaments with Distinct Morphologies in Vitro ', *Journal of Biological Chemistry* , 274(12), pp. 7619–7622. doi: 10.1074/jbc.274.12.7619.

Giasson, B. I. *et al.* (2000) 'Oxidative damage linked to neurodegeneration by selective α-synuclein nitration in synucleinopathy lesions', *Science*. doi: 10.1126/science.290.5493.985.

Giasson, B. I. *et al.* (2002) 'Neuronal α-Synucleinopathy with Severe Movement Disorder in Mice Expressing A53T Human α-Synuclein', *Neuron*. Elsevier, 34(4), pp. 521–533. doi: 10.1016/S0896-6273(02)00682-7.

Gibb, W. R. G. (1997) 'Functional Neuropathology in Parkinson's Disease', *European Neurology*. doi: 10.1159/000113472.

Glaser, C. B. *et al.* (2005) 'Methionine oxidation, α-synuclein and Parkinson's disease', *Biochimica et Biophysica Acta - Proteins and Proteomics*. doi: 10.1016/j.bbapap.2004.10.008.

Goedert, M. *et al.* (2014) 'Prion-like mechanisms in the pathogenesis of tauopathies and synucleinopathies', *Current Neurology and Neuroscience Reports*. doi: 10.1007/s11910-014-0495-z.

Goedert, M., Clavaguera, F. and Tolnay, M. (2010) 'The propagation of prion-like protein inclusions in neurodegenerative diseases', *Trends in Neurosciences*. doi: 10.1016/j.tins.2010.04.003.

Gómez-Tortosa, E. *et al.* (2000) 'alpha-Synuclein immunoreactivity in dementia with Lewy bodies: morphological staging and comparison with ubiquitin immunostaining.', *Acta neuropathologica*. Germany, 99(4), pp. 352–357. doi: 10.1007/s004010051135.

Gosavi, N. *et al.* (2002) 'Golgi fragmentation occurs in the cells with prefibrillar α-synuclein aggregates and precedes the formation of fibrillar inclusion', *Journal of Biological Chemistry*. doi: 10.1074/jbc.M208194200.

Guardia-Laguarta, C. *et al.* (2014) 'α-synuclein is localized to mitochondria-associated ER membranes', *Journal of Neuroscience*. doi: 10.1523/JNEUROSCI.2507-13.2014.

Guo, J. L. and Lee, V. M. Y. (2014) 'Cell-to-cell transmission of pathogenic proteins in neurodegenerative diseases', *Nature Medicine*. doi: 10.1038/nm.3457.

Guzik, A. and Bushnell, C. (2017) 'Stroke Epidemiology and Risk Factor Management', *CONTINUUM Lifelong Learning in Neurology*. doi: 10.1212/CON.0000000000000416.

Haj-Yahya, M. *et al.* (2013) 'Synthetic polyubiquitinated α-Synuclein reveals important insights into the roles of the ubiquitin chain in regulating its pathophysiology.', *Proceedings of the National Academy of Sciences of the United States of America*, 110(44), pp. 17726–17731. doi: 10.1073/pnas.1315654110.

Hasegawa, M. *et al.* (2002) 'Phosphorylated α-synuclein is ubiquitinated in α-synucleinopathy lesions', *Journal of Biological Chemistry*. doi: 10.1074/jbc.M208046200.

Hawkes, C. H., Del Tredici, K. and Braak, H. (2007) 'Parkinson's disease: A dual-hit hypothesis', *Neuropathology and Applied Neurobiology*. doi: 10.1111/j.1365-2990.2007.00874.x.

Hejjaoui, M. *et al.* (2011) 'Towards elucidation of the role of ubiquitination in the pathogenesis of parkinson's disease with semisynthetic ubiquitinated α-synuclein', *Angewandte Chemie - International Edition*, 50(2), pp. 405–409. doi: 10.1002/anie.201005546.

Heman-Ackah, S. M. *et al.* (2017) 'Alpha-synuclein induces the unfolded protein response in Parkinson's disease SNCA triplication iPSC-derived neurons', *Human Molecular Genetics*. doi: 10.1093/hmg/ddx331.

Henderson, M. X. *et al.* (2019) 'Spread of α-synuclein pathology through the brain connectome is modulated by selective vulnerability and predicted by network analysis', *Nature Neuroscience*. doi: 10.1038/s41593-019-0457-5.

Herrera, F. E. *et al.* (2008) 'Inhibition of α-synuclein fibrillization by dopamine is mediated by interactions with five C-terminal residues and with E83 in the NAC region', *PLoS ONE*. doi: 10.1371/journal.pone.0003394.

Hill, A. F. *et al.* (1997) 'The same prion strain causes vCJD and BSE [10]', *Nature*. doi: 10.1038/38925.

Hines, D. J. *et al.* (2009) 'Microglia processes block the spread of damage in the brain and require functional chloride channels', *GLIA*. doi: 10.1002/glia.20874.

Hirsch, E. C. (1994) 'Biochemistry of Parkinson's disease with special reference to the dopaminergic systems', *Molecular Neurobiology*. doi: 10.1007/BF02816113.

Hirsch, E. C. and Hunot, S. (2009) 'Neuroinflammation in Parkinson's disease: a target for neuroprotection?', *The Lancet Neurology*. doi: 10.1016/S1474-4422(09)70062-6.

Hirsch, E., Graybiel, A. M. and Agid, Y. A. (1988) 'Melanized dopaminergic neurons are differentially susceptible to degeneration in Parkinson's disease', *Nature*. doi: 10.1038/334345a0.

Hoban, D. B. *et al.* (2020) 'Impact of α-synuclein pathology on transplanted hESC-derived dopaminergic neurons in a humanized α-synuclein rat model of PD', *Proceedings of the National Academy of Sciences of the United States of America*. doi: 10.1073/pnas.2001305117.

Hodara, R. *et al.* (2004) 'Functional consequences of alpha-synuclein tyrosine nitration: diminished binding to lipid vesicles and increased fibril formation.', *The Journal of biological chemistry*. United States, 279(46), pp. 47746–47753. doi: 10.1074/jbc.M408906200.

Hoffman-Zacharska, D. *et al.* (2013) 'Novel A18T and pA29S substitutions in α-synuclein may be associated with sporadic Parkinson's disease', *Parkinsonism and Related Disorders*. doi: 10.1016/j.parkreldis.2013.07.011.

Höglinger, G. U. *et al.* (2004) 'Dopamine depletion impairs precursor cell proliferation in Parkinson disease', *Nature Neuroscience*. doi: 10.1038/nn1265.

Holmqvist, S. *et al.* (2014) 'Direct evidence of Parkinson pathology spread from the gastrointestinal tract to the brain in rats', *Acta Neuropathologica*. doi: 10.1007/s00401-014-1343-6.

Hoozemans, J. J. M. *et al.* (2007) 'Activation of the unfolded protein response in Parkinson's disease', *Biochemical and Biophysical Research Communications*. doi: 10.1016/j.bbrc.2007.01.043.

Horvath, I. *et al.* (2012) 'Mechanisms of protein oligomerization: Inhibitor of functional amyloids templates α-synuclein fibrillation', *Journal of the American Chemical Society*. doi: 10.1021/ja209829m.

Howard, V. J. *et al.* (2006) 'High prevalence of stroke symptoms among persons without a diagnosis of stroke or transient ischemic attack in a general population: The REasons for Geographic And Racial Differences in Stroke (REGARDS) study', *Archives of Internal Medicine*. doi: 10.1001/archinte.166.18.1952.

Howells, D. W. *et al.* (2010) 'Different strokes for different folks: The rich diversity of animal models of focal cerebral ischemia', *Journal of Cerebral Blood Flow and Metabolism*. doi: 10.1038/jcbfm.2010.66.

Hoyer, W. *et al.* (2004) 'Impact of the acidic C-terminal region comprising amino acids 109-140 on α-synuclein aggregation in vitro', *Biochemistry*. doi: 10.1021/bi048453u.

Hu, X. *et al.* (2006) 'Proteomic analysis of hypoxia/ischemia-induced alteration of cortical development and dopamine neurotransmission in neonatal rat', *Journal of Proteome Research*. doi: 10.1021/pr060209x.

Huang, F. P. and MacPherson, G. G. (2004) 'Dendritic cells and oral transmission of prion diseases', *Advanced Drug Delivery Reviews*. doi: 10.1016/j.addr.2003.09.006.

Huang, Y.-F. *et al.* (2019) 'Stroke in Parkinson's disease', *QJM: An International Journal of Medicine*, 112(4), pp. 269–274. doi: 10.1093/qjmed/hcz015.

Huang, Y.-P. *et al.* (2013) 'Parkinson's Disease Is Related to an Increased Risk of Ischemic Stroke—A Population-Based Propensity Score-Matched Follow-Up Study', *PLoS ONE*. doi: 10.1371/journal.pone.0068314.

Hubble, J. P. *et al.* (1993) 'Risk factors for Parkinson's disease.', *Neurology*. United States, 43(9), pp. 1693–1697. doi: 10.1212/wnl.43.9.1693.

Hunter, N. *et al.* (2002) 'Transmission of prion diseases by blood transfusion', *Journal of General Virology*. doi: 10.1099/0022-1317-83-11-2897.

Hyun, C. H. *et al.* (2013) 'LRRK2 as a Potential Genetic Modifier of Synucleinopathies: Interlacing the Two Major Genetic Factors of Parkinson's Disease', *Experimental Neurobiology*. doi: 10.5607/en.2013.22.4.249.

Iadecola, C. and Anrather, J. (2011) 'The immunology of stroke: From mechanisms to translation', *Nature Medicine*. doi: 10.1038/nm.2399.

Ibáñez, P. *et al.* (2004) 'Causal relation between α-synuclein gene duplication and familial Parkinson's disease', *Lancet*. doi: 10.1016/S0140-6736(04)17104-3.

Inglis, K. J. *et al.* (2009) 'Polo-like kinase 2 (PLK2) phosphorylates α-synuclein at serine 129 in central nervous system', *Journal of Biological Chemistry*. doi: 10.1074/jbc.C800206200.

Iwai, A. *et al.* (1995) 'The precursor protein of non-Aβ component of Alzheimer's disease amyloid is a presynaptic protein of the central nervous system', *Neuron*. doi: 10.1016/0896-6273(95)90302-X.

Jakes, R., Spillantini, M. G. and Goedert, M. (1994) 'Identification of two distinct synucleins from human brain', *FEBS Letters*, 345(1), pp. 27–32. doi: 10.1016/0014-5793(94)00395-5.

Jangula, A. and Murphy, E. J. (2013) 'Lipopolysaccharide-induced blood brain barrier permeability is enhanced by alpha-synuclein expression', *Neuroscience Letters*. doi: 10.1016/j.neulet.2013.06.058.

Jankovic, J. (2008) 'Parkinson's disease: Clinical features and diagnosis', *Journal of Neurology, Neurosurgery and Psychiatry*. doi: 10.1136/jnnp.2007.131045.

Jeong, H. K. *et al.* (2014) 'Astrogliosis is a possible player in preventing delayed neuronal death', *Molecules and Cells*. doi: 10.14348/molcells.2014.0046.

Kahle, P. J. *et al.* (2000) 'Subcellular localization of wild-type and Parkinson's disease-associated mutant α-synuclein in human and transgenic mouse brain', *Journal of Neuroscience*. doi: 10.1523/jneurosci.20-17-06365.2000.

Kalia, L. V. *et al.* (2013) 'α-synuclein oligomers and clinical implications for parkinson disease', *Annals of Neurology*. doi: 10.1002/ana.23746.

Kalia, L. V. and Lang, A. E. (2015) 'Parkinson's disease', *The Lancet*. doi: 10.1016/S0140-6736(14)61393-3.

Kanazawa, T. *et al.* (2008) 'Three-layered structure shared between Lewy bodies and Lewy neurites - Three-dimensional reconstruction of triple-labeled sections', *Brain Pathology*. doi: 10.1111/j.1750-3639.2008.00140.x.

Kang, J.-B. *et al.* (2018) 'Hyperglycemia aggravates decrease in alpha-synuclein expression in a middle cerebral artery occlusion model', *Laboratory Animal Research*. doi: 10.5625/lar.2018.34.4.195.

Khalaf, O. *et al.* (2014) 'The H50Q mutation enhances αα-synuclein aggregation, secretion, and toxicity', *Journal of Biological Chemistry*. doi: 10.1074/jbc.M114.553297.

Kiely, A. P. *et al.* (2013) 'A-synucleinopathy associated with G51D SNCA mutation: A link between Parkinson's disease and multiple system atrophy?', *Acta Neuropathologica*, 125(5), pp. 753–769. doi: 10.1007/s00401-013-1096-7.

Kim, C. *et al.* (2013) 'Neuron-released oligomeric α-synuclein is an endogenous agonist of TLR2 for paracrine activation of microglia', *Nature Communications*. doi: 10.1038/ncomms2534.

Kim, C. *et al.* (2016) 'Exposure to bacterial endotoxin generates a distinct strain of α-synuclein fibril', *Scientific Reports*. doi: 10.1038/srep30891.

Kim, J. H. *et al.* (2010) 'Astrocytes in injury states rapidly produce anti-inflammatory factors and attenuate microglial inflammatory responses', *Journal of Neurochemistry*. doi: 10.1111/j.1471-4159.2010.07004.x.

Kim, S. *et al.* (2019) 'Transneuronal Propagation of Pathologic α-Synuclein from the Gut to the Brain Models Parkinson's Disease', *Neuron*. Elsevier Inc., 103(4), pp. 627-641.e7. doi: 10.1016/j.neuron.2019.05.035.

Kim, T. H. *et al.* (2016) 'Poststroke induction of α-synuclein mediates ischemic brain damage', *Journal of Neuroscience*. doi: 10.1523/JNEUROSCI.1241-16.2016.

Kirik, D. *et al.* (2002) 'Parkinson-Like Neurodegeneration Induced by Targeted Overexpression of α-Synuclein in the Nigrostriatal System', *Journal of Neuroscience*. doi: 10.1523/jneurosci.22-07-02780.2002.

Klegeris, A. *et al.* (2008) 'α-Synuclein activates stress signaling protein kinases in THP-1 cells and microglia', *Neurobiology of Aging*. doi: 10.1016/j.neurobiolaging.2006.11.013.

Koh, P.-O. (2017) 'Cerebral ischemic injury decreases α-synuclein expression in brain tissue and glutamate-exposed HT22 cells', *Laboratory Animal Research*. doi: 10.5625/lar.2017.33.3.244.

Koprich, J. B. *et al.* (2010) 'Expression of human A53T alpha-synuclein in the rat substantia nigra using a novel AAV1/2 vector produces a rapidly evolving pathology with protein aggregation, dystrophic neurite architecture and nigrostriatal degeneration with potential to model the pat', *Molecular Neurodegeneration*. doi: 10.1186/1750-1326-5-43.

Kordower, J. H. *et al.* (2008) 'Lewy body-like pathology in long-term embryonic nigral transplants in Parkinson's disease', *Nature Medicine*. doi: 10.1038/nm1747.

Kramer, M. L. and Schulz-Schaeffer, W. J. (2007) 'Presynaptic α-synuclein aggregates, not Lewy bodies, cause neurodegeneration in dementia with lewy bodies', *Journal of Neuroscience*. doi: 10.1523/JNEUROSCI.4564-06.2007.

Krüger, R. *et al.* (1998) 'Ala30Pro mutation in the gene encoding α-synuclein in Parkinson's disease', *Nature Genetics*. doi: 10.1038/ng0298-106.

Kummer, B. R. *et al.* (2019) 'Associations between cerebrovascular risk factors and parkinson disease', *Annals of Neurology*. doi: 10.1002/ana.25564.

Kuric, E. and Ruscher, K. (2014) 'Dynamics of major histocompatibility complex class II-positive cells in the postischemic brain - influence of levodopa treatment', *Journal of Neuroinflammation*. doi: 10.1186/s12974-014-0145-z.

Kuusisto, E., Kauppinen, T. and Alafuzoff, I. (2008) 'Use of p62/SQSTM1 antibodies for neuropathological diagnosis', *Neuropathology and Applied Neurobiology*. doi: 10.1111/j.1365-2990.2007.00884.x.

Kuusisto, E., Parkkinen, L. and Alafuzoff, I. (2003) 'Morphogenesis of Lewy Bodies: Dissimilar Incorporation of α-Synuclein, Ubiquitin, and p62', *Journal of Neuropathology & Experimental Neurology*, 62(12), pp. 1241–1253. doi: 10.1093/jnen/62.12.1241.

Kuusisto, E., Salminen, A. and Alafuzoff, I. (2001) 'Ubiquitin-binding protein p62 is present in neuronal and glial inclusions in human tauopathies and synucleinopathies.', *Neuroreport*. England, 12(10), pp. 2085–2090. doi: 10.1097/00001756-200107200-00009.

Kuzuhara, S. *et al.* (1988) 'Lewy bodies are ubiquitinated', *Acta Neuropathologica*. doi: 10.1007/bf00687787.

Lakso, M. *et al.* (2003) 'Dopaminergic neuronal loss and motor deficits in Caenorhabditis elegans overexpressing human α-synuclein', *Journal of Neurochemistry*. doi: 10.1046/j.1471-4159.2003.01809.x.

Lamark, T. *et al.* (2009) 'NBR1 and p62 as cargo receptors for selective autophagy of ubiquitinated targets', *Cell Cycle*. doi: 10.4161/cc.8.13.8892.

Lang, Anthony E. and Lozano, A. M. (1998) 'Parkinson's disease: Second of two parts', *New England Journal of Medicine*. doi: 10.1056/NEJM199810153391607.

Lang, A E and Lozano, A. M. (1998) 'Parkinson's disease. First of two parts.', *The New England journal of medicine*. doi: 10.1056/NEJM199810083391506.

Langston, J. W. *et al.* (1999) 'Evidence of active nerve cell degeneration in the substantia nigra of humans years after 1-methyl-4-phenyl-1,2,3,6-tetrahydropyridine exposure', *Annals of Neurology*. doi: 10.1002/1531-8249(199910)46:4<598::AID-ANA7>3.0.CO;2-F.

Lashuel, H. A. *et al.* (2002) 'α-synuclein, especially the parkinson's disease-associated mutants, forms pore-like annular and tubular protofibrils', *Journal of Molecular Biology*. doi: 10.1016/S0022-2836(02)00735-0.

Lavedan, C. *et al.* (1998) 'Identification, localization and characterization of the human γ-synuclein gene', *Human Genetics*. doi: 10.1007/s004390050792.

Lee, B. C. and Gladyshev, V. N. (2011) 'The biological significance of methionine sulfoxide stereochemistry', *Free Radical Biology and Medicine*. doi: 10.1016/j.freeradbiomed.2010.11.008.

Lee, H. J. *et al.* (2010) 'Direct transfer of α-synuclein from neuron to astroglia causes inflammatory responses in synucleinopathies', *Journal of Biological Chemistry*. doi: 10.1074/jbc.M109.081125.

Lee, H. J. *et al.* (2011) 'Dopamine promotes formation and secretion of non-fibrillar alpha-synuclein oligomers', *Experimental and Molecular Medicine*. doi: 10.3858/emm.2011.43.4.026.

Lee, J. K. *et al.* (2007) 'Photochemically induced cerebral ischemia in a mouse model', *Surgical Neurology*. doi: 10.1016/j.surneu.2006.08.077.

Lee, J. T. *et al.* (2008) 'Ubiquitination of α-synuclein by Siah-1 promotes α-synuclein aggregation and apoptotic cell death', *Human Molecular Genetics*, 17(6), pp. 906–917. doi: 10.1093/hmg/ddm363.

Lee, M. K. *et al.* (2002) 'Human α-synuclein-harboring familial Parkinson's disease-linked Ala-53 → Thr mutation causes neurodegenerative disease with α-synuclein aggregation in transgenic mice', *Proceedings of the National Academy of Sciences of the United States of America*. doi: 10.1073/pnas.132197599.

Lee, S. W. *et al.* (2003) 'SSeCKS regulates angiogenesis and tight junction formation in blood-brain barrier', *Nature Medicine*. doi: 10.1038/nm889.

Leverenz, J. B. *et al.* (2007) 'Proteomic identification of novel proteins in cortical lewy bodies.', *Brain pathology (Zurich, Switzerland)*. Switzerland, 17(2), pp. 139–145. doi: 10.1111/j.1750-3639.2007.00048.x.

Li, Y. *et al.* (1997) 'Apoptosis and protein expression after focal cerebral ischemia in rat', *Brain Research*. doi: 10.1016/S0006-8993(97)00524-6.

Lin, L. and Khoshbouei, H. (2019) 'The iPSC-derived human dopamine neurons from a healthy subject and a patient with α-synuclein triplication reveal novel therapeutic target', *The FASEB Journal*. John Wiley & Sons, Ltd, 33(S1), pp. 810.10-810.10. doi: 10.1096/fasebj.2019.33.1_supplement.810.10.

Lipton, P. (1999) 'Ischemic cell death in brain neurons', *Physiological Reviews*. doi: 10.1152/physrev.1999.79.4.1431.

Llewelyn, C. A. *et al.* (2004) 'Possible transmission of variant Creutzfeldt-Jakob disease by blood transfusion', *Lancet*. doi: 10.1016/S0140-6736(04)15486-X.

Lo, E. H., Dalkara, T. and Moskowitz, M. A. (2003) 'Mechanisms, challenges and opportunities in stroke', *Nature Reviews Neuroscience*. doi: 10.1038/nrn1106.

Lohmann, S. et al. (2019) 'Oral and intravenous transmission of α-synuclein fibrils to mice', *Acta Neuropathologica* 138 pp. 515-533. doi: 10.1007/s00401-019-02037-5

Longa, E. Z. *et al.* (1989) 'Reversible middle cerebral artery occlusion without craniectomy in rats', *Stroke*. doi: 10.1161/01.STR.20.1.84.

Lopez, M. S., Dempsey, R. J. and Vemuganti, R. (2015) 'Resveratrol neuroprotection in stroke and traumatic CNS injury', *Neurochemistry International*. doi: 10.1016/j.neuint.2015.08.009.

Lou, X. *et al.* (2017) 'α-Synuclein may cross-bridge v-SNARE and acidic phospholipids to facilitate SNARE-dependent vesicle docking', *Biochemical Journal*. doi: 10.1042/BCJ20170200.

Lowe, J. *et al.* (1988) 'Ubiquitin is a common factor in intermediate filament inclusion bodies of diverse type in man, including those of Parkinson's disease, Pick's disease, and Alzheimer's disease, as well as Rosenthal fibres in cerebellar astrocytomas, cytoplasmic bodies in m', *The Journal of pathology*. England, 155(1), pp. 9–15. doi: 10.1002/path.1711550105.

Luk, K. *et al.* (2009) 'Exogenous α-synuclein fibrils seed the formation of Lewy body-like intracellular inclusions in cultured cells', *Proceedings of the National Academy of Sciences of the United States of America*. doi: 10.1073/pnas.0908005106.

Luk, Kelvin C. *et al.* (2012) 'Intracerebral inoculation of pathological α-synuclein initiates a rapidly progressive neurodegenerative α-synucleinopathy in mice', *The Journal of experimental medicine*. 2012/04/16. The Rockefeller University Press, 209(5), pp. 975–986. doi: 10.1084/jem.20112457.

Luk, Kelvin C *et al.* (2012) 'Pathological α-synuclein transmission initiates Parkinson-like neurodegeneration in nontransgenic mice', *Science*. doi: 10.1126/science.1227157.

Mabbott, N. A. (2017) 'How do PrPSc prions spread between host species, and within hosts?', *Pathogens*. doi: 10.3390/pathogens6040060.

Machiya, Y. *et al.* (2010) 'Phosphorylated alpha-synuclein at Ser-129 is targeted to the proteasome pathway in a ubiquitin-independent manner.', *The Journal of biological chemistry*, 285(52), pp. 40732–40744. doi: 10.1074/jbc.M110.141952.

Maeda, K., Hata, R. and Hossmann, K. A. (1999) 'Regional metabolic disturbances and cerebrovascular anatomy after permanent middle cerebral artery occlusion in C57Black/6 and SV129 mice', *Neurobiology of Disease*. doi: 10.1006/nbdi.1998.0235.

Di Maio, R. *et al.* (2016) 'α-synuclein binds to TOM20 and inhibits mitochondrial protein import in Parkinson's disease', *Science Translational Medicine*. doi: 10.1126/scitranslmed.aaf3634.

Maltsev, A. S. *et al.* (2013) 'Site-specific interaction between α-synuclein and membranes probed by NMR-observed methionine oxidation rates', *Journal of the American Chemical Society*. doi: 10.1021/ja312415q.

Manfredsson, F. P. *et al.* (2018) 'Induction of alpha-synuclein pathology in the enteric nervous system of the rat and non-human primate results in gastrointestinal dysmotility and transient CNS pathology', *Neurobiology of Disease*. doi: 10.1016/j.nbd.2018.01.008.

Manning-Bog, A. B. *et al.* (2002) 'The herbicide paraquat causes up-regulation and aggregation of α-synuclein in mice: Paraquat and α-synuclein', *Journal of Biological Chemistry*. doi: 10.1074/jbc.C100560200.

Mao, L. *et al.* (2017) 'mir-193 targets ALDH2 and contributes to toxic aldehyde accumulation and tyrosine hydroxylase dysfunction in cerebral ischemia/reperfusion injury', *Oncotarget*. doi: 10.18632/oncotarget.21129.

Mao, X. *et al.* (2016) 'Pathological α-synuclein transmission initiated by binding lymphocyte-activation gene 3', *Science*. doi: 10.1126/science.aah3374.

Maroteaux, L., Campanelli, J. T. and Scheller, R. H. (1988) 'Synuclein: A neuron-specific protein localized to the nucleus and presynaptic nerve terminal', *Journal of Neuroscience*. doi: 10.1523/jneurosci.08-08-02804.1988.

Masliah, E. *et al.* (2000a) 'Dopaminergic loss and inclusion body formation in α-synuclein mice: Implications for neurodegenerative disorders', *Science*. doi: 10.1126/science.287.5456.1265.

Masliah, E. *et al.* (2000b) 'Dopaminergic Loss and Inclusion Body Formation in α-Synuclein Mice: Implications for Neurodegenerative Disorders', *Science*, 287(5456), pp. 1265 LP – 1269. doi: 10.1126/science.287.5456.1265.

Masuda-Suzukake, M. *et al.* (2013) 'Prion-like spreading of pathological alpha-synuclein in brain.', *Brain : a journal of neurology*. England, 136(Pt 4), pp. 1128–1138. doi: 10.1093/brain/awt037.

Masuda-Suzukake, M. *et al.* (2014) 'Pathological alpha-synuclein propagates through neural networks', *Acta Neuropathologica Communications*. doi: 10.1186/s40478-014-0088-8.

McColl, B. W. *et al.* (2004) 'Extension of cerebral hypoperfusion and ischaemic pathology beyond MCA territory after intraluminal filament occlusion in C57Bl/6J mice', *Brain Research*. doi: 10.1016/j.brainres.2003.10.028.

McCulloch, L. *et al.* (2011) 'Follicular dendritic cell-specific prion protein (PrP c) expression alone is sufficient to sustain prion infection in the spleen', *PLoS Pathogens*. doi: 10.1371/journal.ppat.1002402.

McGeer, P. L. *et al.* (1987) 'Reactive microglia in patients with senile dementia of the Alzheimer type are positive for the histocompatibility glycoprotein HLA-DR', *Neuroscience Letters*. doi: 10.1016/0304-3940(87)90696-3.

McGeer, P. L. *et al.* (1988) 'Reactive microglia are positive for HLA-DR in the: Substantia nigra of Parkinson's and Alzheimer's disease brains', *Neurology*. doi: 10.1212/wnl.38.8.1285.

Meier, F. *et al.* (2012) 'Semisynthetic, Site-Specific Ubiquitin Modification of α-Synuclein Reveals Differential Effects on Aggregation', *Journal of the American Chemical Society*. American Chemical Society, 134(12), pp. 5468–5471. doi: 10.1021/ja300094r.

Michel, P. P., Hirsch, E. C. and Hunot, S. (2016) 'Understanding Dopaminergic Cell Death Pathways in Parkinson Disease', *Neuron*. doi: 10.1016/j.neuron.2016.03.038.

Miller, D. W. *et al.* (2004) 'α-synuclein in blood and brain from familial Parkinson disease with SNCA locus triplication', *Neurology*. doi: 10.1212/01.WNL.0000127517.33208.F4.

Mirzaei, H. *et al.* (2006) 'Identification of rotenone-induced modifications in α-synuclein using affinity pull-down and tandem mass spectrometry', *Analytical Chemistry*. doi: 10.1021/ac051978n.

Mohr, J. P., Lazar, R. M. and Marshall, R. S. (2011) 'Middle Cerebral Artery Disease', in *Stroke*. doi: 10.1016/B978-1-4160-5478-8.10024-7.

Moon, S. P. *et al.* (2020) 'Ubiquitination Can Change the Structure of the α-Synuclein Amyloid Fiber in a Site Selective Fashion', *Journal of Organic Chemistry*, 85(3), pp. 1548–1555. doi: 10.1021/acs.joc.9b02641.

Morató, L. *et al.* (2014) 'Mitochondrial dysfunction in central nervous system white matter disorders', *GLIA*. doi: 10.1002/glia.22670.

Mozaffarian, D. *et al.* (2016) 'Heart Disease and Stroke Statistics—2016 Update', *Circulation*. doi: 10.1161/cir.0000000000000350.

Murray, I. V. J. *et al.* (2003) 'Role of α-synuclein carboxy-terminus on fibril formation in vitro', *Biochemistry*. doi: 10.1021/bi027363r.

Musgrove, R. E. *et al.* (2019) 'Oxidative stress in vagal neurons promotes parkinsonian pathology and intercellular α-synuclein transfer', *Journal of Clinical Investigation*. doi: 10.1172/JCI127330.

Nakajo, S. *et al.* (1993) 'A new brain-specific 14-kDa protein is a phosphoprotein: Its complete amino acid sequence and evidence for phosphorylation', *European Journal of Biochemistry*. doi: 10.1111/j.1432-1033.1993.tb18337.x.

Nemani, V. M. *et al.* (2010) 'Increased Expression of α-Synuclein Reduces Neurotransmitter Release by Inhibiting Synaptic Vesicle Reclustering after Endocytosis', *Neuron*. doi: 10.1016/j.neuron.2009.12.023.

Nielsen, M. S. *et al.* (2001) 'Ca2+ Binding to α-Synuclein Regulates Ligand Binding and Oligomerization', *Journal of Biological Chemistry*. doi: 10.1074/jbc.M101181200.

Nimmerjahn, A., Kirchhoff, F. and Helmchen, F. (2005) 'Resting microglial cells are highly dynamic surveillants of brain parenchyma in vivo', *Neuroforum*. doi: 10.1515/nf-2005-0304.

Nonaka, T., Iwatsubo, T. and Hasegawa, M. (2004) 'P3-401 Ubiquitination of alpha-synuclein', *Neurobiology of Aging*. doi: 10.1016/s0197-4580(04)81549-5.

Nonaka, T., Iwatsubo, T. and Hasegawa, M. (2005) 'Ubiquitination of alpha-synuclein.', *Biochemistry*. United States, 44(1), pp. 361–368. doi: 10.1021/bi0485528.

O'Leary, K. T. *et al.* (2008) 'Paraquat exposure reduces nicotinic receptor-evoked dopamine release in monkey striatum', *Journal of Pharmacology and Experimental Therapeutics*. doi: 10.1124/jpet.108.141861.

Oh, S. H. *et al.* (2016) 'Mesenchymal Stem Cells Inhibit Transmission of α-Synuclein by Modulating Clathrin-Mediated Endocytosis in a Parkinsonian Model', *Cell Reports*. doi: 10.1016/j.celrep.2015.12.075.

Okochi, M. *et al.* (2000) 'Constitutive phosphorylation of the Parkinson's disease associated α- synuclein', *Journal of Biological Chemistry*. doi: 10.1074/jbc.275.1.390.

Ouchi, Y. *et al.* (2005) 'Microglial activation and dopamine terminal loss in early Parkinson's disease', *Annals of Neurology*. doi: 10.1002/ana.20338.

Oueslati, A., Fournier, M. and Lashuel, H. A. (2010) 'Role of post-translational modifications in modulating the structure, function and toxicity of α-synuclein. Implications for Parkinson's disease pathogenesis and therapies', in *Progress in Brain Research*. doi: 10.1016/S0079-6123(10)83007-9.

Pankratz, N. and Foroud, T. (2004) 'Genetics of Parkinson Disease', *NeuroRx*. doi: 10.1602/neurorx.1.2.235.

Park, J. Y. *et al.* (2008) 'Microglial phagocytosis is enhanced by monomeric α-synuclein, not aggregated α-synuclein: Implications for Parkinson's disease', *GLIA*. doi: 10.1002/glia.20691.

Park, M. *et al.* (2005) 'Consumption of milk and calcium in midlife and the future risk of Parkinson disease', *Neurology*. doi: 10.1212/01.WNL.0000154532.98495.BF.

Park, S. J. *et al.* (2012) ' Astrocytes, but Not Microglia, Rapidly Sense H 2 O 2 via STAT6 Phosphorylation, Resulting in Cyclooxygenase-2 Expression and Prostaglandin Release ', *The Journal of Immunology*. doi: 10.4049/jimmunol.1101600.

Pasanen, P. *et al.* (2014) 'A novel α-synuclein mutation A53E associated with atypical multiple system atrophy and Parkinson's disease-type pathology', *Neurobiology of Aging*. doi: 10.1016/j.neurobiolaging.2014.03.024.

Peelaerts, W. *et al.* (2015a) 'α-Synuclein strains cause distinct synucleinopathies after local and systemic administration', *Nature*, 522(7556), pp. 340–344. doi: 10.1038/nature14547.

Peelaerts, W. *et al.* (2015b) 'α-Synuclein strains cause distinct synucleinopathies after local and systemic administration', *Nature*. doi: 10.1038/nature14547.

Peelaerts, W. *et al.* (2018) 'α-Synuclein strains and seeding in Parkinson's disease, incidental Lewy body disease, dementia with Lewy bodies and multiple system atrophy: similarities and differences', *Cell and Tissue Research*. Cell and Tissue Research, 373(1), pp. 195–212. doi: 10.1007/s00441-018-2839-5.

Peng, C. *et al.* (2018) 'Cellular milieu imparts distinct pathological α-synuclein strains in α-synucleinopathies', *Nature*, 557(7706), pp. 558–563. doi: 10.1038/s41586-018-0104-4.

Perese, D. A. *et al.* (1989) 'A 6-hydroxydopamine-induced selective parkinsonian rat model', *Brain Research*. doi: 10.1016/0006-8993(89)90597-0.

Perez, R. G. *et al.* (2002) 'A role for α-synuclein in the regulation of dopamine biosynthesis', *Journal of Neuroscience*. doi: 10.1523/jneurosci.22-08-03090.2002.

Perfeito, R. *et al.* (2014) 'Linking alpha-synuclein phosphorylation to reactive oxygen species formation and mitochondrial dysfunction in SH-SY5Y cells', *Molecular and Cellular Neuroscience*. doi: 10.1016/j.mcn.2014.08.002.

Van der Perren, A. *et al.* (2015) 'Longitudinal follow-up and characterization of a robust rat model for Parkinson's disease based on overexpression of alpha-synuclein with adeno-associated viral vectors', *Neurobiology of Aging*. doi: 10.1016/j.neurobiolaging.2014.11.015.

Petrucelli, L. *et al.* (2002) 'Parkin protects against the toxicity associated with mutant α-Synuclein: Proteasome dysfunction selectively affects catecholaminergic neurons', *Neuron*. doi: 10.1016/S0896-6273(02)01125-X.

Plotegher, N., Gratton, E. and Bubacco, L. (2014) 'Number and Brightness analysis of alpha-synuclein oligomerization and the associated mitochondrial morphology alterations in live cells', *Biochimica et Biophysica Acta - General Subjects*. doi: 10.1016/j.bbagen.2014.02.013.

Polymeropoulos, M. H. *et al.* (1996) 'Mapping of a gene for Parkinson's disease to chromosome 4q21-q23', *Science*, 274(5290), pp. 1197–1199. doi: 10.1126/science.274.5290.1197.

Polymeropoulos, M. H. *et al.* (1997) 'Mutation in the α-synuclein gene identified in families with Parkinson's disease', *Science*. doi: 10.1126/science.276.5321.2045.

Popp, A. *et al.* (2009) 'Identification of ischemic regions in a rat model of stroke', *PLoS ONE*. doi: 10.1371/journal.pone.0004764.

Prabhakaran, K., Chapman, G. D. and Gunasekar, P. G. (2011) 'α-Synuclein overexpression enhances manganese-induced neurotoxicity through the NF-κB-mediated pathway', *Toxicology Mechanisms and Methods*. doi: 10.3109/15376516.2011.560210.

Prots, I. *et al.* (2013) 'α-synuclein oligomers impair neuronal microtubule-kinesin interplay', *Journal of Biological Chemistry*. doi: 10.1074/jbc.M113.451815.

Prusiner, S. B. (1991) 'Molecular biology of prion diseases', *Science*. doi: 10.1126/science.1675487.

Prusiner, S. B. (1998) 'Prions', in Proceedings of the National Academy of Sciences of the United States of America. doi: 10.1073/pnas.95.23.13363.

Qiu, C. *et al.* (2010) 'Vascular risk profiles for dementia and Alzheimer's disease in very old people: A population-based longitudinal study', *Journal of Alzheimer's Disease*. doi: 10.3233/JAD-2010-1361.

Rannikko, E. H., Weber, S. S. and Kahle, P. J. (2015) 'Exogenous α-synuclein induces toll-like receptor 4 dependent inflammatory responses in astrocytes', *BMC Neuroscience*. doi: 10.1186/s12868-015-0192-0.

Ransohoff, R. M. and Cardona, A. E. (2010) 'The myeloid cells of the central nervous system parenchyma', *Nature*. doi: 10.1038/nature09615.

Ravikumar, B., Duden, R. and Rubinsztein, D. C. (2002) 'Aggregate-prone proteins with polyglutamine and polyalanine expansions are degraded by autophagy', *Human Molecular Genetics*. doi: 10.1093/hmg/11.9.1107.

Rehme, A. K. and Grefkes, C. (2013) 'Cerebral network disorders after stroke: Evidence from imaging-based connectivity analyses of active and resting brain states in humans', *Journal of Physiology*. doi: 10.1113/jphysiol.2012.243469.

Rey, N. L. *et al.* (2016) 'Widespread transneuronal propagation of α-synucleinopathy triggered in olfactory bulb mimics prodromal Parkinson's disease', *Journal of Experimental Medicine*. doi: 10.1084/jem.20160368.

Rideout, H. J., Lang-Rollin, I. and Stefanis, L. (2004) 'Involvement of macroautophagy in the dissolution of neuronal inclusions', *The International Journal of Biochemistry & Cell Biology*, 36(12), pp. 2551–2562. doi: https://doi.org/10.1016/j.biocel.2004.05.008.

Rodriguez-Grande, B. *et al.* (2013) 'Loss of substance P and inflammation precede delayed neurodegeneration in the substantia nigra after cerebral ischemia', *Brain, Behavior, and Immunity*. doi: 10.1016/j.bbi.2012.11.017.

Rostovtseva, T. K. *et al.* (2015) 'α-synuclein shows high affinity interaction with voltage-dependent anion channel, suggesting mechanisms of mitochondrial regulation and toxicity in Parkinson disease', *Journal of Biological Chemistry*. doi: 10.1074/jbc.M115.641746.

Rott, R. *et al.* (2008) 'Monoubiquitylation of alpha-synuclein by seven in absentia homolog (SIAH) promotes its aggregation in dopaminergic cells.', *The Journal of biological chemistry*. United States, 283(6), pp. 3316–3328. doi: 10.1074/jbc.M704809200.

Rott, R. *et al.* (2017) 'SUMOylation and ubiquitination reciprocally regulate α-synuclein degradation and pathological aggregation.', *Proceedings of the National Academy of Sciences of the United States of America*, 114(50), pp. 13176–13181. doi: 10.1073/pnas.1704351114.

Rubinsztein, D. C. (2006) 'The roles of intracellular protein-degradation pathways in neurodegeneration.', *Nature*. England, 443(7113), pp. 780–786. doi: 10.1038/nature05291.

Rudge, P. *et al.* (2015) 'Iatrogenic CJD due to pituitary-derived growth hormone with genetically determined incubation times of up to 40 years', *Brain*. doi: 10.1093/brain/awv235.

Rutherford, N. J. *et al.* (2017) 'Comparison of the in vivo induction and transmission of α-synuclein pathology by mutant α-synuclein fibril seeds in transgenic mice', *Human Molecular Genetics*, 26(24), pp. 4906–4915. doi: 10.1093/hmg/ddx371.

Sacino, A. N., Brooks, M., Thomas, M. A., McKinney, A. B., McGarvey, N. H., *et al.* (2014) 'Amyloidogenic α-synuclein seeds do not invariably induce rapid, widespread pathology in mice', *Acta Neuropathologica*. doi: 10.1007/s00401-014-1268-0.

Sacino, A. N., Brooks, Mieu, Shaw, G., Golde, T. E., Giasson, B. I., McKinney, A. B., *et al.* (2014) 'Brain injection of α-Synuclein induces multiple proteinopathies, gliosis, and a neuronal injury marker', *Journal of Neuroscience*. doi: 10.1523/JNEUROSCI.2102-14.2014.

Sacino, A. N., Brooks, Mieu, McGarvey, N. H., McKinney, A. B., Thomas, M. A., Levites, Y., *et al.* (2014) 'Induction of CNS α-synuclein pathology by fibrillar and non-amyloidogenic recombinant α-synuclein', *Acta Neuropathologica Communications*. doi: 10.1186/2051-5960-1-38.

Sacino, A. N., Brooks, M., Thomas, M. A., McKinney, A. B., Lee, S., *et al.* (2014) 'Intramuscular injection of α-synuclein induces CNS α-synuclein pathology and a rapid-onset motor phenotype in transgenic mice', *Proceedings of the National Academy of Sciences of the United States of America*. doi: 10.1073/pnas.1321785111.

Sargent, D. *et al.* (2017) '"Prion-like" propagation of the synucleinopathy of M83 transgenic mice depends on the mouse genotype and type of inoculum', *Journal of Neurochemistry*. doi: 10.1111/jnc.14139.

Sato, S. *et al.* (2018) 'Loss of autophagy in dopaminergic neurons causes Lewy pathology and motor dysfunction in aged mice', *Scientific Reports*, 8(1), p. 2813. doi: 10.1038/s41598-018-21325-w.

Schulz-Schaeffer, W. J. (2010) 'The synaptic pathology of α-synuclein aggregation in dementia with Lewy bodies, Parkinson's disease and Parkinson's disease dementia', *Acta Neuropathologica*. doi: 10.1007/s00401-010-0711-0.

Sen, N. *et al.* (2009) 'GOSPEL: a neuroprotective protein that binds to GAPDH upon S-nitrosylation.', *Neuron*. doi: 10.1016/j.neuron.2009.05.024.

Sevcsik, E. *et al.* (2011) 'Allostery in a disordered protein: oxidative modifications to α-synuclein act distally to regulate membrane binding.', *Journal of the American Chemical Society*, 133(18), pp. 7152–7158. doi: 10.1021/ja2009554.

Sherer, T. B. *et al.* (2003) 'Subcutaneous rotenone exposure causes highly selective dopaminergic degeneration and α-synuclein aggregation', *Experimental Neurology*. doi: 10.1006/exnr.2002.8072.

Silva, R. M. *et al.* (2005) 'CHOP/GADD153 is a mediator of apoptotic death in substantia nigra dopamine neurons in an in vivo neurotoxin model of parkinsonism', *Journal of Neurochemistry*. doi: 10.1111/j.1471-4159.2005.03428.x.

Singleton, A. B. *et al.* (2003) 'α-Synuclein Locus Triplication Causes Parkinson's Disease', *Science*. doi: 10.1126/science.1090278.

Smith, J. F. *et al.* (2006) 'Characterization of the nanoscale properties of individual amyloid fibrils', *Proceedings of the National Academy of Sciences of the United States of America*. doi: 10.1073/pnas.0604035103.

Smith, W. W. *et al.* (2005) 'Endoplasmic reticulum stress and mitochondrial cell death pathways mediate A53T mutant alpha-synuclein-induced toxicity', *Human Molecular Genetics*. doi: 10.1093/hmg/ddi396.

Sofroniew, M. V. and Vinters, H. V. (2010) 'Astrocytes: biology and pathology', *Acta Neuropathologica*, 119(1), pp. 7–35. doi: 10.1007/s00401-009-0619-8.

Sommer, C. J. (2017) 'Ischemic stroke: experimental models and reality', *Acta Neuropathologica*. doi: 10.1007/s00401-017-1667-0.

Sorrentino, Z. A. *et al.* (2018) 'Motor neuron loss and neuroinflammation in a model of α-synuclein-induced neurodegeneration', *Neurobiology of Disease*. doi: 10.1016/j.nbd.2018.09.005.

Spillantini, M. G. *et al.* (1997) 'α-Synuclein in Lewy bodies', *Nature*, 388(6645), pp. 839–840. doi: 10.1038/42166.

Spillantini, M. G. *et al.* (1998) 'alpha-Synuclein in filamentous inclusions of Lewy bodies from Parkinson's disease and dementia with lewy bodies.', *Proceedings of the National Academy of Sciences of the United States of America*. United States, 95(11), pp. 6469–6473. doi: 10.1073/pnas.95.11.6469.

Stefanovic, A. N. D. *et al.* (2014) 'α-Synuclein oligomers distinctively permeabilize complex model membranes', *FEBS Journal*. doi: 10.1111/febs.12824.

Stirling, D. P. *et al.* (2014) 'Toll-like receptor 2-mediated alternative activation of microglia is protective after spinal cord injury', *Brain*. doi: 10.1093/brain/awt341.

Stokholm, M. G. *et al.* (2016) 'Pathological α-synuclein in gastrointestinal tissues from prodromal Parkinson disease patients', *Annals of Neurology*. doi: 10.1002/ana.24648.

Subramaniam, S. R. *et al.* (2014) 'Region specific mitochondrial impairment in mice with widespread overexpression of alpha-synuclein', *Neurobiology of Disease*. doi: 10.1016/j.nbd.2014.06.017.

Sulzer, D. and Surmeier, D. J. (2013) 'Neuronal vulnerability, pathogenesis, and Parkinson's disease', *Movement Disorders*. doi: 10.1002/mds.25095.

Szalay, G. *et al.* (2016) 'Microglia protect against brain injury and their selective elimination dysregulates neuronal network activity after stroke', *Nature Communications*. doi: 10.1038/ncomms11499.

Tamgüney, G. *et al.* (2009) 'Transmission of scrapie and sheep-passaged bovine spongiform encephalopathy prions to transgenic mice expressing elk prion protein', *Journal of General Virology*. doi: 10.1099/vir.0.007500-0.

Tamgüney, G. and Korczyn, A. D. (2018) 'A critical review of the prion hypothesis of human synucleinopathies', *Cell and Tissue Research*. doi: 10.1007/s00441-017-2712-y.

Tarutani, A. *et al.* (2016) 'The effect of fragmented pathogenic α-synuclein seeds on prion-like propagation', *Journal of Biological Chemistry*. doi: 10.1074/jbc.M116.734707.

Taylor, J. P., Hardy, J. and Fischbeck, K. H. (2002) 'Toxic proteins in neurodegenerative disease', *Science*. doi: 10.1126/science.1067122.

Thul, P. J. and Lindskog, C. (2018) 'The human protein atlas: A spatial map of the human proteome', *Protein Science*. doi: 10.1002/pro.3307.

Tofaris, G. K. *et al.* (2003) 'Ubiquitination of α-Synuclein in Lewy Bodies Is a Pathological Event Not Associated with Impairment of Proteasome Function', *Journal of Biological Chemistry*. doi: 10.1074/jbc.M308041200.

Tremblay, M.-E. *et al.* (2011) 'The Role of Microglia in the Healthy Brain', *Journal of Neuroscience*, 31(45), pp. 16064–16069. doi: 10.1523/JNEUROSCI.4158-11.2011.

Tsacopoulos, M. and Magistretti, P. J. (1996) 'Metabolic coupling between glia and neurons', *Journal of Neuroscience*. doi: 10.1523/jneurosci.16-03-00877.1996.

Tsunemi, T., Hamada, K. and Krainc, D. (2014) 'ATP13A2/PARK9 regulates secretion of exosomes and α-Synuclein', *Journal of Neuroscience*. doi: 10.1523/JNEUROSCI.1629-14.2014.

Tuttle, M. D. *et al.* (2016) 'Solid-state NMR structure of a pathogenic fibril of full-length human α-synuclein', *Nature Structural and Molecular Biology*. doi: 10.1038/nsmb.3194.

Tysnes, O. B. and Storstein, A. (2017) 'Epidemiology of Parkinson's disease', *Journal of Neural Transmission*. doi: 10.1007/s00702-017-1686-y.

Ueda, K. *et al.* (1993) 'Molecular cloning of cDNA encoding an unrecognized component of amyloid in Alzheimer disease', *Proceedings of the National Academy of Sciences of the United States of America*. doi: 10.1073/pnas.90.23.11282.

Uemura, N. *et al.* (2018) 'Inoculation of α-synuclein preformed fibrils into the mouse gastrointestinal tract induces Lewy body-like aggregates in the brainstem via the vagus nerve', *Molecular Neurodegeneration*. doi: 10.1186/s13024-018-0257-5.

Ulusoy, A. *et al.* (2013) 'Caudo-rostral brain spreading of α-synuclein through vagal connections', *EMBO Molecular Medicine*. doi: 10.1002/emmm.201302475.

Unal-Cevik, I. *et al.* (2011) 'Alpha-synuclein aggregation induced by brief ischemia negatively impacts neuronal survival in vivo: A study in A30Palpha-synuclein transgenic mouse', *Journal of Cerebral Blood Flow and Metabolism*. doi: 10.1038/jcbfm.2010.170.

Ungerstedt, U. (1971) 'Postsynaptic Supersensitivity after 6-Hydroxy-dopamine Induced Degeneration of the Nigro-striatal Dopamine System', *Acta Physiologica Scandinavica*. doi: 10.1111/j.1365-201X.1971.tb11000.x.

Uversky, V. and Eliezer, D. (2009) 'Biophysics of Parkinsons Disease: Structure and Aggregation of α- Synuclein', *Current Protein & Peptide Science*. doi: 10.2174/138920309789351921.

Vaikath, N. N. *et al.* (2015) 'Generation and characterization of novel conformation-specific monoclonal antibodies for alpha-synuclein pathology.', *Neurobiology of disease*. United States, 79, pp. 81–99. doi: 10.1016/j.nbd.2015.04.009.

Volpicelli-Daley, L. A. *et al.* (2011) 'Exogenous α-Synuclein Fibrils Induce Lewy Body Pathology Leading to Synaptic Dysfunction and Neuron Death', *Neuron*. Elsevier Inc., 72(1), pp. 57–71. doi: 10.1016/j.neuron.2011.08.033.

Volpicelli-Daley, L. A., Luk, K. C. and Lee, V. M. Y. (2014) 'Addition of exogenous α-synuclein preformed fibrils to primary neuronal cultures to seed recruitment of endogenous α-synuclein to Lewy body and Lewy neurite-like aggregates', *Nature Protocols*. doi: 10.1038/nprot.2014.143.

Vossel, S. *et al.* (2013) 'Anosognosia, neglect, extinction and lesion site predict impairment of daily living after right-hemispheric stroke', *Cortex*. doi: 10.1016/j.cortex.2012.12.011.

Wakabayashi, K. *et al.* (2000) 'NACP/α-synuclein-positive filamentous inclusions in astrocytes and oligodendrocytes of Parkinson's disease brains', *Acta Neuropathologica*. doi: 10.1007/PL00007400.

Wang, S. *et al.* (2015) 'α-Synuclein, a chemoattractant, directs microglial migration via H2O2-dependent Lyn phosphorylation', *Proceedings of the National Academy of Sciences of the United States of America*. doi: 10.1073/pnas.1417883112.

Wanner, I. B. *et al.* (2013) 'Glial scar borders are formed by newly proliferated, elongated astrocytes that interact to corral inflammatory and fibrotic cells via STAT3-dependent mechanisms after spinal cord injury', *Journal of Neuroscience*. doi: 10.1523/JNEUROSCI.2121-13.2013.

Watanabe, Y. *et al.* (2012) 'p62/SQSTM1-Dependent Autophagy of Lewy Body-Like α-Synuclein Inclusions', *PLoS ONE*, 7(12), pp. 1–12. doi: 10.1371/journal.pone.0052868.

Watts, J. C. *et al.* (2013) 'Transmission of multiple system atrophy prions to transgenic mice.', *Proceedings of the National Academy of Sciences of the United States of America*. United States, 110(48), pp. 19555–19560. doi: 10.1073/pnas.1318268110.

Webb, J. L. *et al.* (2003) 'Alpha-Synuclein is degraded by both autophagy and the proteasome.', *The Journal of biological chemistry*. United States, 278(27), pp. 25009–25013. doi: 10.1074/jbc.M300227200.

Wells, A. J. *et al.* (2012) 'A surgical model of permanent and transient middle cerebral artery stroke in the sheep', *PLoS ONE*. doi: 10.1371/journal.pone.0042157.

Wilton, D. K., Dissing-Olesen, L. and Stevens, B. (2019) 'Neuron-Glia Signaling in Synapse Elimination', *Annual Review of Neuroscience*. doi: 10.1146/annurev-neuro-070918-050306.

Winner, B. *et al.* (2011) 'In vivo demonstration that alpha-synuclein oligomers are toxic.', *Proceedings of the National Academy of Sciences of the United States of America*. United States, 108(10), pp. 4194–4199. doi: 10.1073/pnas.1100976108.

Winner, B. *et al.* (2012) 'Role of α-synuclein in adult neurogenesis and neuronal maturation in the dentate gyrus', *Journal of Neuroscience*. doi: 10.1523/JNEUROSCI.2723-12.2012.

Woerman, A. L. *et al.* (2017) 'Familial Parkinson's point mutation abolishes multiple system atrophy prion replication', *Proceedings of the National Academy of Sciences of the United States of America*. doi: 10.1073/pnas.1719369115.

Woerman, A. L. *et al.* (2019) 'Multiple system atrophy prions retain strain specificity after serial propagation in two different Tg(SNCA*A53T) mouse lines', *Acta Neuropathologica*. doi: 10.1007/s00401-019-01959-4.

Wu, Z. *et al.* (2019) 'Alpha-synuclein alterations in red blood cells of peripheral blood after acute ischemic stroke.', *International journal of clinical and experimental pathology*.

Xing, C. *et al.* (2012) 'Pathophysiologic cascades in ischemic stroke', *International Journal of Stroke*. doi: 10.1111/j.1747-4949.2012.00839.x.

Yang, M. S., Min, K. J. and Joe, E. (2007) 'Multiple mechanisms that prevent excessive brain inflammation', *Journal of Neuroscience Research*. doi: 10.1002/jnr.21254.

Yoon, D. K. *et al.* (2006) 'Comparison of α-synuclein immunoreactivity and protein levels in ischemic hippocampal CA1 region between adult and aged gerbils and correlation with Cu,Zn-superoxide dismutase', *Neuroscience Research*. doi: 10.1016/j.neures.2006.04.014.

Ysselstein, D. *et al.* (2017) 'Endosulfine-alpha inhibits membrane-induced α-synuclein aggregation and protects against α-synuclein neurotoxicity', *Heritage Science*. doi: 10.1186/s40478-016-0403-7.

Yun, S. P. *et al.* (2018) 'Block of A1 astrocyte conversion by microglia is neuroprotective in models of Parkinson's disease', *Nature Medicine*. doi: 10.1038/s41591-018-0051-5.

Zaidat, O. O. *et al.* (2012) 'Revascularization grading in endovascular acute ischemic stroke therapy', *Neurology*. doi: 10.1212/WNL.0b013e3182695916.

Zaltieri, M. *et al.* (2015) 'α-synuclein and synapsin III cooperatively regulate synaptic function in dopamine neurons', *Journal of Cell Science*. doi: 10.1242/jcs.157867.

Zarranz, J. J. *et al.* (2004) 'The New Mutation, E46K, of α-Synuclein Causes Parkinson and Lewy Body Dementia', *Annals of Neurology*, 55(2), pp. 164–173. doi: 10.1002/ana.10795.

Zhang, L. *et al.* (2015) 'Focal embolic cerebral ischemia in the rat', *Nature Protocols*. doi: 10.1038/nprot.2015.036.

Zhang, Wei *et al.* (2005) 'Aggregated α-synuclein activates microglia: a process leading to disease progression in Parkinson's disease', *The FASEB Journal*. Federation of American Societies for Experimental Biology, 19(6), pp. 533–542. doi: 10.1096/fj.04-2751com.

Zhang, Y. *et al.* (2016) 'Purification and Characterization of Progenitor and Mature Human Astrocytes Reveals Transcriptional and Functional Differences with Mouse', *Neuron*. doi: 10.1016/j.neuron.2015.11.013.

Zhao, H. Q. *et al.* (2016a) 'A comparative study of the amount of α-synuclein in ischemic stroke and Parkinson's disease', *Neurological Sciences*, 37(5), pp. 749–754. doi: 10.1007/s10072-016-2485-1.

Zhao, H. Q. *et al.* (2016b) 'A comparative study of the amount of α-synuclein in ischemic stroke and Parkinson's disease', *Neurological Sciences*. doi: 10.1007/s10072-016-2485-1.

Zhong, Z. F. *et al.* (2019) 'Neuroprotective effects of salidroside on cerebral ischemia/reperfusion-induced behavioral impairment involves the dopaminergic system', *Frontiers in Pharmacology*. doi: 10.3389/fphar.2019.01433.

Zhou, R. M. *et al.* (2010) 'Molecular interaction of α-synuclein with tubulin influences on the polymerization of microtubule in vitro and structure of microtubule in cells', *Molecular Biology Reports*. doi: 10.1007/s11033-009-9899-2.

Zhou, W. *et al.* (2000) 'Overexpression of human α-synuclein causes dopamine neuron death in rat primary culture and immortalized mesencephalon-derived cells', *Brain Research*. doi: 10.1016/S0006-8993(00)02215-0.

Zhu, M. *et al.* (2006) 'α-synuclein can function as an antioxidant preventing oxidation of unsaturated lipid in vesicles', *Biochemistry*. doi: 10.1021/bi052584t.

Zülch, K. J. (1981) 'Cerebrovascular Pathology and Pathogenesis as a Basis of Neuroradiological Diagnosis', in. doi: 10.1007/978-3-642-95333-0_1.

7 Acknowledgement

First of all I want to thank my supervisor Prof. Dr. Erdem Tamgüney for the opportunity of working on several interesting projects in his lab and for supporting me through my PhD. I am deeply grateful for your scientific guidance, the useful thoughts and scientific discussions and your input and support throughout these past four years. You always took the time to discuss ideas and results – even when you already set up your new group in Jülich. You helped me to develop not only as a scientist but also as a person. Thank you very much for the support and guidance, the patience and flexibility.

I would like to thank Prof. Dr. Jörg Höhfeld for agreeing to be my second examiner and Prof. Dr. Irmgard Förster and Prof. Dr. Anton Bovier for their willingness to be members of the extended examination board and for taking the time to consider my work.

Also, I am very thankful to everyone who contributed to this thesis: Dr. Maria Eugenia Bernis, Dr. Babila Julius Tachu, Dr. Jessica Grigoletto, Alexandra Ziemski, and my Bachelorstudent Alina Hebestreit. I would like to thank the animal caretakers who took such good care of the mice, both at the DZNE in Bonn, but also at the Forschungszentrum Jülich. Moreover, I appreciate the technical support of the Light Microscope Facility (LMF) at the DZNE in Bonn. My gratitude also goes out to all the other current and former members of the Tamgüney lab for the great working atmosphere. In particular, I would like to thank Maria Eugenia Bernis, who not only introduced me to the methods in the lab, always was and still is open for scientific and non-scientific discussions, but also for welcoming me in her family and making me Lauti's german auntie.

I would also like to thank Prof. Dr. Ina Vorberg, for adopting and hosting me in her lab during my last two years at the DZNE. In line with this, I would like to thank the whole Vorberg lab for nicely welcoming me and all the hours inside but also outside the lab.

My sincere acknowledgement also goes out to all of you who have helped and supported me in the past years to manage my life, this thesis, and the Corona lockdown, by giving me great advice, motivating me, proof-reading, starting our Sunday hikes, or just offering me company and a cup of coffee or a glass of wine. This includes in particular: Theresa, Nicole, Nelli, Hana, Moni, Anna, Annika, Alina, Eva, Tanja, Nina, and again Euge.
I also want to acknowledge my Spotify account for keeping me company during all the cutting sessions at the microtome and making them more fun.

Zu guter Letzt möchte ich noch meinen Eltern meinen tiefsten Dank aussprechen. Danke für Eure liebevolle Unterstützung und Euren unerschütterlichen Glauben an mich. Danke, dass Ihr immer für mich da wart und seid, mich bei all meinen Entscheidungen unterstützt und mich immer wieder motiviert!